

## Supplementary Materials for

### **HEx: A heterologous expression platform for the discovery of fungal natural products**

Colin J. B. Harvey, Mancheng Tang, Ulrich Schlecht, Joe Horecka, Curt R. Fischer, Hsiao-Ching Lin, Jian Li, Brian Naughton, James Cherry, Molly Miranda, Yong Fuga Li, Angela M. Chu, James R. Hennessy, Gergana A. Vandova, Diane Inglis, Raeka S. Aiyar, Lars M. Steinmetz, Ronald W. Davis, Marnix H. Medema, Elizabeth Sattely, Chaitan Khosla, Robert P. St. Onge, Yi Tang, Maureen E. Hillenmeyer

Published 11 April 2018, *Sci. Adv.* **4**, eaar5459 (2018)

DOI: 10.1126/sciadv.aar5459

#### **The PDF file includes:**

- Supplementary Text
- fig. S1. Characterization of *S. cerevisiae* P<sub>ADH2</sub>-like promoters.
- fig. S2. Cloning vectors used in this study.
- fig. S3. Improving DNA assembly.
- fig. S4. Schematics of all PKS-containing BGCs examined here.
- fig. S5. UTC-containing BGCs examined here.
- fig. S6. Volcano plot of all spectral features identified in the automated analysis of strains expressing PKS-containing BGCs.
- fig. S8. All features produced by PKS1 in strain 132.
- fig. S9. All features produced by PKS2 in strain 133.
- fig. S10. All features produced by PKS4 in strain 255.
- fig. S11. All features produced by PKS6 in strain 178.
- fig. S12. All features produced by PKS8 in strain 164.
- fig. S13. All features produced by PKS10 in strain 246.
- fig. S14. All features produced by PKS13 in strain 206.
- fig. S15. All features produced by PKS14 in strain 257.
- fig. S16. All features produced by PKS15 in strain 247.
- fig. S17. All features produced by PKS16 in strain 177.
- fig. S18. All features produced by PKS17 in strain 176.
- fig. S19. All features produced by PKS18 in strain 207.
- fig. S20. All features produced by PKS20 in strain 208.

- fig. S21. All features produced by PKS22 in strain 209.
- fig. S22. All features produced by PKS23 in strain 241.
- fig. S23. All features produced by PKS24 in strain 210.
- fig. S24. All features produced by PKS28 in strain 240.
- fig. S25.  $^1\text{H}$  NMR spectrum of compound **6** in  $\text{CDCl}_3$ .
- fig. S26.  $^{13}\text{C}$  NMR spectrum of compound **6** in  $\text{CDCl}_3$ .
- fig. S27.  $^1\text{H}$ - $^1\text{H}$  COSY spectrum of compound **6** in  $\text{CDCl}_3$ .
- fig. S28. HSQC spectrum of compound **6** in  $\text{CDCl}_3$ .
- fig. S29. HMBC spectrum of compound **6** in  $\text{CDCl}_3$ .
- fig. S30.  $^1\text{H}$  NMR spectrum of compound **7** in acetone- $\text{d}_6$ .
- fig. S31.  $^{13}\text{C}$  NMR spectrum of compound **7** in acetone- $\text{d}_6$ .
- fig. S32.  $^1\text{H}$ - $^1\text{H}$  COSY spectrum of compound **7** in acetone- $\text{d}_6$ .
- fig. S33. HSQC spectrum of compound **7** in acetone- $\text{d}_6$ .
- fig. S34. HMBC spectrum of compound **7** in acetone- $\text{d}_6$ .
- fig. S35.  $^1\text{H}$  NMR spectrum of compound **8** in acetone- $\text{d}_6$ .
- fig. S36.  $^{13}\text{C}$  NMR spectrum of compound **8** in acetone- $\text{d}_6$ .
- fig. S37.  $^1\text{H}$ - $^1\text{H}$  COSY spectrum of compound **8** in acetone- $\text{d}_6$ .
- fig. S38. HSQC spectrum of compound **8** in acetone- $\text{d}_6$ .
- fig. S39. HMBC spectrum of compound **8** in acetone- $\text{d}_6$ .
- fig. S40.  $^1\text{H}$  NMR spectrum of compound **9** in  $\text{CDCl}_3$ .
- fig. S41.  $^{13}\text{C}$  NMR spectrum of compound **9** in  $\text{CDCl}_3$ .
- fig. S42.  $^1\text{H}$ - $^1\text{H}$  COSY spectrum of compound **9** in  $\text{CDCl}_3$ .
- fig. S43. HSQC spectrum of compound **9** in  $\text{CDCl}_3$ .
- fig. S44. HMBC spectrum of compound **9** in  $\text{CDCl}_3$ .
- fig. S45.  $^1\text{H}$  NMR spectrum of compound **10** in  $\text{CDCl}_3$ .
- fig. S46.  $^{13}\text{C}$  NMR spectrum of compound **10** in  $\text{CDCl}_3$ .
- fig. S47.  $^1\text{H}$ - $^1\text{H}$  COSY spectrum of compound **10** in  $\text{CDCl}_3$ .
- fig. S48. HSQC spectrum of compound **10** in  $\text{CDCl}_3$ .
- fig. S49. HMBC spectrum of compound **10** in  $\text{CDCl}_3$ .
- fig. S50.  $^1\text{H}$  NMR spectrum of compound **11** in  $\text{CDCl}_3$ .
- fig. S51.  $^{13}\text{C}$  NMR spectrum of compound **11** in  $\text{CDCl}_3$ .
- fig. S52.  $^1\text{H}$  NMR spectrum of compound **12** in  $\text{CDCl}_3$ .
- fig. S53.  $^{13}\text{C}$  NMR spectrum of compound **12** in  $\text{CDCl}_3$ .
- fig. S54.  $^1\text{H}$ - $^1\text{H}$  COSY spectrum of compound **12** in  $\text{CDCl}_3$ .
- fig. S55. HSQC spectrum of compound **12** in  $\text{CDCl}_3$ .
- fig. S56. HMBC spectrum of compound **12** in  $\text{CDCl}_3$ .
- fig. S57. NOESY spectrum of compound **12** in  $\text{CDCl}_3$ .
- fig. S58.  $^1\text{H}$  NMR spectrum of compound **13** in  $\text{CDCl}_3$ .
- fig. S59.  $^{13}\text{C}$  NMR spectrum of compound **13** in  $\text{CDCl}_3$ .
- fig. S60.  $^1\text{H}$ - $^1\text{H}$  COSY spectrum of compound **13** in  $\text{CDCl}_3$ .
- fig. S61. HSQC spectrum of compound **13** in  $\text{CDCl}_3$ .
- fig. S62. HMBC spectrum of compound **13** in  $\text{CDCl}_3$ .
- fig. S63. NOESY spectrum of compound **13** in  $\text{CDCl}_3$ .
- fig. S64.  $^1\text{H}$  NMR spectrum of compound **14** in  $\text{CDCl}_3$ .

- fig. S65.  $^{13}\text{C}$  NMR spectrum of compound **14** in  $\text{CDCl}_3$ .
- fig. S66.  $^1\text{H}$ - $^1\text{H}$  COSY spectrum of compound **14** in  $\text{CDCl}_3$ .
- fig. S67. HSQC spectrum of compound **14** in  $\text{CDCl}_3$ .
- fig. S68. HMBC spectrum of compound **14** in  $\text{CDCl}_3$ .
- fig. S69.  $^1\text{H}$  NMR spectrum of compound **15** in  $\text{CDCl}_3$ .
- fig. S70.  $^{13}\text{C}$  NMR spectrum of compound **15** in  $\text{CDCl}_3$ .
- fig. S71.  $^1\text{H}$ - $^1\text{H}$  COSY spectrum of compound **15** in  $\text{CDCl}_3$ .
- fig. S72. HSQC spectrum of compound **15** in  $\text{CDCl}_3$ .
- fig. S73. HMBC spectrum of compound **15** in  $\text{CDCl}_3$ .
- fig. S74. HMBC spectrum of compound **15** in  $\text{CDCl}_3$ .
- fig. S75.  $^1\text{H}$  NMR spectrum of compound **16** in  $\text{CDCl}_3$ .
- fig. S76.  $^{13}\text{C}$  NMR spectrum of compound **16** in  $\text{CDCl}_3$ .
- fig. S77.  $^1\text{H}$ - $^1\text{H}$  COSY spectrum of compound **16** in  $\text{CDCl}_3$ .
- fig. S78. HSQC spectrum of compound **16** in  $\text{CDCl}_3$ .
- fig. S79. HMBC spectrum of compound **16** in  $\text{CDCl}_3$ .
- table S1. Ion source parameters used in this study.
- table S2. Expression data for selected promoters drawn from genome-wide expression studies.
- table S3. Sequences of HEx promoters.
- table S4. Background strains used throughout this study.
- table S5. Features integrated for the determination of sesquiterpenoid titer in Fig. 2B.
- table S6. Order of promoters and terminators used in the expression of all cryptic fungal BGCs examined in this study.
- table S7. Standard part plasmids and expression vectors used for the assembly of cryptic BGCS in this study.
- table S8. Coordinates of native loci from which all clusters examined here were derived along with the IDs of plasmids expressing the engineered cluster versions.
- table S9. Abbreviations for the functional gene annotations used in Figs. 2, 5, and 6.
- table S10. Strains expressing cryptic fungal BGCs analyzed here.
- table S11. NMR data of compound **6**.
- table S12. NMR data of compound **7**.
- table S13. NMR data of compound **8**.
- table S14. NMR data of compound **9**.
- table S15. NMR data of compound **10**.
- table S16. NMR data of compound **11**.
- table S17. NMR data of compound **12**.
- table S18. NMR data of compound **13**.
- table S19. NMR data of compound **14**.
- table S20. NMR data of compound **15**.
- table S21. NMR data of compound **16**.
- References (70–73)

**Other Supplementary Material for this manuscript includes the following:**  
(available at [advances.sciencemag.org/cgi/content/full/4/4/eaar5459/DC1](https://advances.sciencemag.org/cgi/content/full/4/4/eaar5459/DC1))

- fig. S7 (.pdf format).
- Data file S1 (.gb format).



## Supplementary Text

### **Selection and characterization of P<sub>ADH2</sub>-like promoters:**

Prior to this study, the only promoter set with of sufficient size as to be compatible with the assembly of large, multigene plasmids consisted entirely of strong constitutive promoters(36, 37). In contrast to this large panel, controllable promoter sets based on natural sequences modulated by copper (27), methionine(28), galactose(29), or other carbon sources(30) are limited to 4 or fewer mutually controllable promoters, while synthetic promoters and those employing engineered transcription factor binding sites require stretches of homologous sequence likely to complicate single-step assembly efforts(70, 71). As described in the main text, we sought to identify and characterize a large set of promoters of genes coregulated with ADH2.

Expression values for *Saccharomyces cerevisiae* cultures grown in both YPD (fermentation) and YPE (respiration) were used for the selection of P<sub>ADH2</sub>-like promoters. The values for selected promoters, which had an expression value <2 in YPD and >4.5 in YPE as well as the known constitutive promoters used as controls are listed in table S2. The full dataset used for this analysis is available from the authors of the original study at:

<http://steinmetzlab.embl.de/NFRsharing/index.html>.

The fluorescence profiles for GFP expressed under strong *S. cerevisiae* P<sub>ADH2</sub>-like sequences and all *sensu stricto* ADH2 promoters are illustrated in Fig. 2A of the main text. Shown in fig. S1a is the expression of GFP over time when driven by all *S. cerevisiae* promoters examined here. Figure S1b shows representative fluorescence intensity histograms from flow cytometry experiments and while fig. S1c shows both light field and fluorescence microscopy images with these same strains.

P<sub>ADH2</sub>-like promoters from *sensu stricto* *Saccharomyces* species were chosen by selecting 500 bases upstream of the start codon of the closest homologue of *S. cerevisiae* ADH2 in each genome. Figure S1d shows a phylogenetic tree for the all of the *sensu stricto* P<sub>ADH2</sub> sequences along with a multiple sequence alignment of the upstream activating sequences shown in fig. S1e and the pairwise identities of all *sensu stricto* P<sub>ADH2</sub> sequences are illustrated in fig. S1f. The sequences of all promoters examined in this study are listed in table S4.

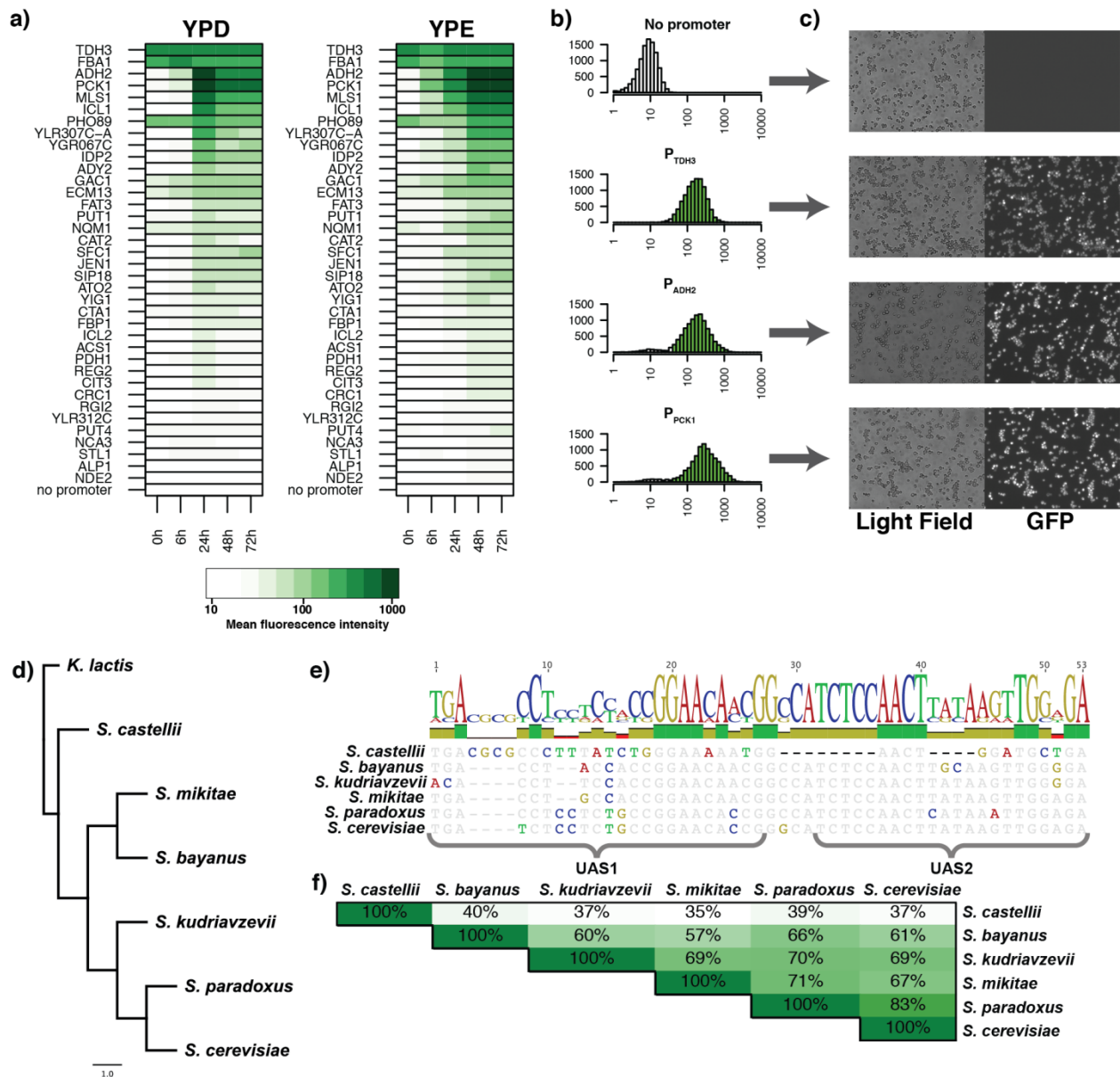


**fig. S1. Characterization of *S. cerevisiae* P<sub>ADH2</sub>-like promoters.** (a) Expression of eGFP under all *S. cerevisiae* promoters examined here. Fluorescence intensity calculated as the mean of 10<sup>4</sup> cells. (b) Histograms from representative flow cytometry experiments. All histograms represent 10<sup>4</sup> cells after 48 h of culture in YPD medium. (c) Light field and fluorescence images taken of eGFP expressing strains 48 h of culture in YPD medium. (d) Cladogram of all *Saccharomyces* P<sub>ADH2</sub> sequences. (e) Multiple sequence alignment of previously characterized upstream activating sequences. (f) Pairwise identities of all *Saccharomyces* P<sub>ADH2</sub> sequences.

### Cloning vectors used in this study:

In addition to the HEx promoters, we also generated and characterized a novel series of vectors based on the pRS42X series of plasmids (72). These vectors all contain a 2 $\mu$  origins of replication and, as such, exist at high copy numbers within cells. While we believe this is an

appropriate context in which to initially examine each BGC, we wanted the ability to easily generate a stable, single copy, genomic integrant for each BGC. In order to facilitate this, we developed the system outline in fig. S2. We established a new set of vectors with the multiple cloning site (MCS) flanked by  $P_{ADH2}$  and  $T_{CYC1}$ . This expression cassette is then flanked by both a 200 bp linker sequence an I-SceI site on each side. These 18 bp nuclease recognition sites are unlikely to occur in any of the cryptic BGCs we wish to express and, as such, allow excision of the entire multigene cassette inserted at the MCS as a single fragment with no requirement for PCR. Linker sequences can then be used to target the multi-gene cassette for integration at any desired genomic locus. When present on the backbone, selectable markers have been moved inside the linker sequences, allowing for selection for correct integrants by plating on the appropriate SDC dropout media.

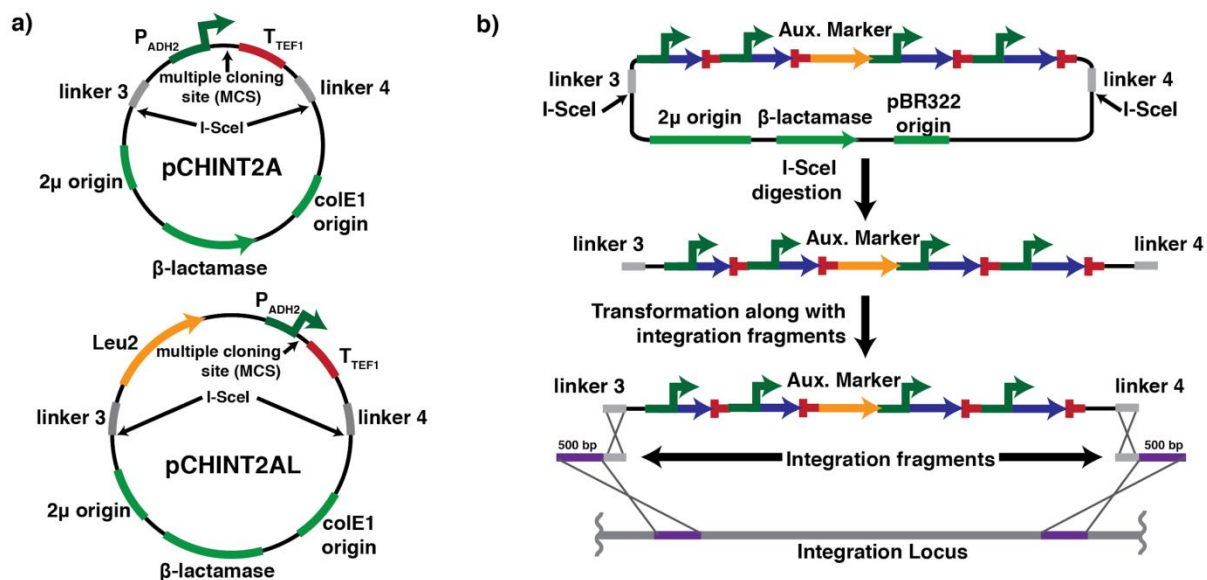


**fig. S2. Cloning vectors used in this study.** (a) Schematics of two representative pCHINT2A and pCHINT2AL, two representative cloning vectors used in this study for the assembly of plasmids with 1-2 genes (pCHINT2AL) or >3 genes (pCHINT2A). Fully annotated sequences for each of these vectors are provided in the Supporting Documents (b) Strategy for the excision and PCR-free integration of entire multigene cassettes at a desired genomic locus.

### High-throughput DNA assembly:

To increase the efficiency of assemblies by YHR, we tested the relative efficiencies of BY4743 and BY4743 $\Delta$ DNL4; a strain in which the *DNL4* ligase, involved in non-homologous endjoining, has been deleted. Figure S3a illustrates efficiencies of several plasmid assemblies done in both strains, demonstrating the deletion of the *DNL4* DNA ligase does consistently lead to more efficient assembly.

The sequencing of plasmid DNA directly out of yeast is one of the major advantages of the HEX pipeline. In establishing this portion of the pipeline we tested multiple means of preparation for both the plasmid DNA and the next-generation sequencing (NGS) library prep. Shown in fig. S3b is a comparison of sequencing efficiency using DNA prepared both from colonies picked

from plates and cell pellets collected from 1 ml of liquid culture. All samples were prepared using Zymo-prep-96 plasmid miniprep (Zymo research, S2007) according to manufacturer's specifications. These data show that these two DNA preparations generate samples of equivalent purity.

Initially, the HEx platform utilized an NGS library preparation in which the purified, exonuclease treated plasmid DNA was ultrasonically sheared, followed by end repair, A-tailing, and adaptor ligation. In order to decrease labor and increase throughput, we transitioned to a recently published modification of the Illumina Nextera transposase based preparation (66) as described in the Methods. Ultrasonic shearing necessitated the serial processing of multiple plates of clones while tagmentation allows for parallel processing of multiple plates. Figure S3c demonstrates that this modified Nextera preparation provides equivalent efficiency as compared to the standard approach.

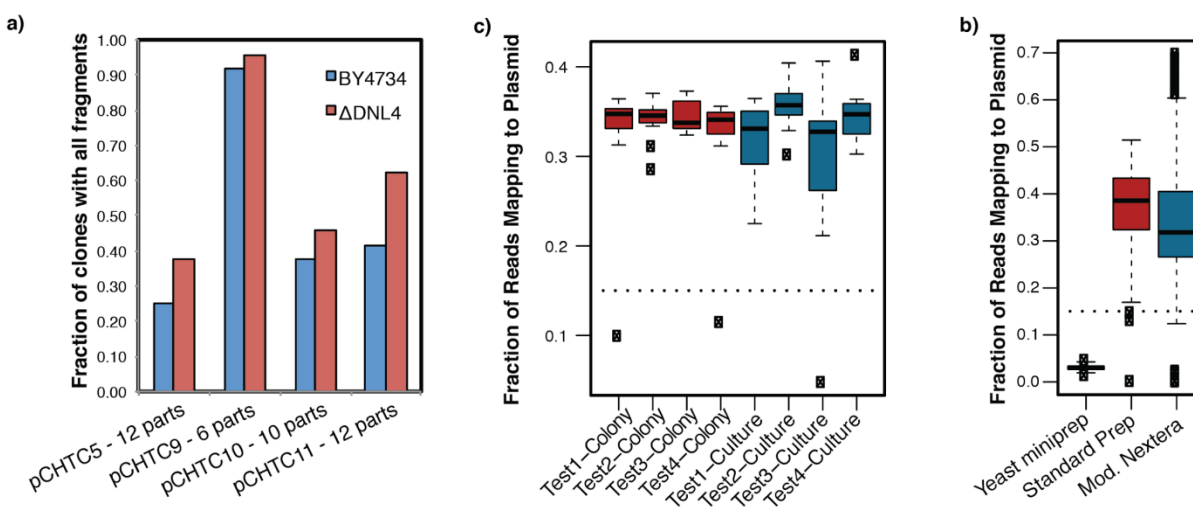


**fig. S3. Improving DNA assembly.** (a) Efficiency of assembly of 4 plasmids in both BY4743 and BY4743ΔDNL4. (b) Sequencing efficiency for DNA directly from picked colonies and cell pellets from 1 ml of 48 h culture for 4 separate assemblies. (c) Sequencing efficiency for libraries prepared by both ultrasonic shearing followed by end-repair and adapter ligation (standard prep) and a modified Nextera tagmentation (Mod Nextera). Detailed protocols are outlined in the Methods.

### Correction of the TC5 terpene cyclase:

For many of the genomes mined in this study for BGCs, transcriptome data were not available. As such, for many of the genes synthesized and expressed here, we relied heavily on intron prediction. For the BGCs analyzed here containing UTCs, we sought to identify gene prediction errors by aligning each UTC that appeared to not produce a novel feature with all of those that did. Such an analysis of the TC5 UTC identified a putative incorrectly predicted intron near the 3' end of the gene, resulting in a premature stop codon and truncation of a well conserved sequence present in all functional UTCs. Shown in fig. S5b is the C-terminal portion the alignment of the all functional sequences along with both the deposited and corrected TC5 UTC, demonstrating that once the incorrect intron boundary is repaired, the well conserved C-

terminus of the protein is present. The ability of the cluster containing the corrected UTC to produce sesquiterpenoids not native to yeast is illustrated in Fig. 4 of the main text.

### Strain analysis and Compound Characterization:

All strains expressing a cryptic fungal polyketide BGCs were cultured and analyzed as described in the Methods using the ionization source parameters defined in (20) table S1. All samples were analyzed using XCMS (20) for untargeted metabolomics resulting in several thousand unique features. Extracted ion chromatograms (EICs) for the top 50 hits when sorted by both p-value and fold change were plotted and subjected to manual inspection in order to identify those spectral features that are specific to the BGC expressing strain as compared to an empty vector control. The necessity of manual inspection is illustrated in the volcano plot shown in fig. S6 in which the p-values and fold changes associated with all automatically identified features are overlaid with those of manually verified “real” features.

These data demonstrate that, with the parameters utilized here, fold-change is a far more useful metric than p-value in determining whether or not a given spectral feature is truly cluster specific. The non-cluster specific features in this quadrant are primarily a result of noise in the spectra or insufficient retention time correction.

**table S1. Ion source parameters used in this study.**

Ion source parameter	Dual AJS	MMI
gas temperature	250 °C	350 °C
drying gas	12 L / min	7.5 L / min
nebulizer	10 psig	20 psig
sheath gas temp.	400 °C	-
sheath gas flow	12 L / min	-
vaporizer	-	250 °C
capillary voltage (Vcap)	3500 V	1500 V
nozzle voltage	1400 V	-
corona discharge	-	4 μA
fragmentor	100 V	120 V
skimmer	50 V	50 V
octopole 1 RF Vpp	750 V	750 V
charging voltage	-	1000 V

Illustrated in figs. S7-S23 are the extracted ion chromatograms (EICs) for all unique features generated by each polyketide producing cluster identified by automated comparative metabolomics using XCMS and deemed real by manual inspection. Strain 137 is a strain constructed with the JHY702 background containing two empty cloning vector and, therefore,

serves as a negative control in all chromatograms shown in figs. S7-S23. For all chromatograms, the ionization source is one of electrospray in either positive (ESI+) or negative (ESI-) mode or multimode ionization in positive mode (MMI+). All m/z values reported here represent the median of the three biological replicates.

For those strains producing isolable amounts of product, compounds were purified as described in the methods and structures were solved using both 1D and 2D NMR. These data are summarized in tables S11-S21 while the spectra themselves are shown in figs. S18-S72.



**fig. S4. Schematics of all PKS-containing BGCs examined here.** Gaps in arrows represent introns in genes. All genes are labelled with the locus tag of the sequence as deposited in GenBank.



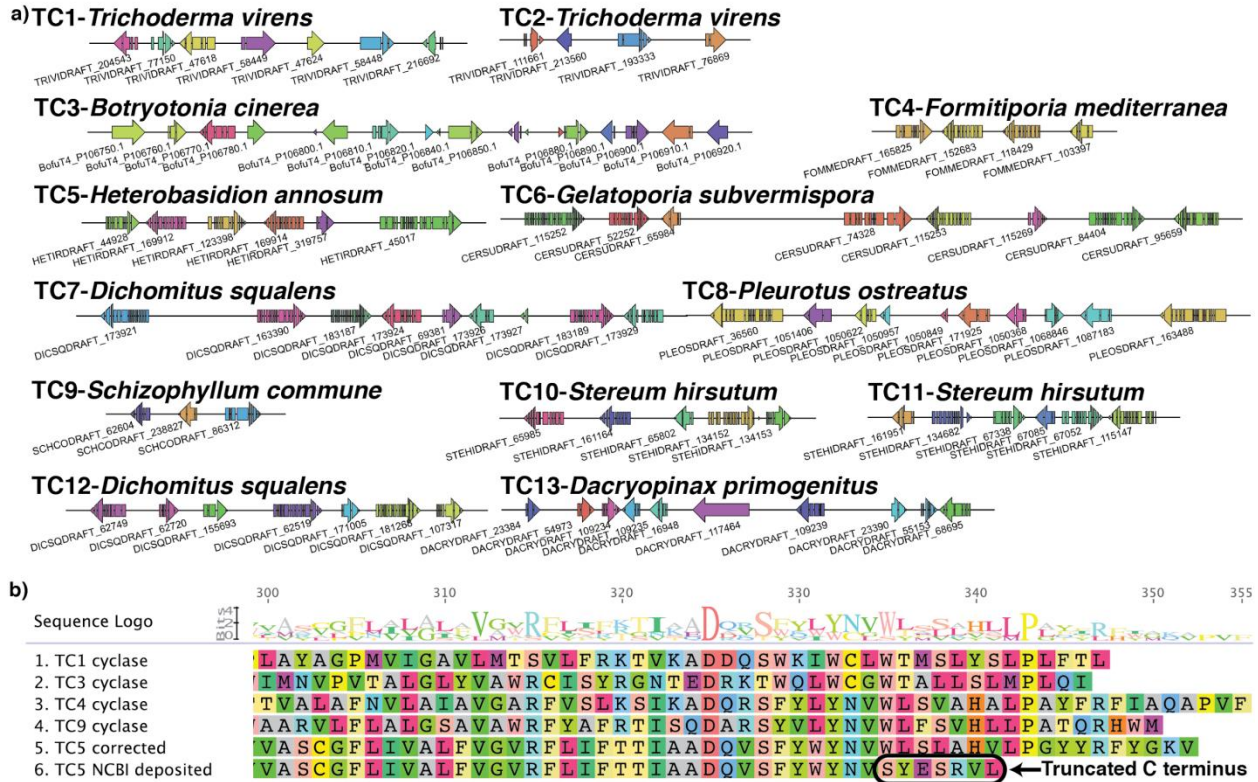


**fig. S5. UTC-containing BGCs examined here.** (a) Schematics of all UTC containing BGCs examined here. Gaps in arrows represent introns in genes. All genes are labelled with the locus tag of the sequence as deposited in GenBank. (b) C-terminus of a multiple sequence alignment of all functional UTC protein sequences along with both the deposited and corrected versions of the TC5 cyclase.



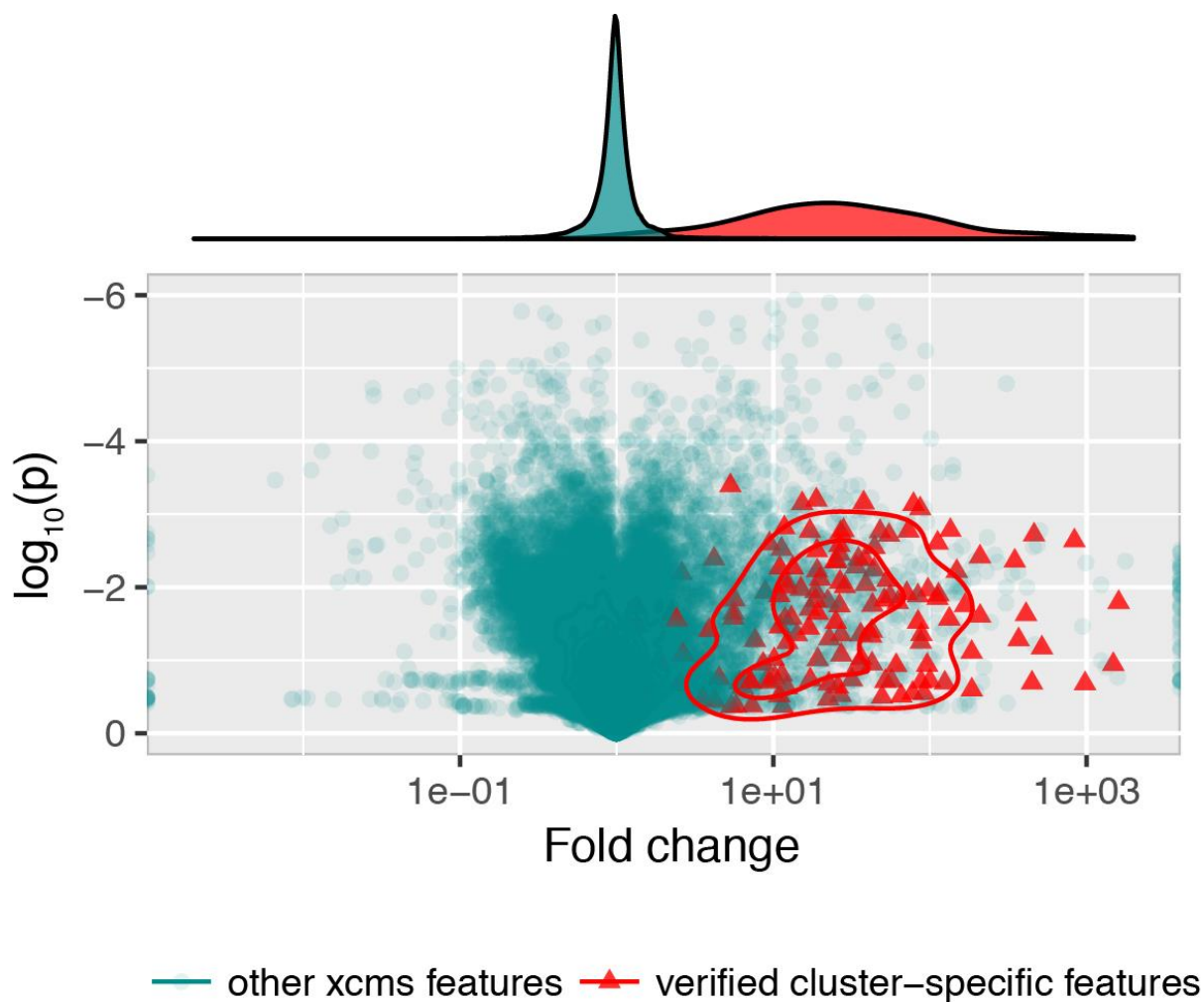


**fig. S6. Volcano plot of all spectral features identified in the automated analysis of strains expressing PKS-containing BGCs.** All features determined to be specific to the BGC expressing strain as compared to a negative vector control. EICs of all BGC specific features are illustrated in figs. S7-S23.

**Supplementary Tables:**

**table S2. Expression data for selected promoters drawn from genome-wide expression studies.**

ORF	Gene	YPD				YPE				YPE/YPD
		1	2	3	Mean	1	2	3	Mean	
YGR192C	TDH3	6.91	6.98	6.97	6.95	6.73	7.27	6.90	6.97	1.0
YKL060C	FBA1	6.67	6.71	6.67	6.68	6.60	6.95	6.56	6.70	1.0
YMR303C	ADH2	1.11	1.15	1.06	1.11	6.38	6.72	6.38	6.50	5.9
YKR097W	PCK1	0.21	0.31	0.19	0.24	7.28	7.49	7.19	7.32	30.8
YNL117W	MLS1	0.24	0.37	0.21	0.27	6.85	6.92	6.64	6.80	25.1
YER065C	ICL1	1.98	1.81	1.94	1.91	6.13	6.22	5.96	6.10	3.2
YBR296C	PHO89	0.58	0.95	1.08	0.87	5.42	5.49	5.13	5.35	6.2
YLR307C-A	YLR307C-A	0.13	0.18	0.12	0.14	4.28	4.74	4.37	4.46	31.5
YGR067C	YGR067C	1.68	1.53	2.26	1.82	6.13	5.98	5.79	5.97	3.3
YLR174W	IDP2	1.68	1.68	1.74	1.70	6.75	6.60	6.32	6.56	3.9
YCR010C	ADY2	0.49	0.63	0.56	0.56	6.61	6.81	6.52	6.65	11.9
YOR178C	GAC1	1.44	1.62	1.75	1.60	5.23	4.66	4.57	4.82	3.0
YBL043W	ECM13	1.54	1.56	1.55	1.55	6.28	6.28	5.92	6.16	4.0
YKL187C	YKL187C	2.63	2.29	2.74	2.55	5.77	5.42	5.24	5.48	2.1
YLR142W	PUT1	1.31	1.67	1.56	1.51	4.71	4.84	4.62	4.73	3.1
YGR043C	NQM1	0.67	1.03	0.83	0.84	4.53	4.53	4.26	4.44	5.3
YML042W	CAT2	0.17	0.22	0.18	0.19	5.62	5.82	5.50	5.65	29.4
YJR095W	SFC1	0.28	0.50	0.33	0.37	6.81	6.85	6.52	6.72	18.2
YKL217W	JEN1	0.66	0.68	0.53	0.62	6.68	6.80	6.48	6.65	10.7
YMR175W	SIP18	0.97	1.09	0.80	0.95	6.27	6.34	5.85	6.15	6.5
YNR002C	ATO2	0.84	0.83	1.01	0.89	5.27	5.44	5.17	5.29	5.9
YPL201C	YIG1	0.46	0.47	0.42	0.45	5.58	5.57	5.35	5.50	12.3
YDR256C	CTA1	1.06	0.89	0.92	0.96	5.68	5.81	5.51	5.67	5.9
YLR377C	FBP1	0.26	0.36	0.22	0.28	6.67	6.92	6.56	6.72	23.8
YPR006C	ICL2	0.43	0.52	0.37	0.44	5.64	5.27	4.95	5.28	12.0
YAL054C	ACS1	0.33	0.42	0.29	0.35	6.02	6.14	5.87	6.01	17.3
YPR002W	PDH1	0.92	1.15	1.36	1.14	5.70	5.89	5.43	5.67	5.0
YBR050C	REG2	0.82	1.07	1.16	1.02	5.25	4.73	4.52	4.84	4.7
YPR001W	CIT3	0.73	0.70	0.86	0.76	5.01	5.15	4.70	4.96	6.5
YOR100C	CRC1	0.51	0.64	0.68	0.61	5.41	5.16	4.86	5.14	8.5
YIL057C	YIL057C	0.14	0.33	0.11	0.19	5.73	6.23	5.79	5.92	30.6
YLR312C	QNQ1	1.26	1.41	1.11	1.26	4.89	4.92	4.52	4.78	3.8
YOR348C	PUT4	0.56	0.63	0.48	0.56	5.86	5.74	5.41	5.67	10.2
YJL116C	NCA3	1.37	1.07	1.17	1.20	4.42	4.75	4.54	4.57	3.8
YDR536W	STL1	0.18	0.28	0.17	0.21	6.04	5.79	5.47	5.77	27.2
YNL270C	ALP1	0.74	0.77	1.08	0.86	5.06	4.72	4.46	4.75	5.5
YDL085W	NDE2	0.24	0.38	0.21	0.28	4.66	4.41	4.27	4.45	16.1



		TCACAATTATTTATTGTTTTCTCACATAGAAAATTCGCCATACTGCGATTATA
YKL187C	FAT3	GAAAGCTTATTACTGAGTTTTGCGGAGCATCGCTCGGAGCGCGGAATTGAATCGAACCCCGCTGCTATTACCGAACAAAAAATTCG AAAGCATAAAGCTAGTAGTAAAAAATTCGAGAAATTTTCAGATGAGTGGCGACTTTCCAGTCCCTTGGCGTTTTGTCACTTAGTCAGCTA GTAAAGGAGCCGTGTGGTTAGAGTGGCTACAATTCCTCAAAGGGCACTTCTAGAACCACCGGTGAATTTTTTTGGCATGATAAATCG GTAGAATCGGTGAAGTAATACCCAAAAAAGGATCGGATTGTGTTTTCTCGTAATCCGTATTATTGCCGATGGCATCGACTACTTCTT TTTTAGAAACCCCAACAGGGTCTATTGTAATGTATATAAACCTTTTTGTAATGGATATATACATGTGGTACTATTCTCCTCATCCTG CTCCATCGAAAAATCCTCATACGAAGAGTTAGGAAAGCAAAGAAAAACAACAAAAAC
YLR142W	PUT1	AGACACAATGCGAAAAATCGCGCAGGGACATAATTTTTGTTTTTTCATTATTTCTTTCGCTTATCCCTCCGTTAGCTCCACCCTTTTTTGA TTGGAATTTCTTTTCGCAATGGCTTTCCGGTTACCACGCCTCGGGTTTCGATCCCGAAAAAGCATATCTACACAAGAAAAATGAATGA TAAACAATGATGAGTGGCGCTATTTCCCTTATCATCTCATTATTGACTTAGTATCGTCTATTATCAGGAGAATCGCATGAACAAAGC CCATTTTCTCACCTTCTGCCTTTTATATAAAGCTTGTGGAAACCGAACACAACTCCACAAGTCCGTAGCAGCTTCTCTTTTTGT CTTTTATATATCAAAACATCGCTACATAGTAATAACACTAACGCACGTAGAA
YGR043C	NQM1	AGGGGTAGCGGCTTTTTCATCAACTCGATTATACCCTTTAGAGACCTTCCCTAAAGTGAAGCGCAATTTTCCGGATGTTAGTAGGG TAATATGGTTACGGATTGTGACACAAAAAGGGCTTTCAACAGCTCGGTCGGGTTGAAGGATTTTCCAGGATGACGAAGCTTTCAATAAG AGGGACTGGACTGTTAACCGCGGGAATTAAGTTACTTTCCCTGATCTGGCTCTGGCTCTGCTGATTTTGGCTCTGTACTCCT CGGACTTCTGACTTGAACGAATACGCTTTTTGCTCTCTCTTCCATAGTAGGGGCAATGAGGGGAGCATAGTGGATCCT TCTAACCATCTAGAATGGGGTGACACATATAAAGAAAGAGCACTTTCGAGCGCAGTCAATTTATGCTAAGTATATCATTATTTCTT GCTAGCGTAAGTCATAAAAAATAGGAAATAATACATATATACAAGAAATTAAT
YML042W	CAT2	TCCGAAGAGCGTGCTACCAATTTCTCATCTCGTTAACAACTGGTTCCGTTAAAAATTTGCTATATGCTCTATAAGCCAACCTCTATC TATATCTTTTTCTTTAGTCCCTACTTTGGTACTGTTACCACCATTTTAGATTGCTTTTTCTTTTGGCCCTAGCCTTACAATATTTGGCAAA CTTTTTTTTTTAGCCCGGAGACTCTTGTATCTATGCGCGGGCAAGGGCAAAATGACTGCTTATCCCGCCATCCTCCCGCCG CAAGGTTTGAATGGGATTAAGTAAAAACGAATGACTATTCCTCAAAGTCACTTTGTCGACAAAAAAGAAATGAATATACATA TTGGAACAATTTATCCTCTTTTCCCATTTTCGCATATAAGAGCAACTAAACCGCGGTGAGTAAAGTCCCTTCCCTACAGACTCTTT ACTCAGGTATATATATATATATATCCCTTAAAAAATCAAAGAAAGCACTC
YJR095W	SFC1	AGCCTAGTCCCGTAAACCGCAACGGACCTTAATTTGACGAAGGGCCCAATTTGATGGTGGGTTAATGATTAGTCCCTATTG TCATAAATAAGTGTGATGATGGAGGAATGATGATACCGTAGTACTACTGCTCGAGGTGCTATCTTTTAAACCAATCCTTTGAGATT TTGTCGCCACGGAGTACTACCTTTTACAACCGTAATGTACATTTTGCATATATCTTATGTATAAATATATAGTTCACTTACTACTTGT TCTCGTTTTGTAACCTTCTGTTGTAGTTCTTCTGTTCTGGCGTTTCCCTTTGTTTTCTATCTGCTTATAAGTAAAGTGAACAG ATTTTGGAAAGTATTATCAATTTGAGTCAATGAAAGAACTTGGCATCTCCCTATTACTAAAACTAAGAATCTTGATTTCAAGAAAGAA TTATATTAGTTTTAGCCGTAAGATAACATAACAAAGAAAGAAAGAAAA
YKL217W	JEN1	TCGATCAGCTCCAAATTAATGAAGACTATTGCGCGTACCCTTCCAGATGGGTGCGAAAGTCAAGTATGATGAGGAAAGTTATTGAGCGC CGGCTTGAACATTTTCCCATCTCAGAGCCGCAAGCCTACCATTATTCTCCACCGAAAGTTAGTTTGAAGCTTCTGCACACCATC CGGACGTCATAATTTCTCACTTAACGGTCTTTTCCCGCCCTTCTACTATAATGCATTAGAACGTTACCTGGTCAATTTGATGGAGAT CTAAGTAACACTTACTATCTCCTATGTTACTATCCTTTACCAAAAAAAAAAAAAAAAAAAAAAAAAAATCAGCAAGTGAAGTACC CTCTGATGTATAAATACATTGCACATCTTTGAGAAATAGTTTTGGAAGTTGTCTAGTCCCTTCCCTTAGATCTAAAAGAAAGAA AGTAACAGTTTCAAAGTTTTTCCCTCAAAGAGATTAAATACTGCTACTGAAAAAT
YMR175W	SIP18	ACATAGTACTGTACGATTACTGTACGATTAATCTATCCACTTCAGATGTTCAACAATTCCTTTTGGCATTACGTATTAATACTTCATAGGA TCGGCACCCCTCCCTTAAAGCCTCCCTAAATGCTTTGCGTACCCTTTAAGACAATATCTTAACTCTGTATTTACTTGCATGTTAC GTTGAGTCTCATTGGAGTTTGCATCATATGTTTAGTTTTTGGAAACGTTGGAGGCTCATAGTATTGGTAAATGGGAGTTACGAA TAAACGTATCTTAAAGGGAGCGGTATGTAATAAGGATAGATGATGATGAATACAGTACGAGGTGAAGAATGATGGGACTGAGAGGG CAATTATCCTCCCTCAGAATCAACATCAAAACATATATAAAGCTCCCAATTCGCCCAAAAGTTTTGTCCTAGGCATTTTTAATCTTT GTATCTGTGCTCTTACTTTAGTAGAAAGGTATATAAAAAAGTATAGTCAAG
YNR002C	ATO2	AAGTCTTGACTACCCTATCTCACACTAGTACGTAATCAATGTATCATTGTTAGTATGATAGTAGAGACCAATACAGGAAAGCT GACCTTCCCTTCCAATCACCACGGCTGAAATGCTTTGTTGACCAATACGGAGCGTTAAGAGCGGACCGGCTGGAACGGCTCCATC TAAATCGCGGAGGAGGAACCTCCGATACCAGCCGACATGGCAATAATAGTACAGTATGATGCTACAGCCCGCAATAATTTACAG TAGATCATCAACAGTCTCCTCATTCTGGAATGATCAGCAACTTCGACGGATTTAACTCTCAAGCAGTTACGCACTCCGAGAACAGCC GTGATCATCTTTGAACAAGCAAAATATAAAGCAGGAGAACTGCTCCTACCTAGAGTGAATAGCCATAAATAACTATGTAACATTCTA CAGATCAATCAAAACAATCTTCAATCACAGAAAAAATAAAGGC
YPL201C	YIG1	TTTTCTAGTTCTTCTGCAATATTGCTTTTTGGGAAGAAGGATCGAAAGTACGATTTGCAGACACGTTTTTACTATATTTACTGTATC TTGATTGCGCGGCTAAAGTTGCCATATTATTTATATTGACGCTCAACCCCGCATTTCGGAGTTTTCTTTTTTTTTTTTGGGGTAA TTTTGGAGTTCGGCGCTATTGGTGGCCGGAATGGTGACACACTTGTAAATATAAAGGAGGAAATCCTACATGTGTATAAGCGAAAT CACAAGGATAAATGATTGCTAAACACCCTCAAGAAAGAAAAATATCAATCAACGAAATC
YDR256C	CTA1	AGCGGTTGTTCTAACCACTATTTAAAGCCGCAATTAGTAAATGCAAAAAAGTTGGCCGGAATTTAGCCGCGCAAGTTGGTGGGGTCCCTTA ATCCGAAAAAGGACGGCTTAAACAAATATAAATCCGAAAAATCCCAAGTACAGAGAATGGAGAAACAACAGTTTTGATATCGCCAT ACATATAAAGAGATGTAGAAAGCATTCTTCACTGTAATGTTCCAAATCGTACATTTGAATTTCTTGTAGGTTTTTAAAGAGTAAAGTAAA TAAATATAAGTACTTACAATAAATTTGAAACCCCTAGAAG
YLR377C	FBP1	CGGATGGAATCGCCGCTTTTGAATTCACCTCCGGGTATTATTATTCTTAGTAGTCCGGCTCGTGGGACACCCGGAGTTATGCG GGCCCGAAAGCTCATTATGTAGTAAAGCTAGGTAATGTTAAGGGCCTAAGAGCCAAAGCAGCAATAGCCGTGATTTCCACAT ATCAAGAAAGCTTAAAGTTGAGACAGGGAATTTGAAGCGAAGATTGCCGAAGTGGCAATACCCACTCTTTTTTTGGTTGCT TGGTTTTCTCTGCTGCTTGGCAACTTGTGGCATCTCCCACTATATTATAAGGATCGTCTATGTATAGGCAATATTATCCATTT ACTCGTAAACAATGTACGTATATATGAGAGCAACAGTGTGCAATACAGACGTTGATTTTGTCTTGTCTTTTGTATGATA GGCCTAAGAATAACAGTGGCAACATATAAAGAACATCCCTCATACCCACACAT
YPR006C	ICL2	AATTTTTATTTCTCCTTCCATATGAGCGACAGCGGTTACTAGCCGCTGTCTCAGGTTAATGATCCAAGTCCGAGATCCGGCCGAAT ATGCTTGGCGGGAAGAAATAAAGTGCATTGGAGAGAAAGGATATGCTCTTCAATTAAGAGCCGCAAACTAACATCATGCTA GCGATATCATACGTACACTATATAAATAAGGCTTAAAGAAATGCTTCTTATTTCTTAACTTTTTTGGCGGTTGAAGAGCTTATA AAAGTACTAGTGGCCTAAGAAGCTACAGCGCCGATAAATAATCGATTTCGACTTTTCTAGTATTTCCGCG
YAL054C	ACS1	TGTGCACATACGTCAGAAATGATATCAAGATAAATGGCACGCTGATGACGGCTGTGAAATATGATAATCATCTCGGACGAACGGCG TAGCACTCTCCATCCCTAAAAATGTTACGTGTGACTGCTCATTTCGCGGATGTCGAGATGACCCCGCCCTCAAAGGCACTC ACCTGTTGACATGCCGTGGCAAAATGATGGGGTCACTTTTTTTCTGTTATCTTAAAGTCCAAAGAAAGTAAAAAAGGTTGG GGTACGAATTCGCCCGGAGCCTCGGATGCAATTAATCAATGGGATTTGCAAGTGGGGTACAGTTCCTCGGTGGCAAAATAGTTCCCT CTTTTTGTATATAAAGTGGCGCTATTCTAAGCATTTCTCCCTTAGTTATCTGGTAGTACGTTATATCTTGTCTTATATTTCTA TCTATAAGCAAAACCAACATATCAAACTACTAGAAGACATTTGCCACTGTGCT

YPR002W	PDH1	AATATAAATAAAATTCATACAGCATGTCTAATCATAGCTAATTTATACATATTCATCATGAAAAACATATAGGGGAAAAATATGGTCGGTTA ACACACCTATCAAAAAATTTACAGCAATTCGAATCTCGTTAGTAAAAATATCTTATTTTTTTTTTTCTGATTGATTTATTTCTGG AGTTTTGACTTATTTTTTACACATCGCGCTTTTCGTCCCAATCTCTCTGATATATGATGCTGTCTATAGGTAGCCACTCCCGGATG TCGGACCTCGGGCCGTTTACAACTTTATGAGATGACCTTATTTCTCCACATTTAGTCATTCAACTTTTACCCCTCATATGTTACCTT CACTAATGTAAAGCATGACCAAGAAAGGTATAAGGTATAAATCTGCCATAATGTATGTATAAATTATTAGGACTTTCTCAAATAG TATTTTTGGTATTTTCTACTGTTCTGTGATGTCGAGAACAAACAGA
YBR050C	REG2	AAGTACGATATGGTATAACTGTAACTTGAAGGACTGAAGGACTGAAGGACTGAAGGACTATAGTCAAGGGCCAATGGGGAAGGTC CTTCCAGGCCATTTGCCCGATAGTTTGTCTTCTCTTCTTTCCGACGGCCCGATTGCATGTGGCGGGGACGACTGGATAAAAAA CGTGGGGGAGTATTAATTTTACGCTTATTTGTCAACACGGAACCTTATAGTTATCATTACTAACATCGCAACAAAGCTGCTTTT TACTCGTTTTAGCCACACCATACCCCTTTAATTAACATAAATGCATAAAATAGTTATTTGCTTCTGAGTTGACGCTTCTCTCGGAC GTACTGTTATATGGCATGTCTTCCGATGCTTCAAAATTTAGCGTTGTCTCGAAACTTAGGCTGTCTTCTGCTGTCTGCTTCTGA TAAAAATAATATTGGAAATAGAAAAAATAAGGAACAAGAAAGTGTGTGAGA
YPR001W	CIT3	ATATTATTCAGTTGAAAGACAAAAACATAAATTTCTATGAGCAACAATTTGAACGAAAAATAAAATTTGGGGAAGTGACACCA TGGTAGCGGTTCTAAAGCGAAATCGGCAAGCGGCTAAATAGCAGTTTTGATGACTTACTCCACTGAAAAATGGATGACCTTAAATA GGAGATAAAGCTTTTTCATCCCTATGATTTAAGTAGCTGGCTTGTCAAGCATTCTAATCATAAAAAAGATCGTATTTGATCAAGAA TTTATACATAGACGGCGCTAAATAATTGAATACAAA
YOR100C	CRC1	CTCGTTTGGCGTTACATTGCATTGATGGTACAATAAAGGGCATGCTTTATATCGAGATGTTTCAGTGTATATGAGGGGAAACAGAAAA CGTATTCTGCCATTTTTTGGTCACTGCTTTTTCTGCTATGAGTAATGGTGAAGTTCCCTGTGGGCAACGCTTATGCTATCGGGTTA CTGCTCCTAATATCCGCATATAAGCTTTATGCAGGGATCAGTTGGCGGCTATTTTCTACACCCAGTCATCCGGCGTACTGGATCT CCACTTGGCCCAATAAGTCGGTGGCAAAATGGAGATTTAAGAGTAAAGATGCATGATGGTATAAATCTTCTTAGTCGAAATAGATATAT TCAAGCGCATATATAGGACAGCCTGTACTGTGAAATAGCCGATTTCAATTCGCTCTATGTGTGTTTTTATCCAGGTTTTCTTTG GATTCTACGTATTGTACGACTTTCTTATCTCCACAACGTCATCGTGTGAGT
YIL057C	RGI2	CCCAACAGATTTCAAGTCTGTGCGCTTAACTACTCGGCATAGTGCCTAAAAAATGTAGGTTATTTAAGCAAGTATTGTAGATACTTTT CGTAATAAACTACAATGCACCCAGACTCGCGGTGAATGATGGCATGAAATCATTGAACGAAGTTTTGCGGCTATACGGCTGAAGGA CGAGACTAAAGGGACAGGAATTTAATCGGGGTATAATTTGAATAGTATTACGGGCACTGCCGTTTAGCCATCAAAATGCTATTGTT GGGGTATTCTCTACTTTTTTGTCTTGGCTTGAACCTTTTCCGGCGTTGGCAATCGTCCGATATAAAGCATCGGCTGTCCAAATCCTC TATTGCCTTTTCCCTTGCACCTCTTCAATTTCTGTATCTTTCCGCTAAAGGTAGATCTTGATTCACCTATCTGTGCAAAACAGAT TAAGTGCAACGAAACAACGTACAGTATATAACAAGTATTTTAAATAAATAAGA
YLR312C	QNQ1	CATCAATTAGGGCAAACTTGAATAGTCAAGTGGTGCATATATTTAAATCAATTAGCCCTATGACTACATTAGGTTTTATTGTTAGGTCCTT ACGGCTGCATATTTGCTTTTCGCGCTTTCGCGGGTCTCGCAGCATTTCGCGCGCTTGTATGGGTGGAGTTTATCTGCTTACCCCT CCGGACCCCTACCCCGGTGTGCCCGGTCATCTATCCATTTTGGGTAACCCCTTTCGCGGACAGCTGCTTATCAAGGTACCTG GATCGAGCCATAAAATGATCTACACAGATGAGATGGGCGATTGGGATATATTATTAGTCGGAGTATCATTATAGTTATTCAGTTTTAT GCAGGTTACTGGCCAAACGTTTTTCTTCAATTTGGAAATCGTTTAGGAGCTACTGTTCCGGTATAAAGTAACAACGACAGTAGCAGAG TAATACGACGTGACGATAATAGAGACTAGTAAACAGTCGAGTTGTGCGGACCTAAA
YOR348C	PUT4	GCTATGACGTTTTGGGTGGCCTAGCCGTTTCGCGTGTGCGCTGCTGCTTTTTCGCTTTTCAACTTGTGCCGATATTTCTATCAAAGG AAAAATGGGACGTTTTCAACCCCTCGCTATCATCTGCGCTGCACTCTGCTATCGCAACTACACCGGGTTTTTATCTGCTTACCCCT CCATCCAGTGTGATAACAAGAAGAACCTTGCAGGGTAGGGCAGGACCTACGGCCAAATACTAATATGTCTGTTTATGTACATGCC CCAATCTGAATATTCATGAATGTAGGCACAGCATATCTCCATCCATGACTGATACAGACGATAAACAATATATGTATATACATCTTA TACACTCGAATATTTGTAGACTGTACTTCTATATATATAGGGGGTTTTGTGTTCTCTTCTTCTTTTTTCTCTCTTCCCTTTC CAGTTTTCTTTATCTTTGCTGTTTTGGAAGAACACACCATCAATGAATAAATC
YJL116C	NCA3	TAGATGCGCCATCTCCGAGAAAAATCTAGACAATAACAGCGACAATTAACCTAAAGAGGATAGAAGATCGAGCAAAAAATTTTTTTA ATATGGGTCAGTGGCGATATTACTATAGGAGTTAAAGAGTAAGTTGAGTGAAGGTGGTGAATATGAACTCCGAACTAA GCGCCGATTATGGGTGGCAAGCGGACAGCTTTTGTATATAATCGATCGCTCTCGTAGTTGATATCTCTCTCTTCTTCTTTTCC TGATATAGTATATGTGTACATACAGATACGAATATACCTCAGTTAGTTGTTTTAACATTAATAATCAACAGTTGCCAGTAGCAAAAA AATATATCCATTCATTTCGAGCTTTTTCTGCTCTACTACTGATATCAACAAGCCCTTTATTGATTTTGAATAATTTTTGTATACGTGTTCTAGC TATAACTAGTATAGTCGCACATACTTAACTCGTCTCTCTAACACATA
YDR536W	STL1	CTACGTCGCTGTTTCGAGCGGCTGTTGCTGTCATGAACTAAAAAAGCGGAAAGTGTCCAGCCATCCACTACGTGAGAAAGAAAT AATGGTTGTACACTGTTTCTCGCTATATACCGTTTTTGGTTGGTAACTTCTCGCCAGGTGCAGTTATGCGCTTGGCTGCTCGGAT AGTAGTAATCTGAGAAAGTGCAGATCCCGTAAGGGAACACTTTTGGTTACCTTTGATAGGGCTTTTATTGGGGCATTGTAACAA AAAGGAAGTAGATAGAGAAATGAGAAAGCTTAAAGTGAATGTTTTAGCTTCAATTTTTCGCCCTTCAACCGCTGCTTGGCCTTAGAGGG TCAGAAATGCAGTTCAGGAGTGCACACTCATAGTATATAACAAGCCCTTTATTGATTTTGAATAATTTTTGTATACGTGTTCTAGC ATACAAGTTAGAATAAATAAAAAATAGAAAAATAGAAATAGAAAGTTTATAGACC
YNL270C	ALP1	GAGCTATAGTCTTTTTGCGCTTTCAATACGTGTAGCGGTGACCAAAAGTTGCACAAAAATGTAGTTGTCAATGAAAGCGCACTACGTAT ATAATGACTATTTTTTTTTCTGCGTTGCATGGGTAATTTGTTAATATGCGATTTTCTTGGGAAAAAGGTGCATAGCGCCAAAG ACTGCCGTGCGGCACAGTATGATGTTTTGAGTCCGCGGCTTTAAGGGCTTGCATAAAAAGTGGTTCAAGCGAGTGATAAGTTGG CGCAATGTCGCTTTTTTGTAAACATGCTTTTCTGAAAACAACCTGTAGGACGCTCCACTCCACATAAGGGCTTTCTCCAATGGCAAT GGAGCTCGGAACACCGGAGTAGAAAAATTTAATGTGTATTGTATAAAACTTGTCTTGTATGCAAGTTTTGTTTTTTTGTACTCTTC CGTAGCACAATAGACATATATTAGCGGCAAAATGTAGTGTGCGATTATTGCC
YDL085W	NDE2	GTGTAGTATTGATCTTTGTTGTTATGTAGAAATGCTTACGCAACTGTATAAAATATGGAACAGTTGCCATGGCAAGACAAAAAAG TGATCTTGAGTGAATAATAGAGCCCGGATGGCCGGTAAATTAACCGCTCGTACCCTTTAATACGCATAAACGCCGAAAAATGTC TCTATTTTGTGATTTCCCGAGGTGCGGATTTGGGTACACCTGTATGCGTTCCTTAGTGCCGATAGATATACTAATATCGATGCGTCA CAGTAGCAGATCATCTGACACTGTTTTCCCATTTTTTTTTTCAATTTTTTAAAGGGTTCTCTACAGCCTACAGGCTCCCTAATAA GTCAGCCCTCCCTTTGGAGTGCCTGTTGACCTGCTATATAAGAGGTATATCAGTGCCAGTAGGTAACCCATCTTGGGGGATTG TACCAGGAACATAGTAGAAAGACAAAAACAACCCGCTTTGCCATTGATAG
<i>S. bayanus ADH2</i>		GATCCAGTTCTCCAGTGACACAGCCTTTATCTGGTCAAACTTTCTTTCTAATCACCTATGCTGATGCTTAATTAAGGGATTTTTGTCTC CATCAACGGCATGCGCCAAAAATGACGTTTTTTTTTAAACCATAGACACGAACTACCCATTTTCCACCGGCTGACCTACCACCGGA ACAAACGGCCATCCAACTTGCAGTTGGGAAATTAAGAGCATCGCAGTTTAAATGGAAAGAAAAAAGGTACAGCACAGCCGAA ATGGAGTTAGTCCCTTATGTGCACACACTCACACAGTCCGTCAGATCAAGCTACTGGGTGCGTATAAATAGAGTGGCCATTGCCA CCCTGTTTATCTCAAAATCTGCTTGTAGTGGTCTTCTCCCTTTTTCAGGTTACAATTTCTTTGTTTCTACTTATAGTATAAGTATATCAA GCTATATTAAGCATACTACTCACTGTCAACTTATCTCCAAATACAAATACAAA
<i>S. castellii ADH2</i>		TGTCGTGGACGAAATACGCCACAATTTGCCGAGAAGGTCATTAGTATGTCCAAAGAACCCCTAGGTTGAAAGTCGGGAAATCCGAAATC TCCGATTTTGGAGGGGCCATGCCCTACTTTTTTTCGCGAGGGGTGAAATTTCAAACCCGTCGCGGTTCTTGGAAATTTGACAGCGCAT TGAGTATGTCTGCGTATTTCCCACTATCATACCGCCCTTTTCTGGGAAAAATGGAACCTGGATGCTGAAATATTTCACTCTCAGATC ACATATCCCAATCTCTGAGTGAATTTTGGTTCAGGCGACCAACAGGAATATGGAATAGATTCTATTCTCGGATTTCACAATATC CATTGTAGCAAAACAAAAAAGCTGGTGTATATATTCAGAGCCTAAAAATTAAGGTTGGATCTCAATTTTAAAGTTTTTCATTCTG TTTTGTTTTTGTCTTCTTAGCTACGAAATACCAAAACAAAAACAATCAATA

<p><i>S. kudriavzevii</i> ADH2</p>	<p>CTCTCAAATCTTTTAGCGCCAAGGACTCCAACATAATTGTATCTTGAATTTGCCTTTACGATCCGTTTGTCCAGTCACGGCATGTATATCT TATTAATCCTGCCTTTCTAATCACGTATTCTAATGTTCAATTAAGGGATTTTATCTTCATCAACGGCTCCCACGCAAAAAATGACGTTTTG CACACAGACACGAAATACACCTTCCACCGGAACAACGGCCATCTCCAACCTATAAGTTGGGGAAATAAGACAATTTAGACTTCAGAG AATGAAAAAAAAAAGGTACATCACAGATGGGGTTCAGGTTTGTACAATTGCAGGGAGCCTGTCACATATAAATAGACCTCCAGTG ATGATATCTTTCAGTCTTCAAACGTCTCTTGTACAGTTCTGGTCTATATCACATCTCTTGGTTCTACTTATTGTCTATAATATC AAGCTACAGCAAGCATAACAATCAACTATCTACCATAACCATAATACACA</p>
<p><i>S. mikitae</i> ADH2</p>	<p>TTTCCCAAAAAGTATTATTTTAAAGTGATAATTGATAAAAGGGGCAAAACGTAGACGCAAATAAAACGAAATAATGATTCTCAGACCTT TTAGCGTCAAGAAGTCAACTAATCTTATCTTAAATTTATCTTTATAATCCGTTTCTCCCGTCACAGTCTGTGTATCTGATTAATCCTGCC TTTCTAATCACCTATTCTAATGTTCAATTAAGGGATTTTGTCTTACCAACGGCTTCCACCCAAAAGTAAAAATGACGTTGTACCCACA GACATCTTACCAGCCTGACCTGCCACCGGAACAACGGCCATCTCCAACCTATAAATGGAGAAATAAGAGAATTTAGATTCTGGAG GATGAAAAAAAAAAGGTACAGCATAAATGGGGTTTTATGTGGGTACAATTACACTAGGACTATCACATATAAATAGACGGGCAATGTA GGTTCTTTTCCACCCTTGAGACAGAGTTATTC</p>
<p><i>S. paradoxus</i> ADH2</p>	<p>TAGTCTTATCTAAAAATTTGCCTTTATAGTCCGTCTCCAGTCACGGCCTGTGTAACCTGATTAATCCTGCCTTTCTAATCACCTTCTAC TGTTAATTAAGGGATTTTGTCTTTCATCAACGGCTTCCGCCAAAAAAGTATGACGTTTTGCCCGCAGGCGTGAAGCTGCCCATCTT CACGGGCTGACCTCCTCTGCCGGAACACCGCCATCTCCAACCTATAAATGGAGAAATAAGAGAATTTAGATTTTCAGAGGATGA AAAAAAAAAGGTAGAGACATAAAAAATGGGGTTCACTTTTTGGCAAAGTTACAGTATGCTTATTACATATAAATAGAGTGCCGATAATG GCTTTTTTTCATCTTCGAAATACGCTTGTACTGCTCTTCCAGCGTTTTTATTACTTCTTTCTTCTTCTCCTTAGTATATAAATATCAAG CTACAACAAGCATAACAATCAACTGTCAATTATATAAATACACT</p>

**table S4. Background strains used throughout this study.**

Strain	Parent	Genotype	Reference
BY4741	S288C	MATa his3Δ1 leu2Δ0 met15Δ0 ura3Δ0	(38)
BY4743	S288C	MATa/α his3Δ1/his3Δ1 leu2Δ0/leu2Δ0 LYS2/lys2Δ0 met15Δ0/MET15 ura3Δ0/ura3Δ0	(38)
BJ5464		MATα ura3-52 trp1 leu2-Δ1 his3-Δ200 pep4::HIS3 prb1-Δ1.6R can1 GAL	(43)
BY4743ΔDNL4	S288C	MATa/Matα dnl4Δ/dnl4Δ	(73)
Y800		MATa ade2-1 leu2-Δ98 ura3-52 lys2-801 trp1-1 his3-Δ200 [cir0]	(51)
DHY213	BY4741	MATa his3Δ1 leu2Δ0 ura3Δ0 met15Δ0 SAL1+ HAP1+ CAT5(91M) MIP1(661T) MKT1(30G) RME1(INS-308A) TAO3(1493Q)	This study
JHY693	DHY213	MATa his3Δ1 leu2Δ0 ura3Δ0 met15Δ0 SAL1+ HAP1+ CAT5(91M) MIP1(661T) MKT1(30G) RME1(INS-308A) TAO3(1493Q) prb1Δ pep4Δ	This study
JHY651	DHY213	MATα his3Δ1 leu2Δ0 ura3Δ0 SAL1+ HAP1+ CAT5(91M) MIP1(661T) MKT1(30G) RME1(INS-308A) TAO3(1493Q)prb1Δ pep4Δ lys2Δ0	This study
JHY692	DHY213	MATa his3Δ1 leu2Δ0 ura3Δ0 met15Δ0 SAL1+ HAP1+ CAT5(91M) MIP1(661T) MKT1(30G) RME1(INS-308A) TAO3(1493Q) prb1Δ pep4Δ ADH2p-npgA-ACS1t	This study
JHY705	DHY213	MATα his3Δ1 leu2Δ0 ura3Δ0 SAL1+ HAP1+ CAT5(91M) MIP1(661T) MKT1(30G) RME1(INS-308A) TAO3(1493Q) prb1Δ pep4Δ ADH2p-CPR-ACS1t lys2Δ0	This study
JHY686	DHY213	MATα his3Δ1 leu2Δ0 ura3Δ0 SAL1+ HAP1+ CAT5(91M) MIP1(661T) MKT1(30G) RME1(INS-308A) TAO3(1493Q) prb1Δ pep4Δ ADH2p-npgA-ACS1t lys2Δ0	This study
JHY702	DHY213	MATa/MATα his3Δ1/his3Δ1 leu2Δ0/leu2Δ0 ura3Δ0/ura3Δ0 SAL1+/SAL1+ HAP1+/HAP1+ CAT5(91M)/CAT5(91M) MIP1(661T)/MIP1(661T) MKT1(30G)/MKT1(30G) RME1(INS- 308A)/RME1(INS-308A) TAO3(1493Q)/TAO3(1493Q) prb1Δ/prb1Δ pep4Δ/pep4Δ ADH2p-npgA-ACS1t/ADH2p- CPR-ACS1t met15Δ0/+ lys2Δ0/+	This study

**table S5. Features integrated for the determination of sesquiterpenoid titer in Fig. 2B.**

M/Z	Formula	Ion
203.1794	C <sub>15</sub> H <sub>22</sub> + H <sup>+</sup>	SQ - H <sub>2</sub>
205.195	C <sub>15</sub> H <sub>24</sub> + H <sup>+</sup>	SQ
221.1899	C <sub>15</sub> H <sub>24</sub> O + H <sup>+</sup>	SQ + O
227.1776	C <sub>15</sub> H <sub>24</sub> + Na <sup>+</sup>	SQ
237.1848	C <sub>15</sub> H <sub>24</sub> O <sub>2</sub> + H <sup>+</sup>	SQ + 2O
239.2005	C <sub>15</sub> H <sub>26</sub> O <sub>2</sub> + H <sup>+</sup>	SQ + H <sub>2</sub> O + O
241.2161	C <sub>15</sub> H <sub>28</sub> O <sub>2</sub> + H <sup>+</sup>	SQ + 2H <sub>2</sub> O
243.1725	C <sub>15</sub> H <sub>24</sub> O + Na <sup>+</sup>	SQ + O
259.1674	C <sub>15</sub> H <sub>24</sub> O <sub>2</sub> + Na <sup>+</sup>	SQ + 2O
261.183	C <sub>15</sub> H <sub>26</sub> O <sub>2</sub> + Na <sup>+</sup>	SQ + H <sub>2</sub> O + O

**SQ = Sesquiterpene (C<sub>15</sub>H<sub>24</sub>)**

**table S6. Order of promoters and terminators used in the expression of all cryptic fungal BGCs examined in this study.**

Gene order	Promoter	Terminator
1	P <sub>ADH2-S. cerevisiae</sub>	T <sub>ADH2</sub>
2	P <sub>ADH2-S. bayanus</sub>	T <sub>PGI1</sub>
3	P <sub>PCK1</sub>	T <sub>ENO2</sub>
4	P <sub>MLS1</sub>	T <sub>TDH2</sub>
5	P <sub>ADH2-S. paradoxus</sub>	T <sub>ADH1</sub>
6	P <sub>ADH2-S. kudriavzevii</sub>	T <sub>CYC1</sub>
7	P <sub>ICL1</sub>	T <sub>TEF1</sub>
Last	-	T <sub>TEF1</sub>



**table S7. Standard part plasmids and expression vectors used for the assembly of cryptic BGCS in this study.**

Plasmid	Insert	Yeast Marker	Description
pCH900	T <sub>ADH2</sub> -P <sub>ADH2</sub> - <i>S. bayanus</i>	None	Template for amplification of terminator one fused to promoter two.
pCH901	T <sub>PGI1</sub> -P <sub>PCK1</sub>	None	Template for amplification of terminator two fused to promoter three.
pCH902	T <sub>ENO2</sub> -P <sub>MLS1</sub>	None	Template for amplification of terminator three fused to promoter four.
pCH903	T <sub>TDH2</sub> -P <sub>ADH2</sub> - <i>S. paradoxus</i>	None	Template for amplification of terminator four fused to promoter five.
pCH904	T <sub>ADH1</sub> -P <sub>ADH2</sub> - <i>S. kudriavzevii</i>	None	Template for amplification of terminator five fused to promoter six.
pCH905	T <sub>CYC1</sub> -P <sub>ICL1</sub>	None	Template for amplification of terminator six fused to promoter seven.
pCH906	T <sub>PGI1</sub> -Ura3-P <sub>PCK1</sub>	None	Template for amplification of terminator two fused to the Ura3 cassette and promoter three.
pCH907	T <sub>PGI1</sub> -His3-P <sub>PCK1</sub>	None	Template for amplification of terminator two fused to the His3 cassette and promoter three.
pCHINT2A	L3-P <sub>ADH2</sub> -flag-MCS-T <sub>TEF1</sub> -L4	None	Cloning vectors generated for this study for assembly of >3 genes. Yeast selectable marker must be included on an assembly fragment
pCHINT3A	L5-P <sub>ADH2</sub> -flag-MCS-T <sub>TEF1</sub> -L6	None	
pCHINT2LA	L3-Leu2-P <sub>ADH2</sub> -flag-MCS-T <sub>TEF1</sub> -L4	Leu2	Cloning vectors generated for this study for assembly of 1-2 genes. Yeast selectable marker is included on the vector backbone
pCHINT3HA	L5-His3-PADH2-flag-MCS-TTEF1-L6	His3	

**table S8. Coordinates of native loci from which all clusters examined here were derived along with the IDs of plasmids expressing the engineered cluster versions.** Annotated Genbank files for all plasmids is included in the Supporting files.

Cluster	Native Locus				Engineered Cluster Plasmids		
	Genbank ID	Start	End	Length	Plasmid 1	Plasmid 2	Plasmid 3
PKS1	KV441552	530394	546723	16329	pCHCS100.1-2.2	pCHCS100.2-2.2	-
PKS2	KV441551	60641	83767	23126	pCHCS163.1-2.2	pCHCS163.2-2.2	-
PKS3	Deposition pending			9892	pCHAK200.1-2.2	pCHAK200.2-2.2	-
PKS4	AM270992	578654	603367	24713	pCHKU27.1-2.2	pCHKU27.2-2.2	-
PKS5	CP003009	8730831	8753560	22729	pCHKU28.1-2.2	pCHKU28.2-2.2	-
PKS6	ABDF02000052	9685	28459	18774	pCHKU30.1-2.2	pCHKU30.2-2.2	-
PKS7	JPJY01000093	2671	30026	27355	pCHKU31.1-2.2	pCHKU31.2-2.2	-
PKS8	JOWA01000110	1607857	1643205	35348	pCHKU32.1-2.2	pCHKU32.2-2.2	-
PKS9	KE384750	270098	292755	22657	pCHKU33.1-2.2	pCHKU33.2-2.2	-
PKS10	KB445572	91380	115199	23819	pCHKU34.1-2.2	pCHKU34.2-2.2	-
PKS11	JPKB01001000	12749	37136	24387	pCHKU35.1-2.2	pCHKU35.2-2.2	-
PKS12	JPJU01000852	23274	38823	15549	pCHKU36.1-2.2	pCHKU36.2-2.2	-
PKS13	JPJR01000396	848	19416	18568	pCHKU37.1-2.2	pCHKU37.2-2.2	-
PKS14	KN847553	300827	326489	25662	pCHKU38.1-2.2	pCHKU38.2-2.2	-
PKS15	AWSO01000045	179446	203577	24131	pCHKU39.1-2.2	pCHKU39.2-2.2	-
PKS16	JH687542	431482	465332	33850	pCHKU42.1-2.2	pCHKU42.2-2.2	pCHKU42.3-2.2
PKS17	KN839868	143119	188013	44894	pCHKU43.1-2.2	pCHKU43.2-2.2	pCHKU43.3-2.2
PKS18	DS989828	1389449	1407499	18050	pCHSU62.1-2.2	pCHSU62.2-2.2	pCHKU62.3-2.2
PKS19	KB908593	409171	443069	33898	pCHSU64.1-2.2	pCHSU64.2-2.2	-
PKS20	GL532685	4724	17845	13121	pCHSU65.1-2.2	pCHSU65.2-2.2	-
PKS21	AMGW01000002	1294251	1322017	27766	pCHSU67.1-2.2	pCHSU67.2-2.2	-
PKS22	DF933843	225991	254307	28316	pCHSU68.1-2.2	pCHSU68.2-2.2	-
PKS23	KE720645	48853	80314	31461	pCHSU70.1-2.2	pCHSU70.2-2.2	-
PKS24	DF933834	523551	558018	34467	pCHSU71.1-2.2	pCHSU71.2-2.2	-
PKS25	AWSO01000633	5071	30440	25369	pCHSU72.1-2.2	pCHSU72.2-2.2	-
PKS26	KN817529	130968	152240	21272	pCHSU73.1-2.2	pCHSU73.2-2.2	-
PKS27	KB445800	1362248	1403385	41137	pCHSU74.1-2.2	pCHSU74.2-2.2	-
PKS28	AWSO01000632	8804	37857	29053	pCHSU75.1-2.2	pCHSU75.2-2.2	-

TC1	ABDF02000086	384012	368868	15144	pCHTV86.1-2.2	pCHTV86.2-2.2	-
TC2	ABDF02000083	37740	49247	11507	pCHTV83.1-2.2	-	-
TC3	FQ790293	97750	131296	33546	pCHBFT4.1-2.2	pCHBFT4.2-2.2	-
TC4	JH717969	858521	869226	10705	pCHKU11.1-2.2	-	-
TC5	KI925459	2412992	2432365	19373	pCHKU12.1-2.2	pTC_KU12_trans	-
TC6	KB445798	581049	618823	37774	pCHKU13.1-2.2	-	-
TC7	JH719450	83620	114270	30650	pCHKU15.1-2.2	-	-
TC8	KL198014	1718438	1746540	28102	pCHKU16.1-2.2	-	-
TC9	GL377319	205808	212935	7127	pCHKU17.1-2.2	-	-
TC10	JH687394	99692	114281	14589	pCHKU19.1-2.2	-	-
TC11	JH687396	33983	48346	14363	pCHKU20.1-2.2	-	-
TC12	JH719415	280135	300470	20335	pCHKU21.1-2.2	-	-
TC13	JH795868	73132	97338	24206	pCHKU22.1-2.2	-	-

**table S9. Abbreviations for the functional gene annotations used in Figs. 2, 5, and 6.**

<b>Abbreviation</b>	<b>Domain Annotation</b>
A	Adenylation domain
a,b-h	a,b-hydrolase
ABC	ATP-binding cassette transporter
ACP	Acyl carrier protein
ADH	Alcohol dehydrogenase
AK-red	Aldo-keto reductase
AmOx	Aminooxidase
AmT	Aminotransferase
ArST	Arylsulfotransferase
AT	Acyltransferase domain
cMT	C-methyltransferase
Cyc	Terpene cyclase
DH	Dehydratase
DUF4246	Domain of unknown function 4246
FAD	Flavin adenine dinucleotide (FAD) binding protein
Fe-ADH	Iron dependent alcohol dehydrogenase
FMO	Flavin-dependent monooxygenase
GGPPS	Geranyl-geranyl pyrophosphate synthase
glycos.	Glycosidase
GMC	Glucose-methanol-choline oxidoreductase
Halo	Halogenase
HR-PKS	Highly reducing polyketide synthase
Hyp	Hypothetical protein
IAS	Indole-3-acetic acid-amido synthetase
KS	Ketosynthase domain
mBla	metallo-B-lactamase
MCP	Mitochondrial phosphate carrier protein
MFS	Major facilitator superfamily transporter
MH	Metallohydrolase
MT	Methyl transferase
NAD-DH	Nicotine adenine dinucleotide dependent dehydrogenase
NADP-R	Nicotine adenine dinucleotide phosphate (NADP) dependent reductase
nMT	N-methyltransferase
NR-PKS	Non reducing polyketide synthase
O-suc-SH	O-succinylhomoserine sulfhydrylase
oMT	O-methyltransferase
OxR	Oxidoreductase
p450	Cytochrome p450

Pep	Dipeptidyl peptidase
PrT	Prenyl transferase
PT	Product template domain
RibD	Riboflavin biosynthesis protein RibD
RNAh	RNA helicase
SAT	starter unit:ACP transacylase domain
SDH	Short-chain dehydrogenase
SDR	Short-chain dehydrogenase/reductase
SH	Serine hydrolase
ST	Sugar transport protein
T	Thiolation domain
TD	Terminal domain
TE	Thioesterase domain
TF	Transcription factor
UTC	UbiA-type terpene cyclase

**table S10. Strains expressing cryptic fungal BGCs analyzed here.**

Strain Number	Mating	Background	Cluster	Plasmid		
				1	2	3
106	-	JHY692	NC	pRS426	-	-
107	-	JHY705	NC	pCHINT2AL	-	-
108	-	JHY705	NC	pRS426	-	-
137	105 x 108	JHY702	NC	pRS426	pCHINT2AL	-
290	266 x 108	JHY702	DHZ	pCHDHZ-2.2	pRS426	-
304	-	JHY692	DHZ	pCHDHZ-2c	-	-
305	304 X 108	JHY702	DHZ	pCHDHZ-2c	pRS426	-
266	-	JHY692	DHZ	pCHDHZ-2.2	-	-
286	182 x 107	JHY702	IDT	pCHIDT-2.2	pCHINT2AL	-
287	183 x 107	JHY702	IDT	pCHIDT-2c	pCHINT2AL	-
95	-	JHY692	PKS01	pCHCS100.1-2.1	-	-
100	-	JHY705	PKS01	pCHCS100.2-2.1	-	-
132	95 x 100	JHY702	PKS01	pCHCS100.1-2.1	pCHCS100.2-2.1	-
96	-	JHY692	PKS02	pCHCS163.1-2.1	-	-
101	-	JHY705	PKS02	pCHCS163.2-2.1	-	-
133	96 x 101	JHY702	PKS02	pCHCS163.1-2.1	pCHCS163.2-2.1	-
97	-	JHY692	PKS03	pCHAK200.1-2.1	-	-
102	-	JHY705	PKS03	pCHAK200.2-2.1	-	-
134	97 x 102	JHY702	PKS03	pCHAK200.1-2.1	pCHAK200.2-2.1	-
124	-	JHY692	PKS04	pCHKU27.1-2.2	-	-
248	-	JHY705	PKS04	pCHKU27.2-2.2	-	-
255	124 x 248	JHY702	PKS04	pCHKU27.1-2.2	pCHKU27.2-2.2	-
117	-	JHY692	PKS05	pCHKU28.1-2.2	-	-
249	-	JHY705	PKS05	pCHKU28.2-2.2	-	-
256	117 x 249	JHY702	PKS05	pCHKU28.1-2.2	pCHKU28.2-2.2	-
118	-	JHY692	PKS06	pCHKU30.1-2.2	-	-
171	-	JHY705	PKS06	pCHKU30.2-2.2	-	-
178	118 x 171	JHY702	PKS06	pCHKU30.1-2.2	pCHKU30.2-2.2	-
110	-	JHY705	PKS07	pCHKU31.2-2.2	-	-
125	-	JHY692	PKS07	pCHKU31.1-2.2	-	-
163	110 x 125	JHY702	PKS07	pCHKU31.1-2.2	pCHKU31.2-2.2	-
111	-	JHY705	PKS08	pCHKU32.2-2.2	-	-
126	-	JHY692	PKS08	pCHKU32.1-2.2	-	-
164	111 x 126	JHY702	PKS08	pCHKU32.2-2.2	pCHKU32.2-2.2	-
112	-	JHY705	PKS09	pCHKU33.2-2.2	-	-

114	-	JHY692	PKS09	pCHKU33.1-2.2	-	-
165	112 x 114	JHY702	PKS09	pCHKU33.1-2.2	pCHKU33.2-2.2	-
242	-	JHY692	PKS10	pCHKU34.1-2.2	-	-
243	-	JHY705	PKS10	pCHKU34.2-2.2	-	-
246	242 x 243	JHY702	PKS10	pCHKU34.1-2.2	pCHKU34.2-2.2	-
115	-	JHY692	PKS11	pCHKU35.1-2.2	-	-
191	-	JHY705	PKS11	pCHKU35.2-2.2	-	-
205	191 x 115	JHY702	PKS11	pCHKU35.1-2.2	pCHKU35.2-2.2	-
113	-	JHY705	PKS12	pCHKU36.2-2.2	-	-
127	-	JHY692	PKS12	pCHKU36.1-2.2	-	-
166	113 x 117	JHY702	PKS12	pCHKU36.1-2.2	pCHKU36.2-2.2	-
128	-	JHY692	PKS13	pCHKU37.1-2.2	-	-
192	-	JHY705	PKS13	pCHKU37.2-2.2	-	-
206	192 x 128	JHY702	PKS13	pCHKU37.1-2.2	pCHKU37.2-2.2	-
167	-	JHY692	PKS14	pCHKU38.1-2.2	-	-
250	-	JHY705	PKS14	pCHKU38.2-2.2	-	-
257	167 x 250	JHY702	PKS14	pCHKU38.1-2.2	pCHKU38.2-2.2	-
228	-	JHY692	PKS15	pCHKU39.1-2.2	-	-
244	-	JHY705	PKS15	pCHKU39.2-2.2	-	-
247	244 x 228	JHY702	PKS15	pCHKU39.1-2.2	pCHKU39.2-2.2	-
122	-	JHY692	PKS16	pCHKU42.1-2.2	-	-
172	-	JHY705	PKS16	pCHKU42.2-2.2	-	-
177	172 x 122	JHY702	PKS16	pCHKU42.1-2.2	pCHKU42.2-2.2	pCHKU42.3-2.2
121	-	JHY705	PKS17	pCHKU43.2-2.2	-	-
168	-	JHY692	PKS17	pCHKU43.1-2.2	-	-
176	168 x 121	JHY702	PKS17	pCHKU43.1-2.2	pCHKU43.2-2.2	pCHKU43.3-2.2
185	-	JHY692	PKS18	pCHSU62.1-2.2	-	-
193	-	JHY705	PKS18	pCHSU62.2-2.2	-	-
207	193 x 185	JHY702	PKS18	pCHSU62.1-2.2	pCHSU62.2-2.2	-
158	-	JHY692	PKS19	pCHSU64.1-2.2	-	-
252	-	JHY705	PKS19	pCHSU64.2-2.2	-	-
259	158 x 252	JHY702	PKS19	pCHSU64.1-2.2	pCHSU64.2-2.2	-
187	-	JHY692	PKS20	pCHSU65.1-2.2	-	-
194	-	JHY705	PKS20	pCHSU65.2-2.2	-	-
208	194 x 187	JHY702	PKS20	pCHSU65.1-2.2	pCHSU65.2-2.2	-
188	-	JHY692	PKS21	pCHSU67.1-2.2	-	-
253	-	JHY705	PKS21	pCHSU67.2-2.2	-	-
260	188 x 253	JHY702	PKS21	pCHSU67.1-2.2	pCHSU67.2-2.2	-

189	-	JHY692	PKS22	pCHSU68.1-2.2	-	-
195	-	JHY705	PKS22	pCHSU68.2-2.2	-	-
209	195 x 189	JHY702	PKS22	pCHSU68.1-2.2	pCHSU68.2-2.2	-
173	-	JHY692	PKS23	pCHSU70.1-2.2	-	-
229	-	JHY705	PKS23	pCHSU70.2-2.2	-	-
241	173 x 229	JHY702	PKS23	pCHSU70.1-2.2	pCHSU70.2-2.2	-
174	-	JHY692	PKS24	pCHSU71.1-2.2	-	-
196	-	JHY705	PKS24	pCHSU71.2-2.2	-	-
210	196 x 174	JHY702	PKS24	pCHSU71.1-2.2	pCHSU71.2-2.2	-
160	-	JHY692	PKS25	pCHSU72.1-2.2	-	-
197	-	JHY705	PKS25	pCHSU72.2-2.2	-	-
211	197 x 160	JHY702	PKS25	pCHSU72.1-2.2	pCHSU72.2-2.2	-
175	-	JHY692	PKS26	pCHSU73.1-2.2	-	-
198	-	JHY705	PKS26	pCHSU73.2-2.2	-	-
212	198 x 175	JHY702	PKS26	pCHSU73.1-2.2	pCHSU73.2-2.2	-
162	-	JHY692	PKS27	pCHSU74.1-2.2	-	-
199	-	JHY705	PKS27	pCHSU74.2-2.2	-	-
213	199 x 162	JHY702	PKS27	pCHSU74.1-2.2	pCHSU74.2-2.2	-
230	-	JHY692	PKS28	pCHSU75.1-2.2	-	-
231	-	JHY705	PKS28	pCHSU75.2-2.2	-	-
240	231 x 230	JHY702	PKS28	pCHSU75.1-2.2	pCHSU75.2-2.2	-
226	-	JHY705	TC01	pCHTV86.1-2.2	-	-
278	-	JHY705	TC01	pCHTV86.1-1.0	-	-
280	-	JHY705	TC01	pCHTV86.1-2.1	-	-
282	-	JHY692	TC01	pCHTV86.2-1.0	-	-
283	-	JHY692	TC01	pCHTV86.2-2.1	-	-
292	280 x 283	JHY702	TC01	pCHTV86.1-2.1	pCHTV86.2-2.1	-
293	278 x 282	JHY702	TC01	pCHTV86.1-1.0	pCHTV86.2-1.0	-
227	-	JHY705	TC03	pCHBFT4.1-2.1	-	-
279	-	JHY705	TC03	pCHBFT4.1-1.0	-	-
281	-	JHY705	TC03	pCHBFT4.1-2.1	-	-
284	-	JHY692	TC03	pCHBFT4.2-2.1	-	-
288	106 x 279	JHY702	TC03	pCHBFT4.1-1.0	pRS426	-
289	106 x 281	JHY702	TC03	pCHBFT4.1-2.1	pRS426	-
291	281 x 284	JHY702	TC03	pCHBFT4.1-2.1	pCHBFT4.2-2.1	-
217	-	JHY705	TC04	pCHKU11.1-2.2	-	-
269	-	JHY705	TC05 Corrected	pCHKU12-2.2	pTC-KU12_Trans	-
218	-	JHY705	TC05 Deposited	pCHKU12-2.2	-	-



219	-	JHY705	TC06	pCHKU13.1-2.2	-	-
220	-	JHY705	TC07	pCHKU15.1-2.2	-	-
271	-	JHY705	TC08	pCHKU16.1-2.2	-	-
221	-	JHY705	TC09	pCHKU17-2.2	-	-
222	-	JHY705	TC10	pCHKU19-2.2	-	-
223	-	JHY705	TC11	pCHKU20-2.2	-	-
224	-	JHY705	TC12	pCHKU21-2.2	-	-
225	-	JHY705	TC13	pCHKU22.1-2.2	-	-

## Compound Characterization Data:

### LC-MS Data:

#### Strain 132 - PKS1 - *Corniothyrium sporulosum*

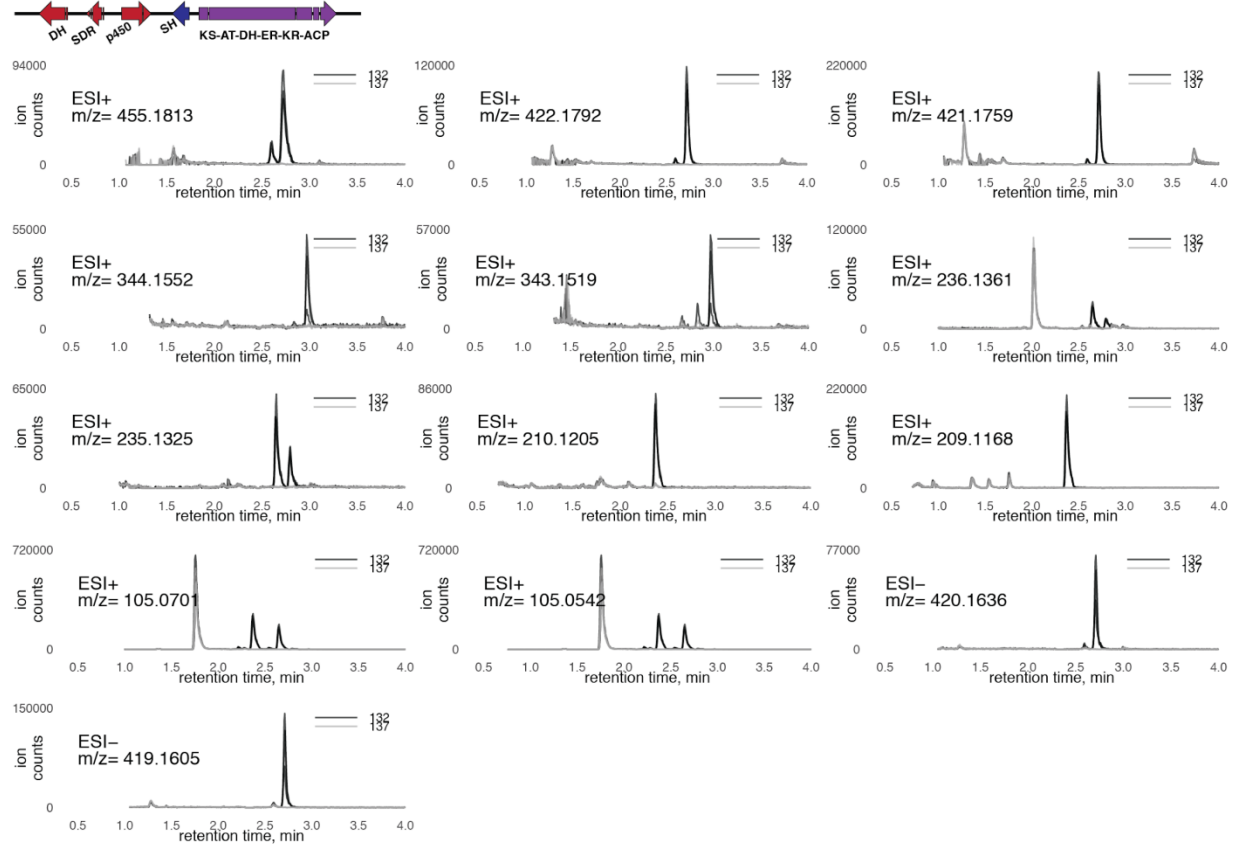
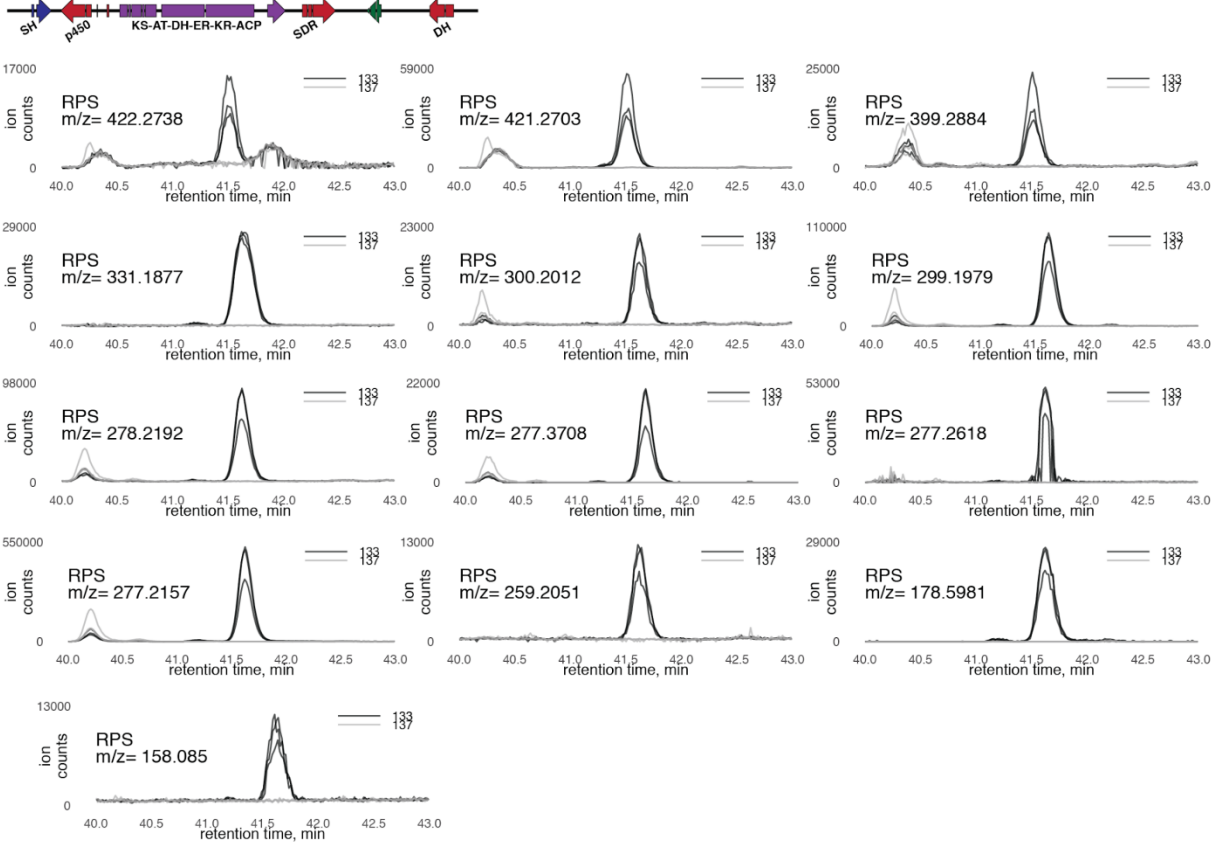


fig. S8. All features produced by PKS1 in strain 132.

**Strain 133 - PKS2 - *Corniothyrium sporulosum***



**fig. S9. All features produced by PKS2 in strain 133.**

**Strain 255 - PKS4 - *Aspergillus niger***

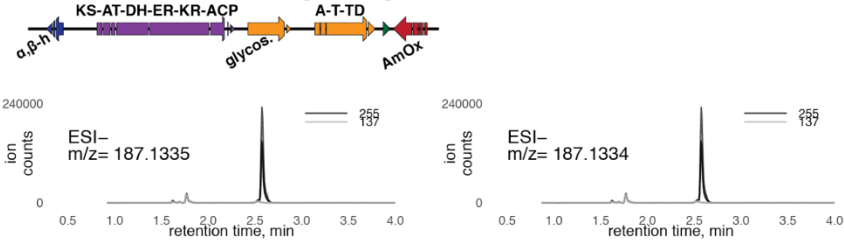


**fig. S10. All features produced by PKS4 in strain 255.**

**Strain 178 - PKS6 - *Trichoderma virens***

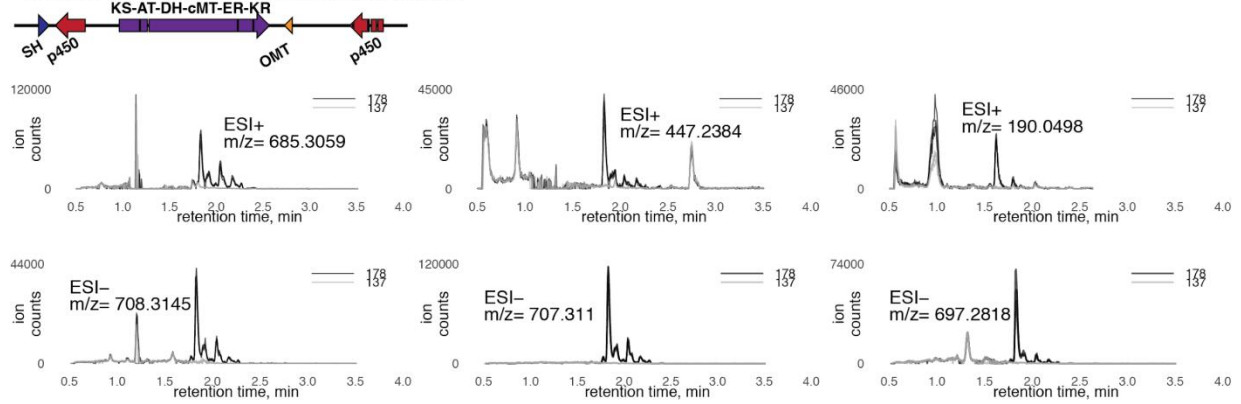


**fig. S11. All features produced by PKS6 in strain 178.**

**Strain 164 - PKS8 - *Scedosporium apiospermum***

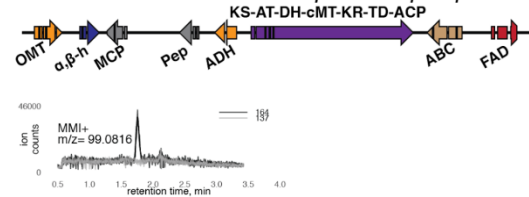


**fig. S12. All features produced by PKS8 in strain 164.**

**Strain 246 - PKS10 - *Cochliobolus heterostrophus***

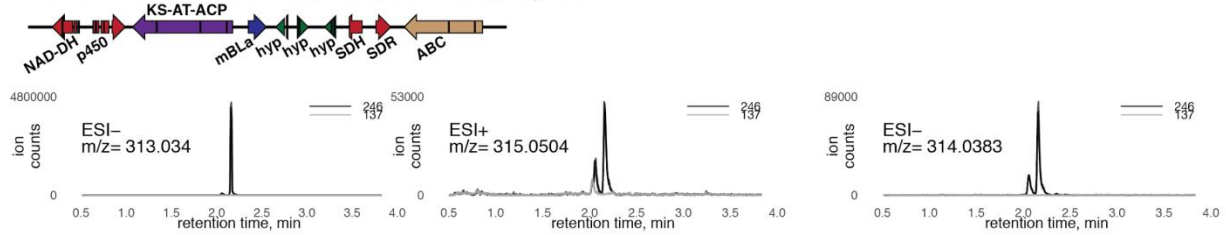


**fig. S13. All features produced by PKS10 in strain 246.**

**Strain 206 - PKS13 - *Pseudogymnoascus pannorum***

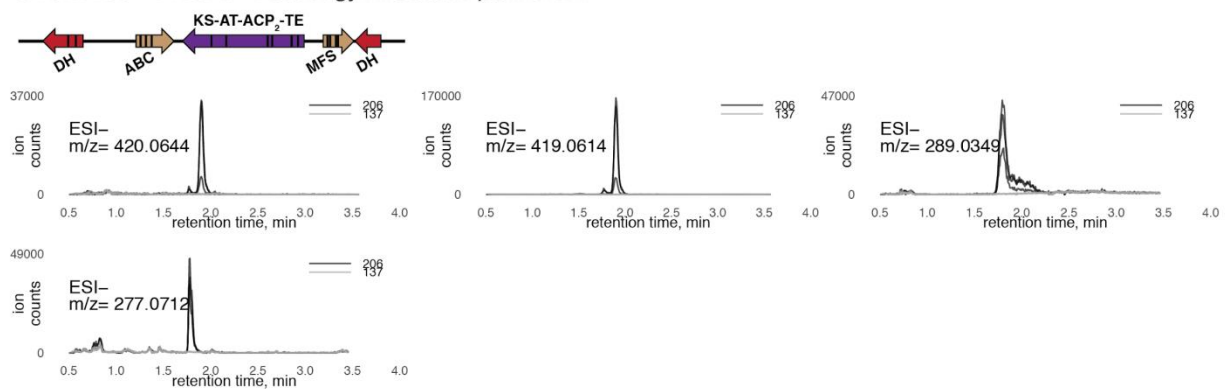


**fig. S14. All features produced by PKS13 in strain 206.**

Strain 257 - PKS14 - *Verruconis gallopava*

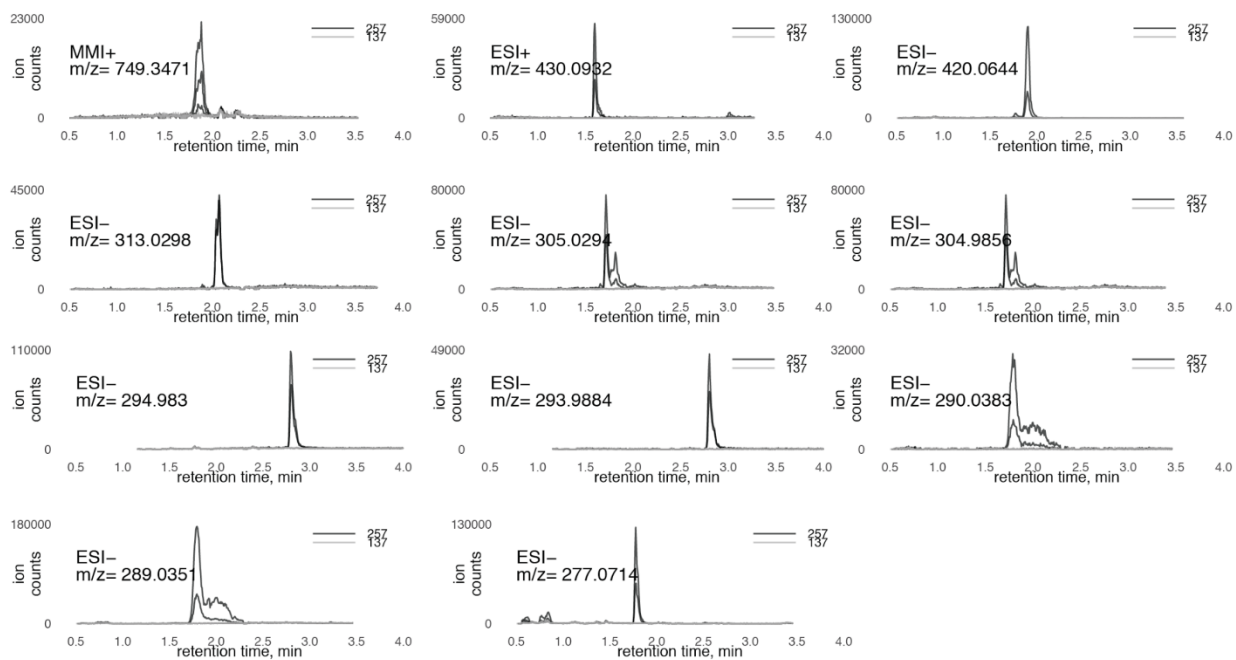
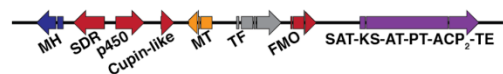


fig. S15. All features produced by PKS14 in strain 257.

Strain 247 - PKS15 - *Moniliophthora roreri*

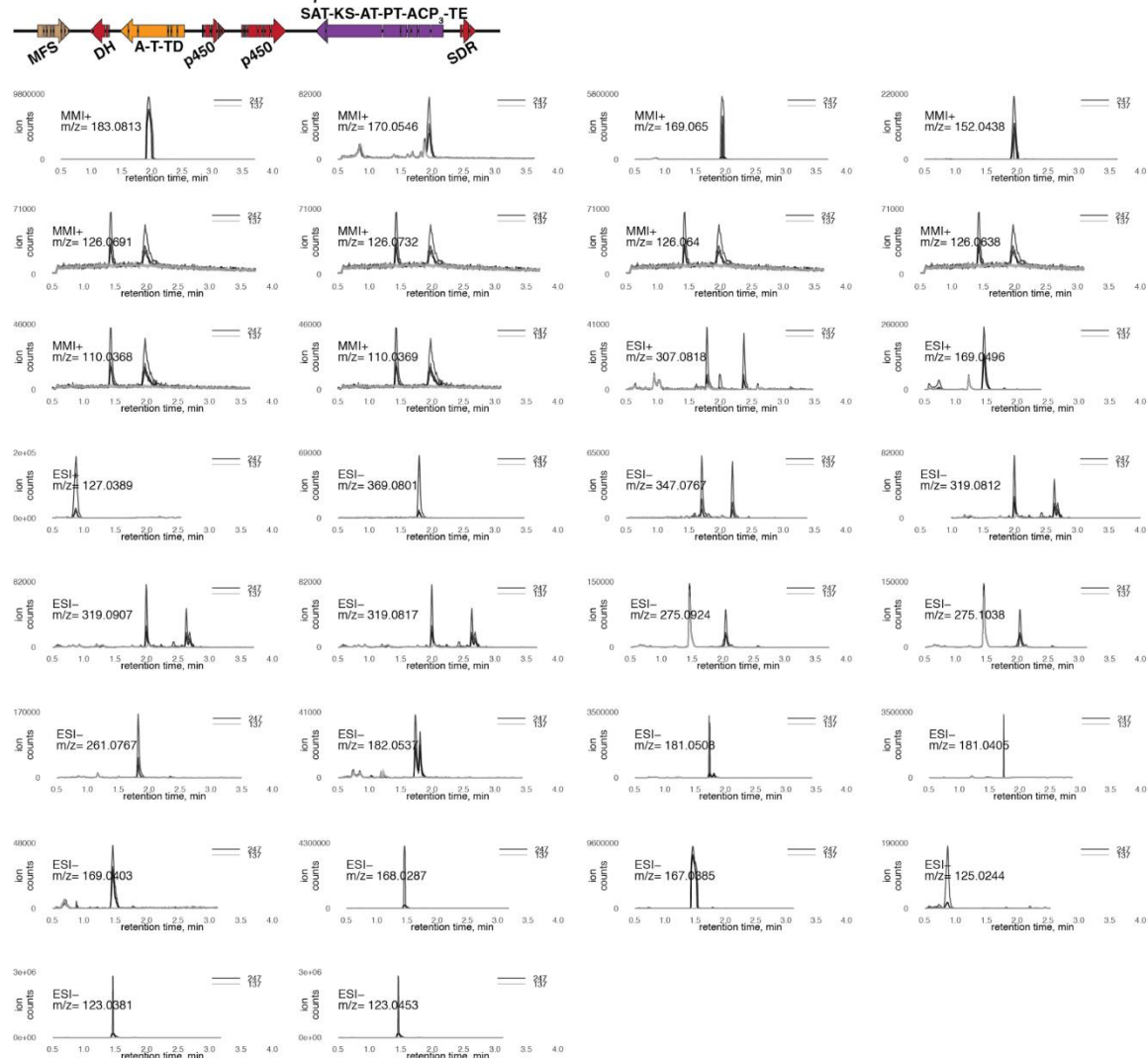


fig. S16. All features produced by PKS15 in strain 247.

Strain 177 - PKS16 - *Puntularia strigosonata*

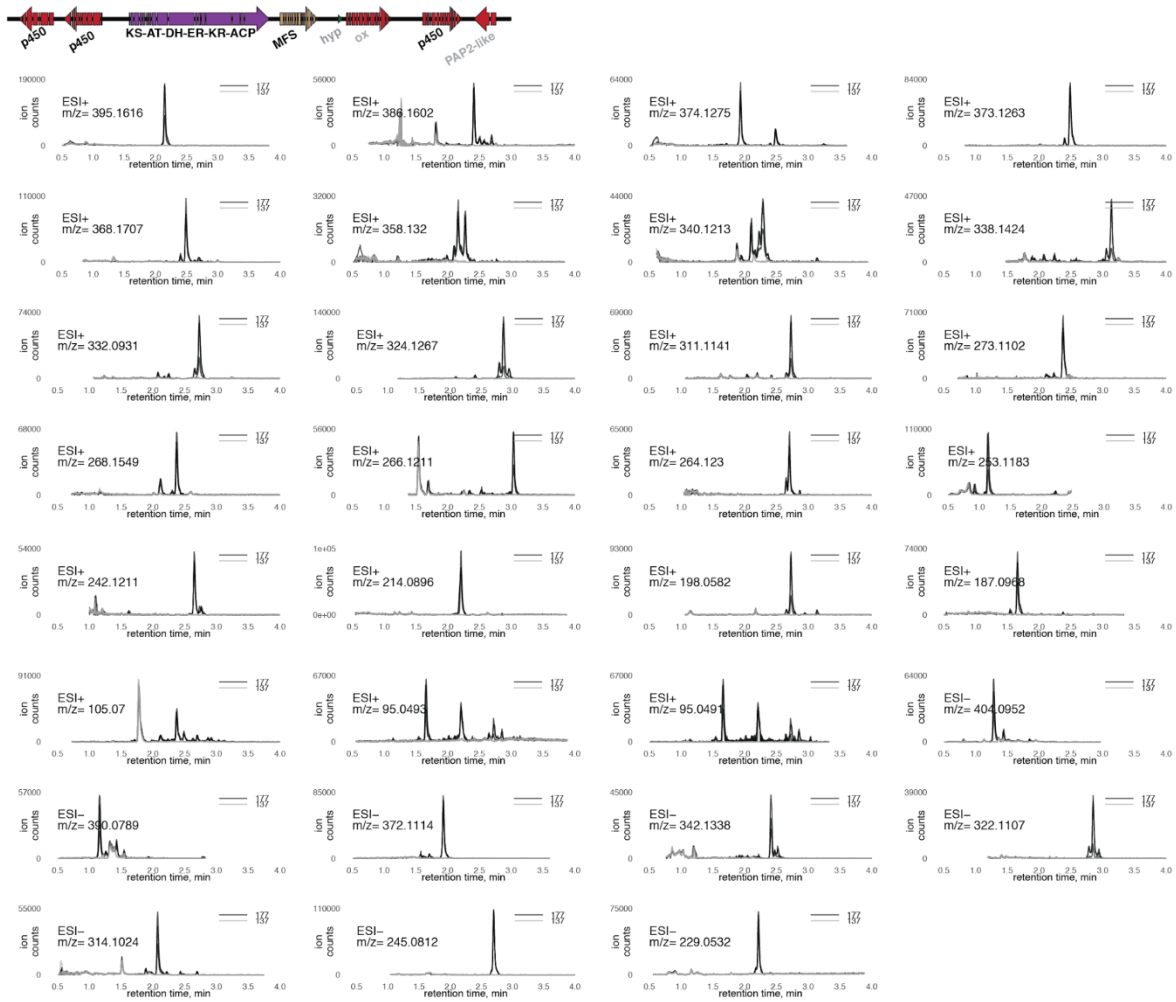
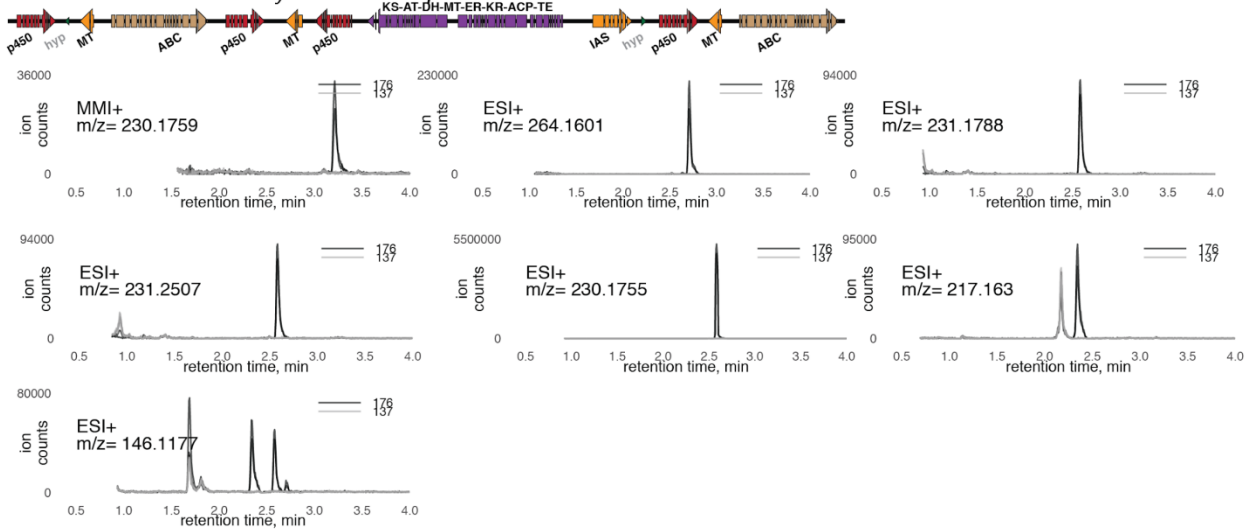


fig. S17. All features produced by PKS16 in strain 177.

**Strain 176 - PKS17 - *Hydnomerulius pinastri***



**fig. S18. All features produced by PKS17 in strain 176.**

**Strain 207 - PKS18 - *Arthroderma gypseum***

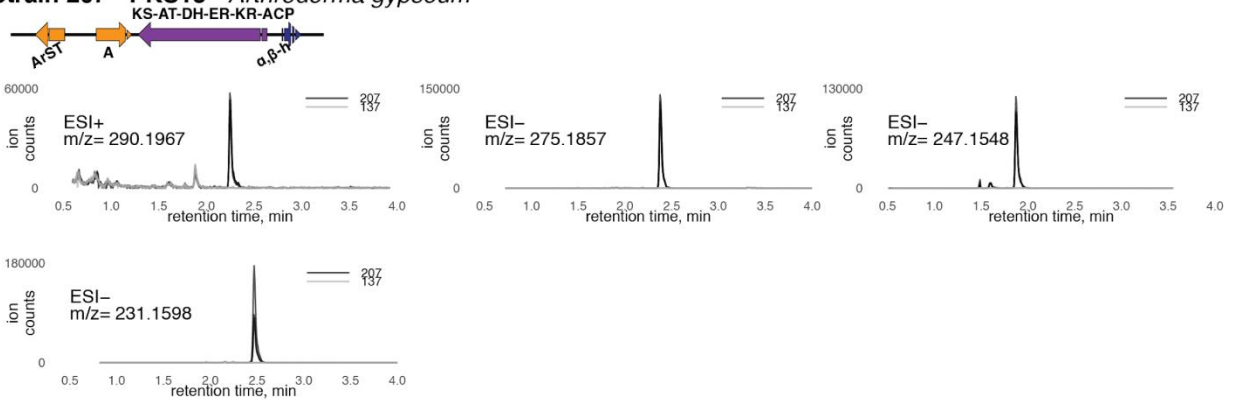


**fig. S19. All features produced by PKS18 in strain 207.**



**Strain 208 - PKS20 - *Pyrenophora teres***

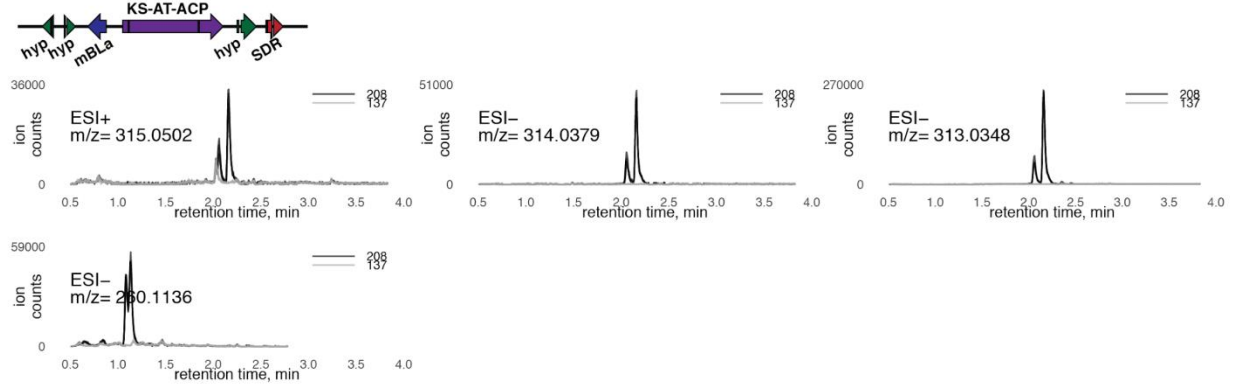


**fig. S20. All features produced by PKS20 in strain 208.**

**Strain 209 - PKS22 - *Talaromyces cellulolyticus***

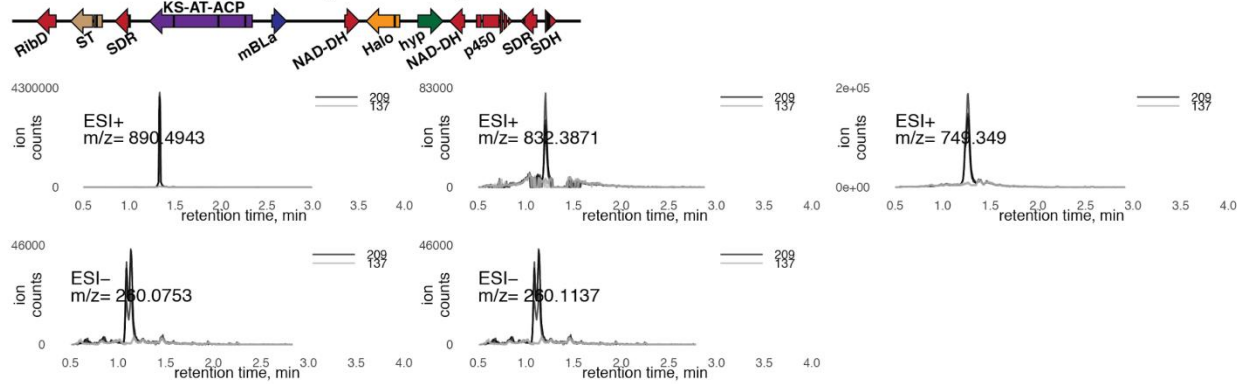


**fig. S21. All features produced by PKS22 in strain 209.**

Strain 241 - PKS23 - *Endocarpon pusillum*

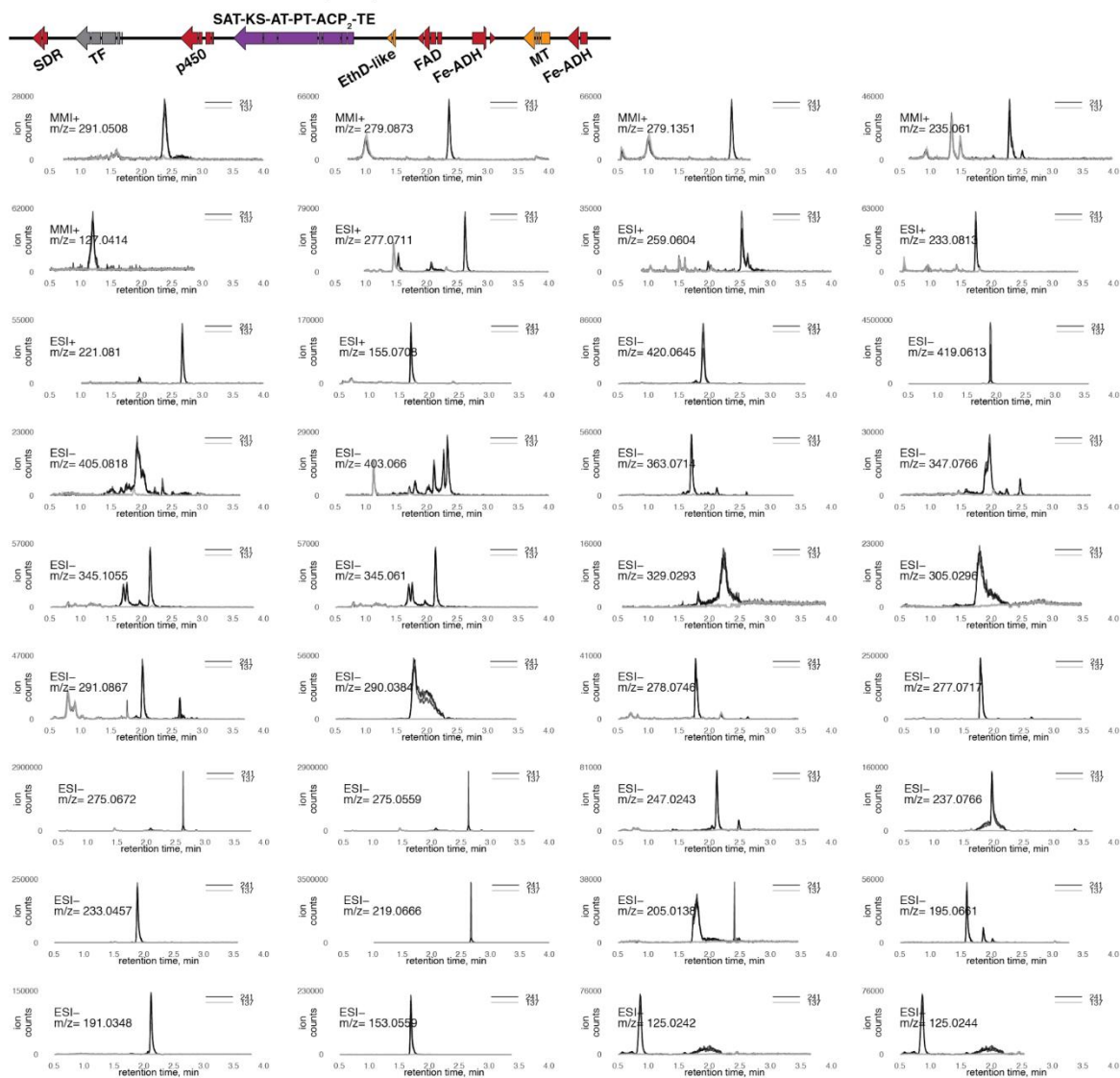
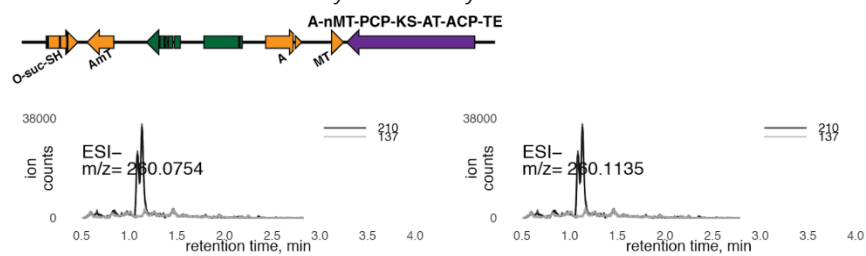


fig. S22. All features produced by PKS23 in strain 241.

**Strain 210 - PKS24 - *Talaromyces cellulolyticus***



**fig. S23. All features produced by PKS24 in strain 210.**

**Strain 240 - PKS28 - *Moniliophthora roreri***

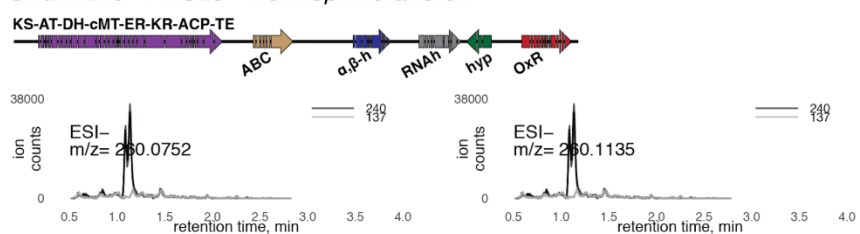
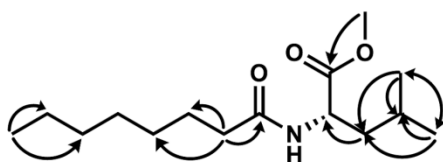
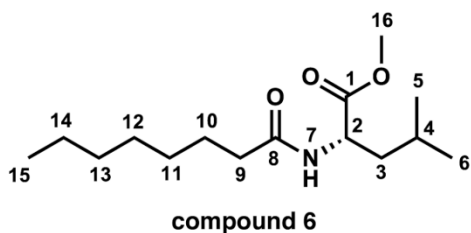


**fig. S24. All features produced by PKS28 in strain 240.**

## NMR Data:

table S11. NMR data of compound 6.

$^1\text{H}$  NMR spectrum (500 MHz),  $^{13}\text{C}$  NMR spectrum (125 MHz),  $\text{CDCl}_3$

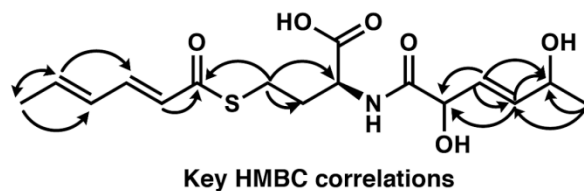
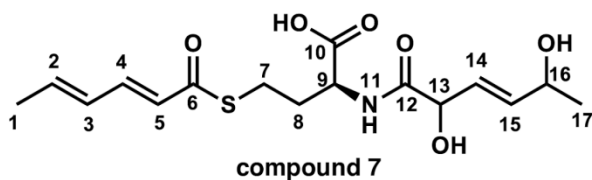


position	$\delta_{\text{H}}$ , mult ( $J$ in Hz)	$\delta_{\text{C}}$	COSY
1		173.92	
2	4.66, td (4.9, 8.8)	50.65	H3, H7
3	1.51, m, overlap 1.64, m, overlap	41.98	H2, H4
4	1.64, m, overlap	25.04	
5 <sup>a</sup>	0.94, m, overlap	22.96	H4
6 <sup>a</sup>	0.94, m, overlap	22.14	H4
7-NH	5.76, d (8.5)		H2
8		173.02	
9	2.21, m	36.77	H8
10	1.64, m, overlap	25.73	H9
11	1.28, m, overlap	29.32	
12	1.28, m, overlap	29.13	
13	1.28, m, overlap	31.83	
14	1.28, m, overlap	22.75	
15	0.88, t (7.2)	14.22	H14
16	3.73, s	52.42	

Note: <sup>a</sup> Assignments denoted by superscript letters are interchangeable.

table S12. NMR data of compound 7.

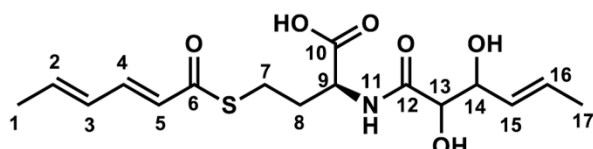
$^1\text{H}$  NMR spectrum (500 MHz),  $^{13}\text{C}$  NMR spectrum (125 MHz), Acetone- $d_6$



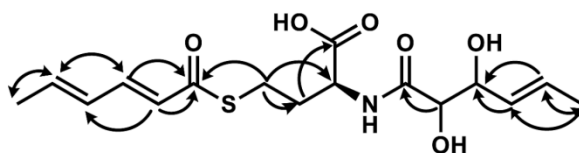
position	$\delta_{\text{H}}$ , mult ( $J$ in Hz)	$\delta_{\text{C}}$	COSY
1	1.87, d (6.2)	18.85	H2
2	6.26, m	143.36	H1, H3
3	7.35, m	129.90	H2, H4
4	6.45, t (11.2)	142.64	H3, H5
5	5.88, d (11.2)	122.27	H4
6		188.99	
7	2.99, m	25.86	H8
8	2.08, m 2.19, m	33.12	H7, H11
9	4.59, m, overlap	51.89	H11
10		172.86	
11-NH	7.58, d (7.2)		H9
12		173.11	
13	4.59, m, overlap	72.71	H14
14	5.80, m	127.68	H13, H14
15	5.91, m	137.57	H14, H16
16	4.26, m	67.72	H15, H17
17	1.17, d (6.4)	23.95	H16

**table S13. NMR data of compound 8.**

$^1\text{H}$  NMR spectrum (500 MHz),  $^{13}\text{C}$  NMR spectrum (125 MHz), Acetone- $d_6$



**compound 8**

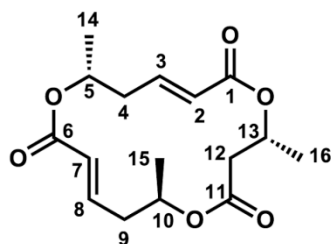


**Key HMBC correlations**

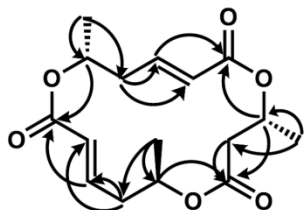
position	$\delta_{\text{H}}$ , mult (J in Hz)	$\delta_{\text{C}}$	COSY
1	1.86, dd (7.0, 1.7)	18.84	H2
2	6.26, m	143.35	H1, H3
3	7.35, m	129.90	H2, H4
4	6.45, t (11.2)	142.63	H3, H5
5	5.89, dd (11.2, 0.85)	122.27	H4
6		188.97	
7	3.01, m	25.89	H8
8	2.09, m 2.19, m	33.03	H7, H11
9	4.60, m	52.03	H11
10		172.89	
11-NH	7.64, d (8.1)		H9
12		173.38	
13	4.06, d (3.6)	74.89	H14
14	4.34, m	73.73	H13, H14
15	5.61, m	131.40	H14, H16
16	5.75, m	127.51	H15, H17
17	1.66, dt (6.5, 1.4)	17.95	H16

**table S14. NMR data of compound 9.**

$^1\text{H}$  NMR spectrum (500 MHz),  $^{13}\text{C}$  NMR spectrum (125 MHz),  $\text{CDCl}_3$



**compound 9**

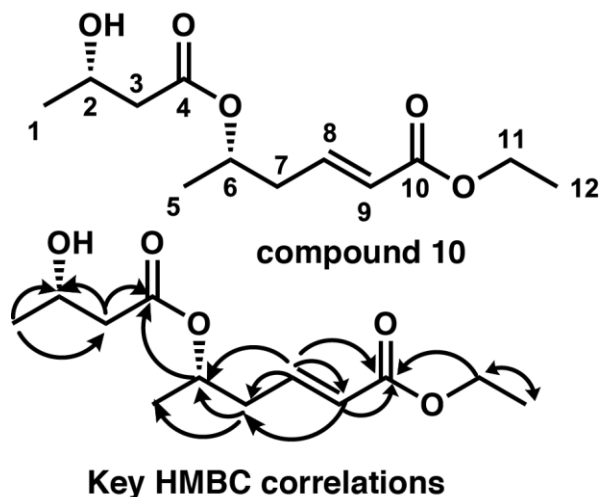


**Key HMBC correlations**

position	$\delta_{\text{H}}$ , mult (J in Hz)	$\delta_{\text{C}}$	COSY
1		165.07	
2	5.80, m	125.02	H3
3	6.84, m, overlap	143.61	H2, H4
4	2.31, m 2.49, m	38.99	H3, H5
5	5.05, m	68.72	H4, H14
6		165.46	
7	5.77, m	123.84	H8
8	6.80, m, overlap	144.69	H7, H9
9	2.39, m	39.50	H8, H10
10	5.11, m	70.21	H9, H15
11		170.30	
12	2.47, dd (15.3, 2.3) 2.57, dd (15.3, 10.6)	41.63	H13
13	5.35, m	67.81	H12, H16
14	1.34, d (6.3)	21.16	H5
15	1.27, d (6.3)	20.68	H10
16	1.30, d (6.3)	20.21	H13

**table S15. NMR data of compound 10.**

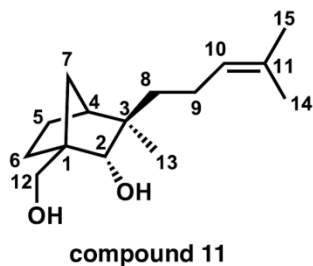
$^1\text{H}$  NMR spectrum (500 MHz),  $^{13}\text{C}$  NMR spectrum (125 MHz),  $\text{CDCl}_3$



position	$\delta_{\text{H}}$ , mult ( $J$ in Hz)	$\delta_{\text{C}}$	COSY
1	1.22, d (6.3)	22.56	H2
2	4.19, m, overlap	64.41	H1, H3
3	2.45, m, overlap	43.70	H2
4		172.48	
5	1.28, m, overlap	19.81	H6
6	5.07, m	69.71	H5, H7
7	2.45, m, overlap	38.48	H6, H8
8	6.86, dt (15.5, 7.4)	143.31	H7, H9
9	5.87, dt (15.5, 1.4)	124.51	H8
10		166.27	
11	4.19, m, overlap	60.55	H12
12	1.28, m, overlap	14.38	H11

**table S16. NMR data of compound 11.**

$^1\text{H}$  NMR spectrum (500 MHz),  $^{13}\text{C}$  NMR spectrum (125 MHz),  $\text{CDCl}_3$

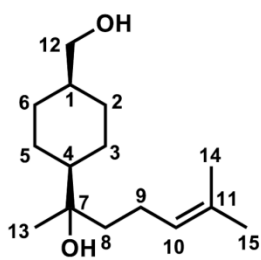


position	$\delta_{\text{H}}$ , mult ( $J$ in Hz)	$\delta_{\text{C}}$
1		53.82
2	3.63, brs	82.59
3		42.57
4	1.88, m	46.26
5	1.46, m 1.74, m	25.83
6	1.20, m 1.88, m	22.16
7	1.09, d (10.1) 1.45, m	36.59
8	1.31, m	42.81
9	1.96, m	22.95
10	5.09, m	124.95
11		131.47
12	3.75, d (10.5) 3.84, d (10.5)	68.54
13	0.87, s	16.47
14	1.61, s	17.79
15	1.68, s	25.85

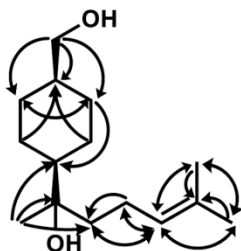
Note: The NMR data is identical to the data previously reported (9).

**table S17. NMR data of compound 12.**

$^1\text{H}$  NMR spectrum (500 MHz),  $^{13}\text{C}$  NMR spectrum (125 MHz),  $\text{CDCl}_3$



**compound 12**



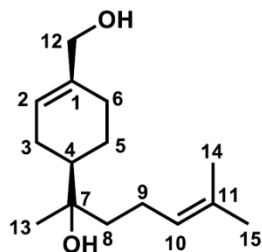
**Key HMBC correlations**

position	$\delta_{\text{H}}$ , mult ( $J$ in Hz)	$\delta_{\text{C}}$	COSY
1	1.43, m	40.63	H2, H6, H12
2 <sup>a</sup>	0.95, m, overlap 1.87, m, overlap	29.71	H1, H3
3 <sup>b</sup>	1.08, m, overlap 1.81, m	26.95	H2, H4
4	1.32, m	47.52	H3, H5
5 <sup>b</sup>	1.12, m, overlap 1.89, m, overlap	26.22	H4, H6
6 <sup>a</sup>	0.95, m, overlap 1.87, m, overlap	29.76	H1, H5
7		74.61	
8	1.49, dd (9.9, 6.8)	39.90	H9
9	2.05, m	22.27	H8, H10
10	5.13, t (7.3)	124.70	H9
11		131.92	
12	3.46, d (6.3)	68.78	
13	1.11, s	24.03	
14	1.62, s	17.83	
15	1.69, s	25.88	

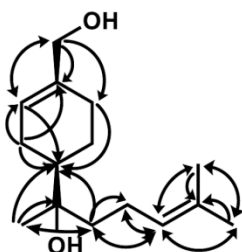
Note: <sup>a, b</sup> Assignments denoted by superscript letters are interchangeable.

**table S18. NMR data of compound 13.**

$^1\text{H}$  NMR spectrum (500 MHz),  $^{13}\text{C}$  NMR spectrum (125 MHz),  $\text{CDCl}_3$



**compound 13**



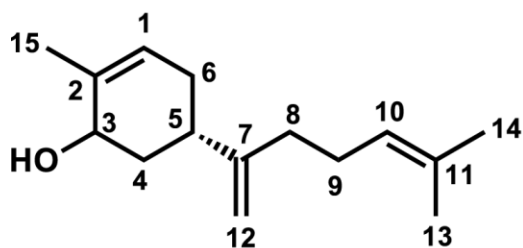
**Key HMBC correlations**

position	$\delta_{\text{H}}$ , mult ( $J$ in Hz)	$\delta_{\text{C}}$	COSY
1		137.73	
2	5.68, m	122.58	H3
3	2.13, m, overlap 2.15, m	26.75	H2, H4
4	1.60, m, overlap	43.28	H3, H5
5	1.29, m 1.89, m, overlap	23.41	H4, H6
6	1.86, m 2.05, m, overlap	26.75	H5
7		74.44	
7-OH <sup>a</sup>	1.25, brs		
8	1.51, m	40.21	H9
9	2.06, m, overlap	22.23	H8, H10
10	5.13, t (7.3)	124.59	H9
11		132.03	
12	4.02, m	67.31	
12-OH <sup>a</sup>	1.15, brs		
13	1.12, s	23.41	
14	1.62, s	17.85	
15	1.69, s	25.88	

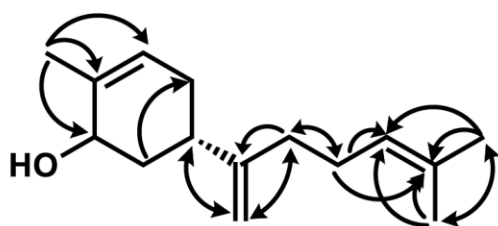
Note: <sup>a</sup> Assignments denoted by superscript letters are interchangeable.

table S19. NMR data of compound 14.

<sup>1</sup>H NMR spectrum (500 MHz), <sup>13</sup>C NMR spectrum (125 MHz), CDCl<sub>3</sub>



compound 14

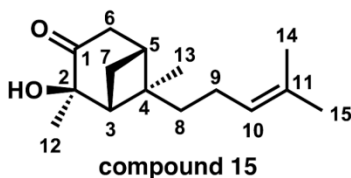


Key HMBC correlations

position	$\delta_H$ , mult (J in Hz)	$\delta_C$	COSY
1	5.59	125.69	H6
2		134.41	
3	4.02, brs	68.81	H4
4	1.59, m, overlap 1.95, m	37.34	H3, H5
5	2.33, m	34.14	H4, H6
6	1.83, m 2.16, m, overlap	31.74	H1, H5
7		153.42	
8	2.08, m	35.04	H9
9	2.13, m, overlap	26.90	H8, H10
10	5.12	124.30	H9
11		131.79	
12	4.78, s	107.88	
13	1.61, s	17.90	
14	1.68, s	25.85	
15	1.80, s	20.99	

table S20. NMR data of compound 15.

<sup>1</sup>H NMR spectrum (500 MHz), <sup>13</sup>C NMR spectrum (125 MHz), CDCl<sub>3</sub>



compound 15



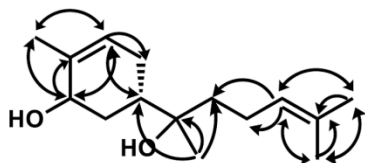
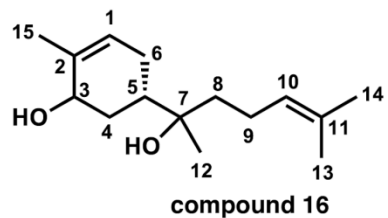
Key HMBC correlations

position	$\delta_H$ , mult (J in Hz)	$\delta_C$	COSY
1		214.32	
2		77.27	
2-OH	2.14, brs		
3	2.21, m, overlap	48.00	H7
4		42.59	
5	2.18, m, overlap	36.94	H6, H7
6	2.62, m	43.12	H5
7	1.68, m, overlap 2.43, m	28.77	H3, H5
8	1.66, m, overlap 1.80, m	39.12	H9
9	2.00, m	23.78	H8, H10
10	5.16, m	124.51	H9
11		131.82	
12	1.39, s	25.51	
13	0.88, s	19.90	
14	1.63, s	17.77	
15	1.70, s	25.87	



table S21. NMR data of compound 16.

$^1\text{H}$  NMR spectrum (500 MHz),  $^{13}\text{C}$  NMR spectrum (125 MHz),  $\text{CDCl}_3$



position	$\delta_{\text{H}}$ , mult (J in Hz)	$\delta_{\text{C}}$	COSY
1	5.56, m	125.41	H6
2		134.61	
3	4.04, m	68.78	
4	1.42, td (13.2, 3.8, 1) 2.03, m, overlap	32.18	H5
5	1.78, m, overlap	36.99	H4, H6
6	1.74, m, overlap 2.04, m, overlap	27.32	H1, H5
7		73.96	
8	1.50, m	40.41	H9
9	2.06, m, overlap	22.20	H8, H10
10	5.12, m	124.57	H9
11		131.98	
12	1.11, s	23.39	
13	1.61, s	17.84	
14	1.68, s	25.86	
15	1.78, s	21.00	

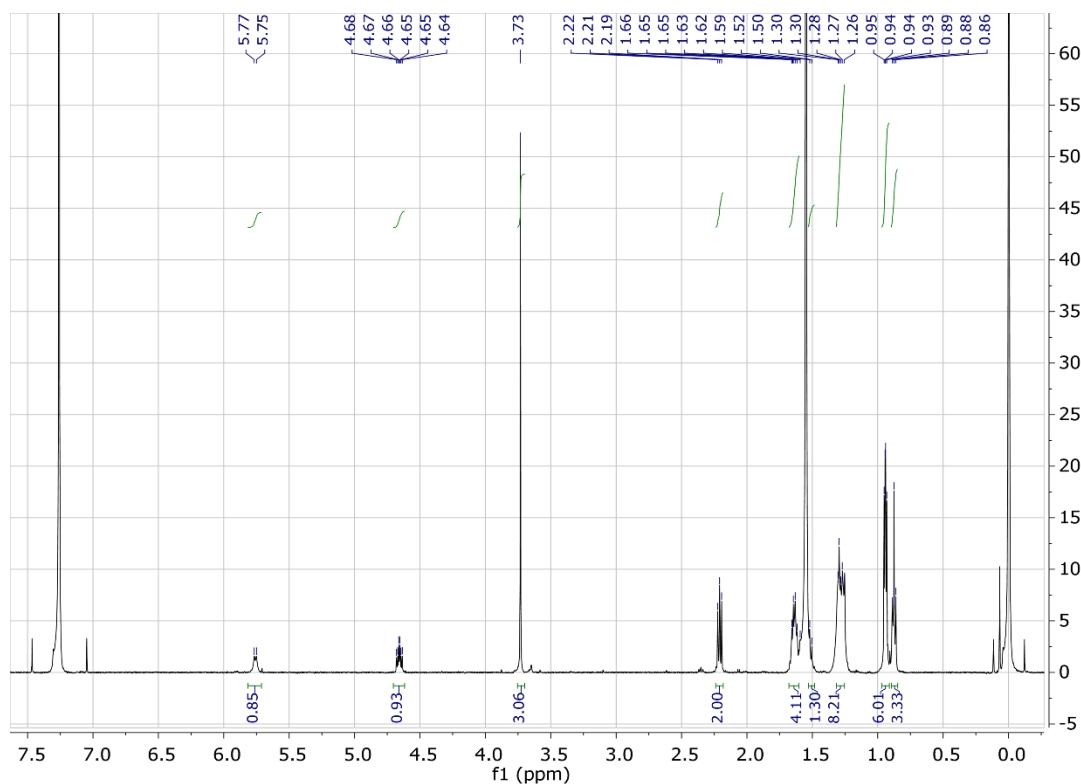


fig. S25.  $^1\text{H}$  NMR spectrum of compound 6 in  $\text{CDCl}_3$ .

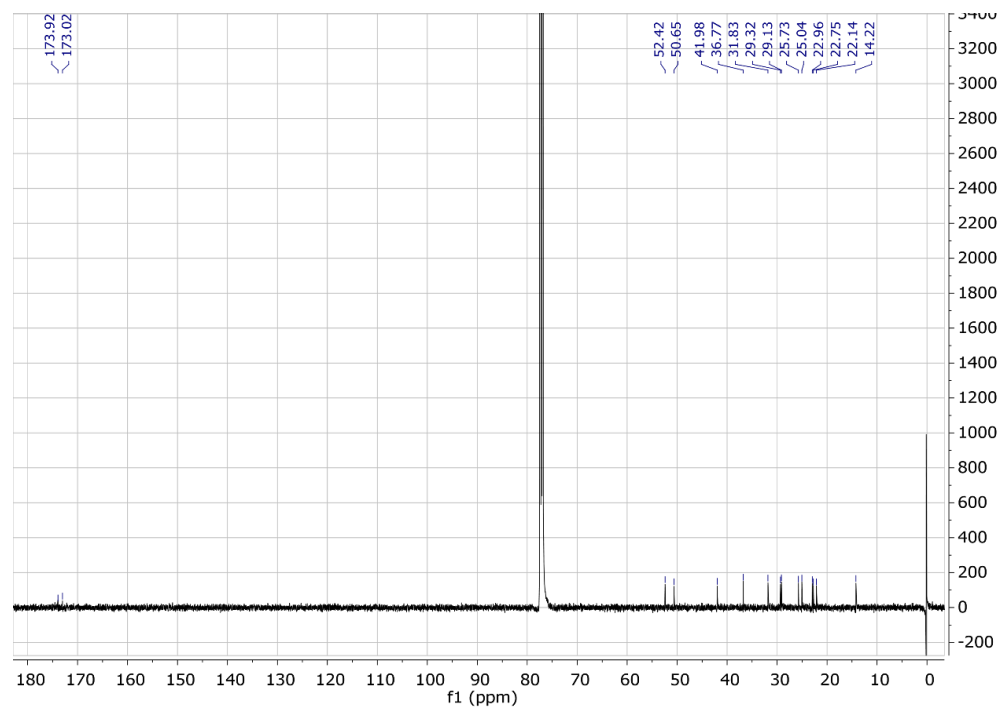


fig. S26.  $^{13}\text{C}$  NMR spectrum of compound 6 in  $\text{CDCl}_3$ .

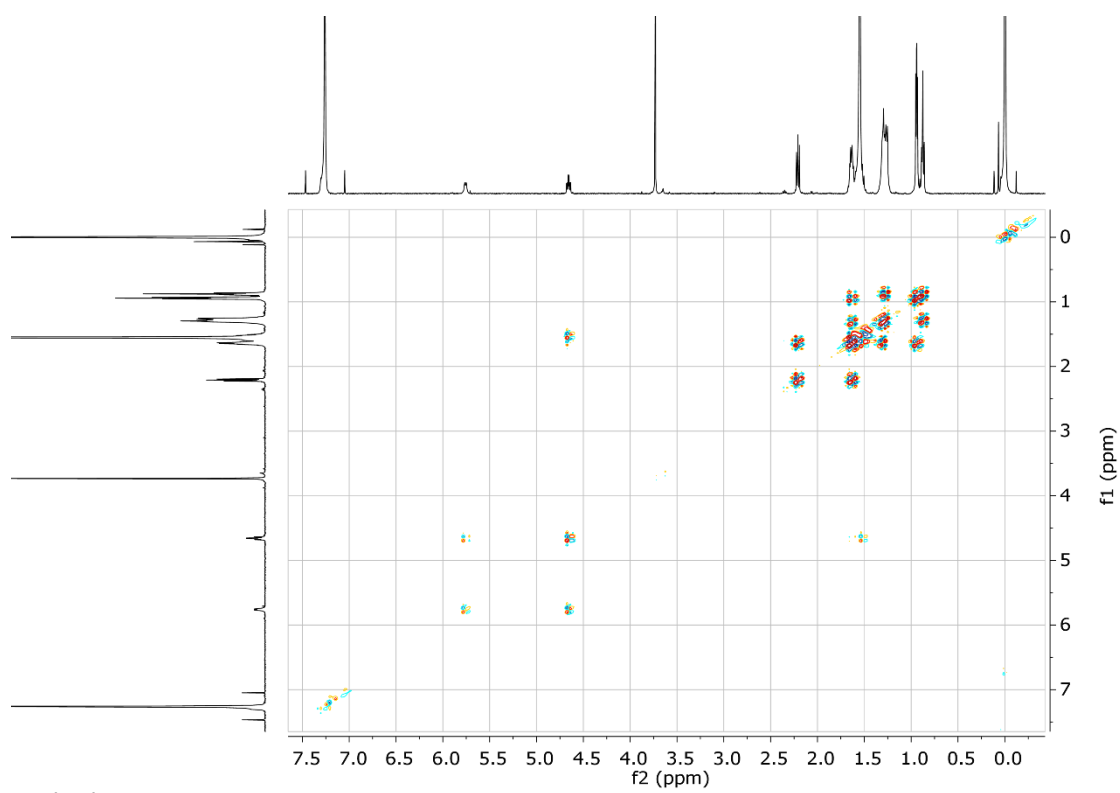


fig. S27.  $^1\text{H}$ - $^1\text{H}$  COSY spectrum of compound 6 in  $\text{CDCl}_3$ .

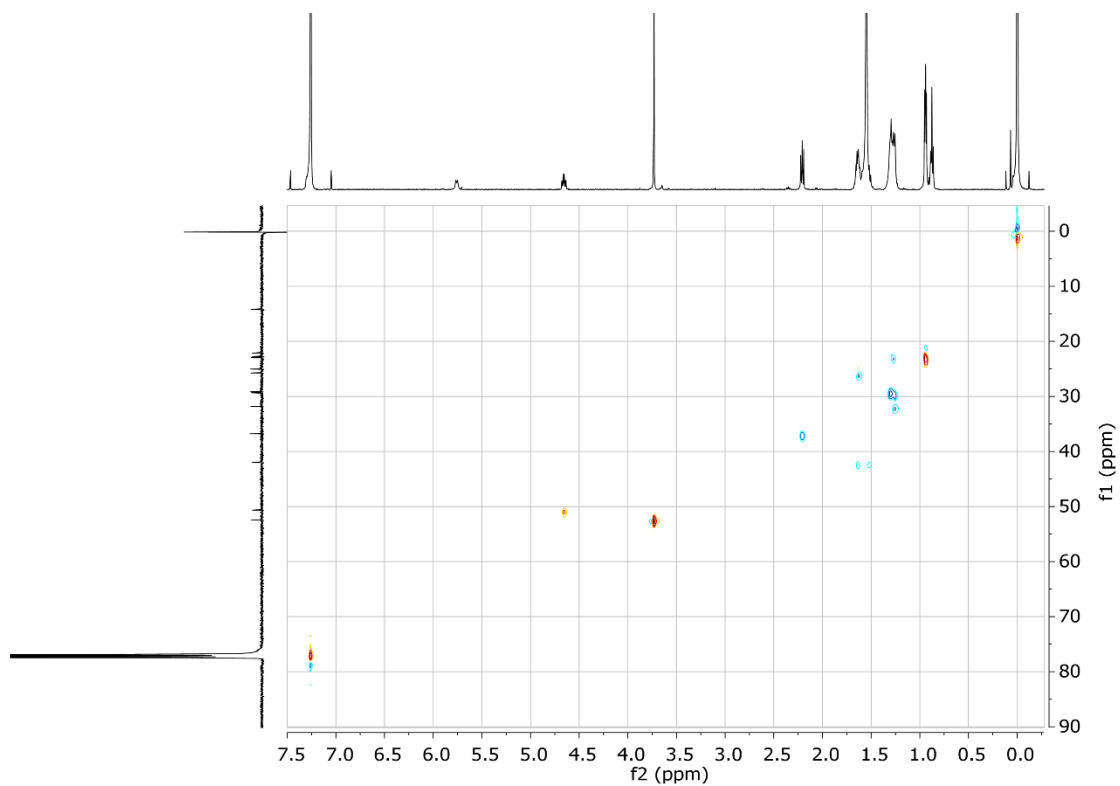


fig. S28. HSQC spectrum of compound 6 in CDCl<sub>3</sub>.

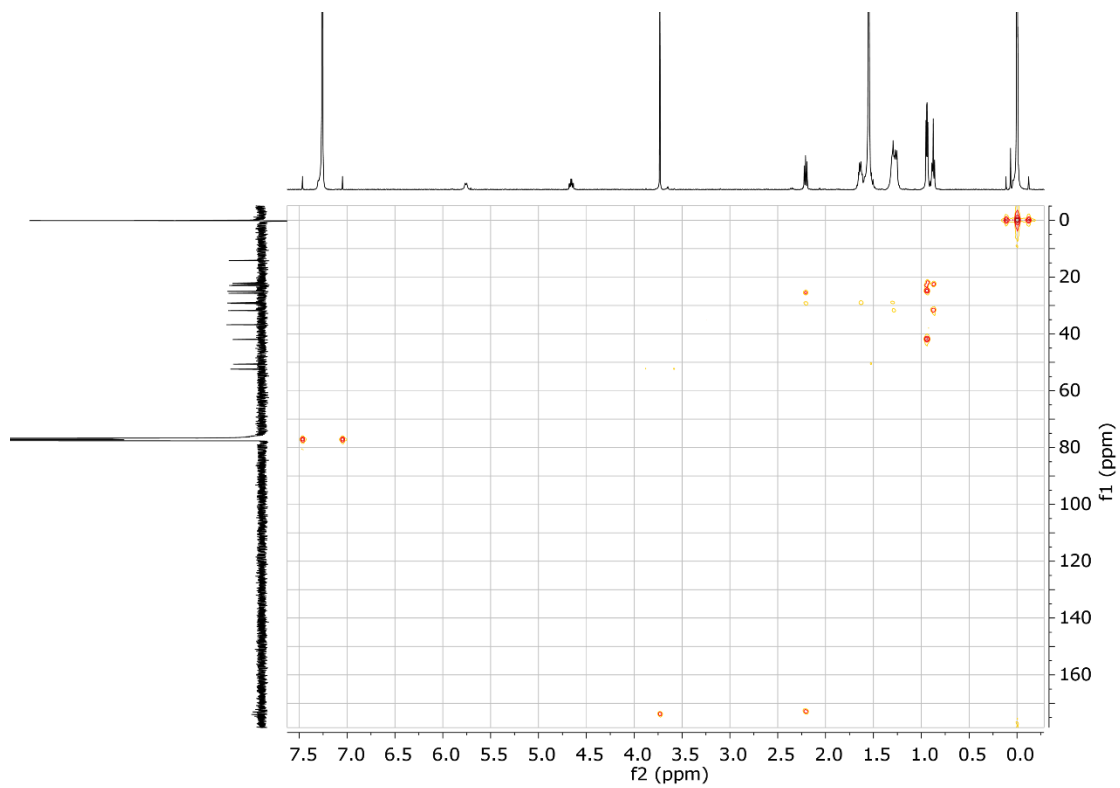


fig. S29. HMBC spectrum of compound 6 in CDCl<sub>3</sub>.

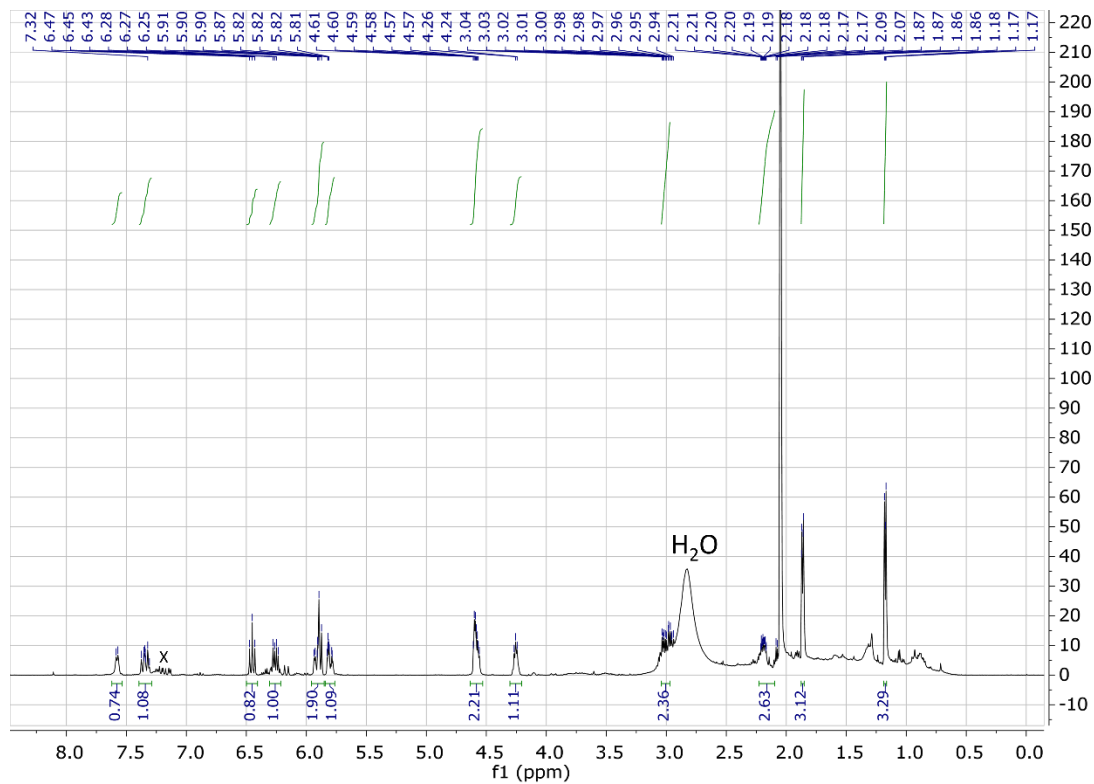


fig. S30. <sup>1</sup>H NMR spectrum of compound 7 in acetone-d<sub>6</sub>.

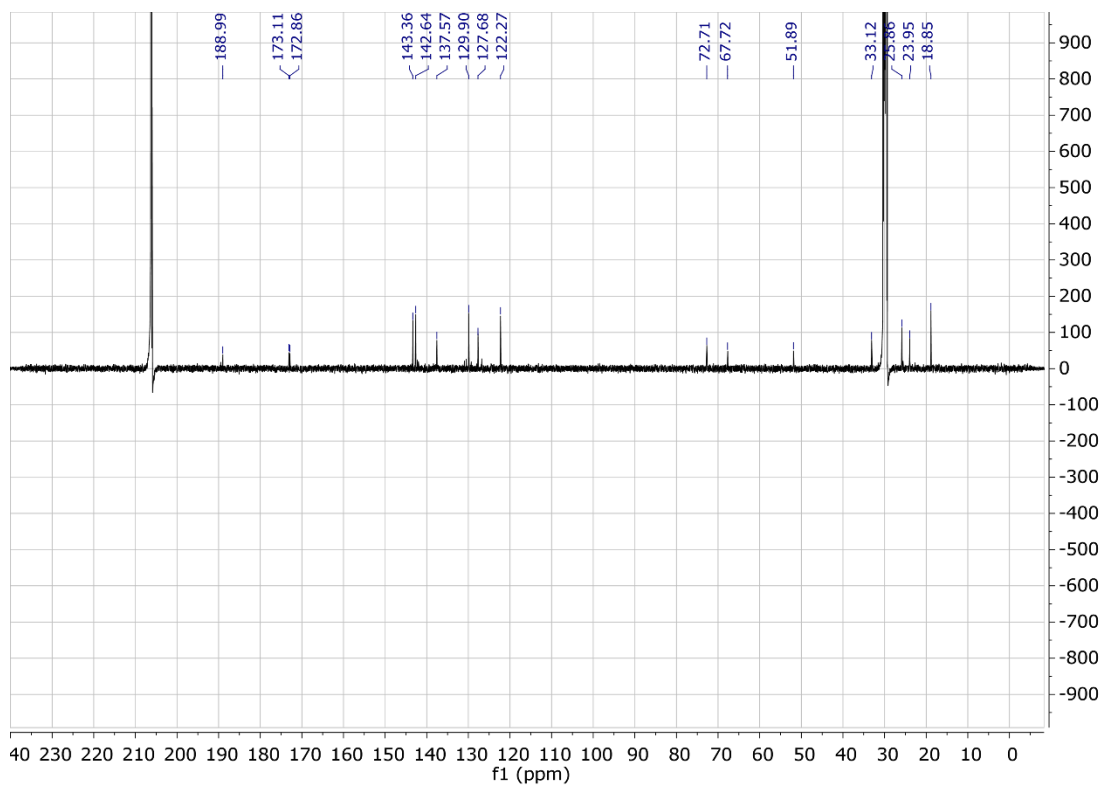


fig. S31. <sup>13</sup>C NMR spectrum of compound 7 in acetone-d<sub>6</sub>.

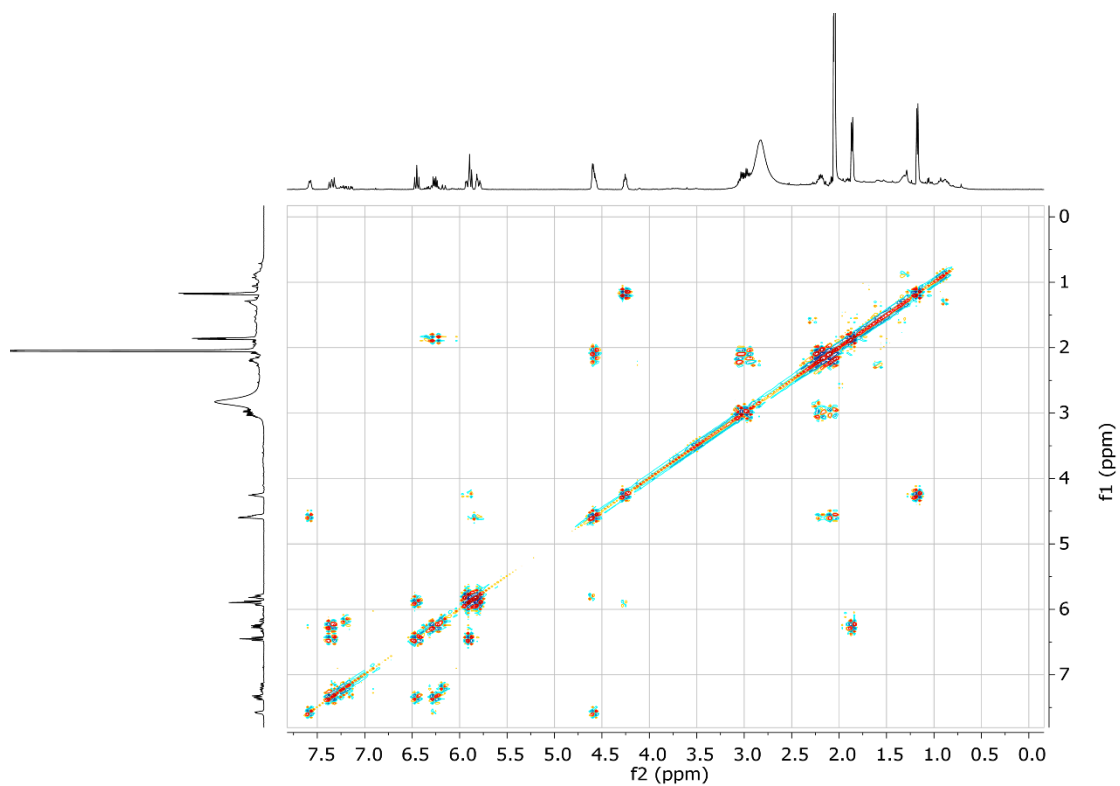


fig. S32.  $^1\text{H}$ - $^1\text{H}$  COSY spectrum of compound 7 in acetone- $\text{d}_6$ .

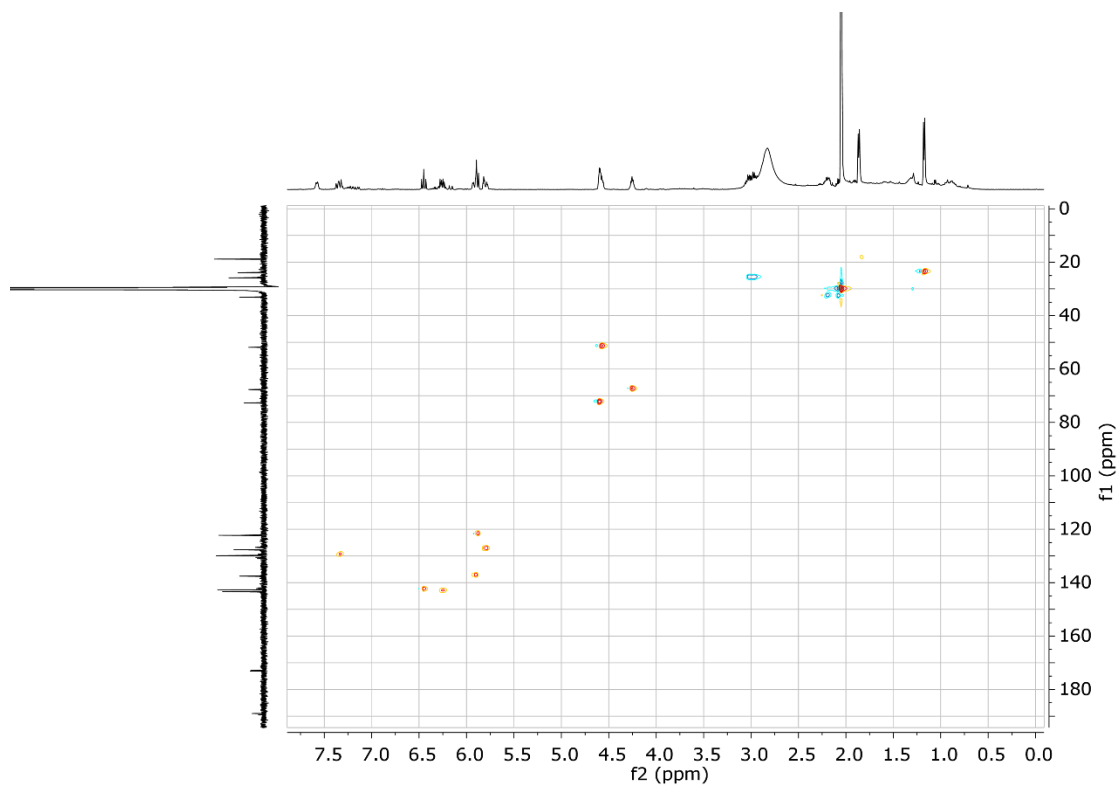


fig. S33. HSQC spectrum of compound 7 in acetone- $\text{d}_6$ .

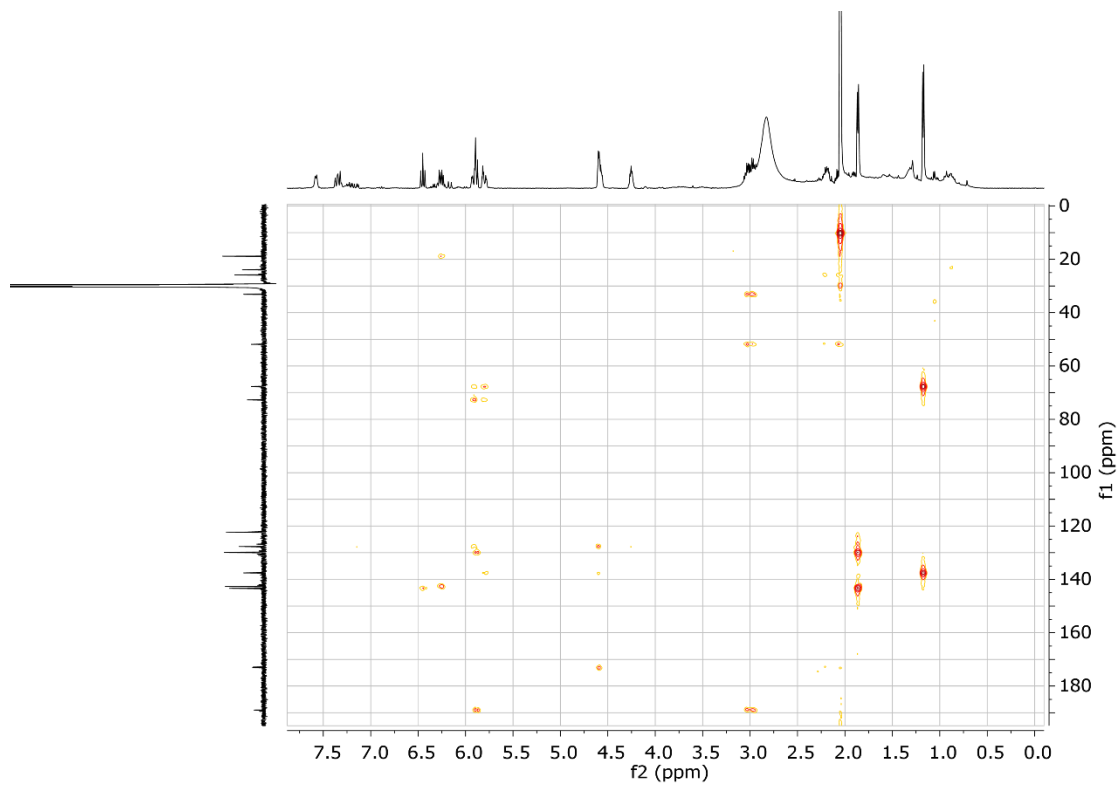


fig. S34. HMBC spectrum of compound 7 in acetone-d<sub>6</sub>.

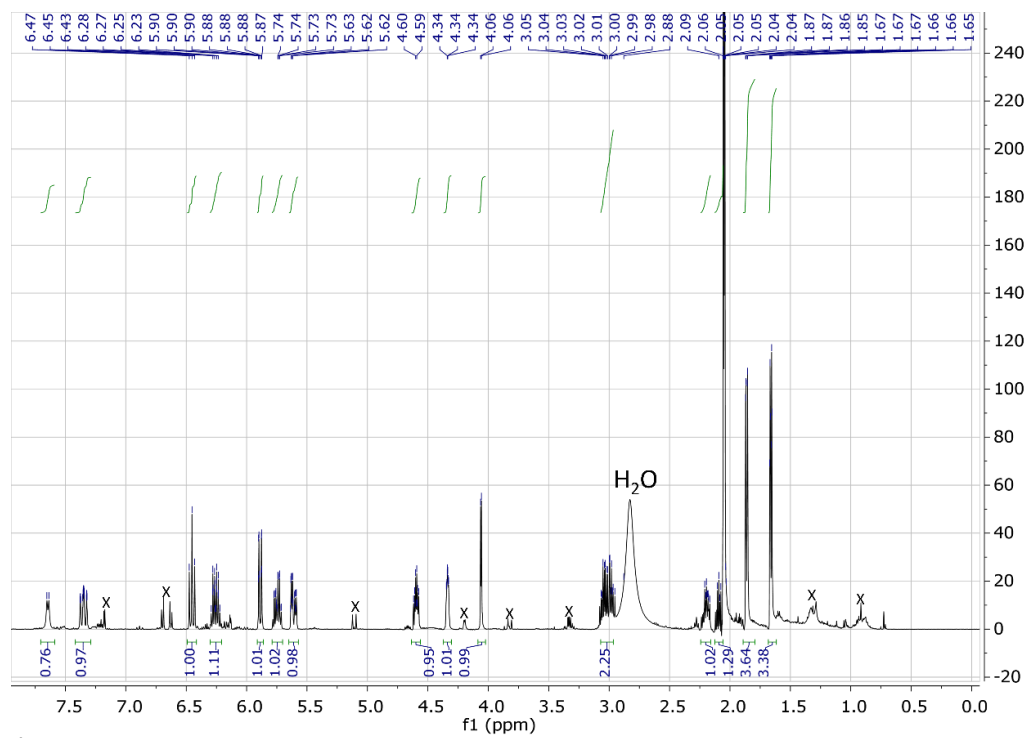


fig. S35. <sup>1</sup>H NMR spectrum of compound 8 in acetone-d<sub>6</sub>.

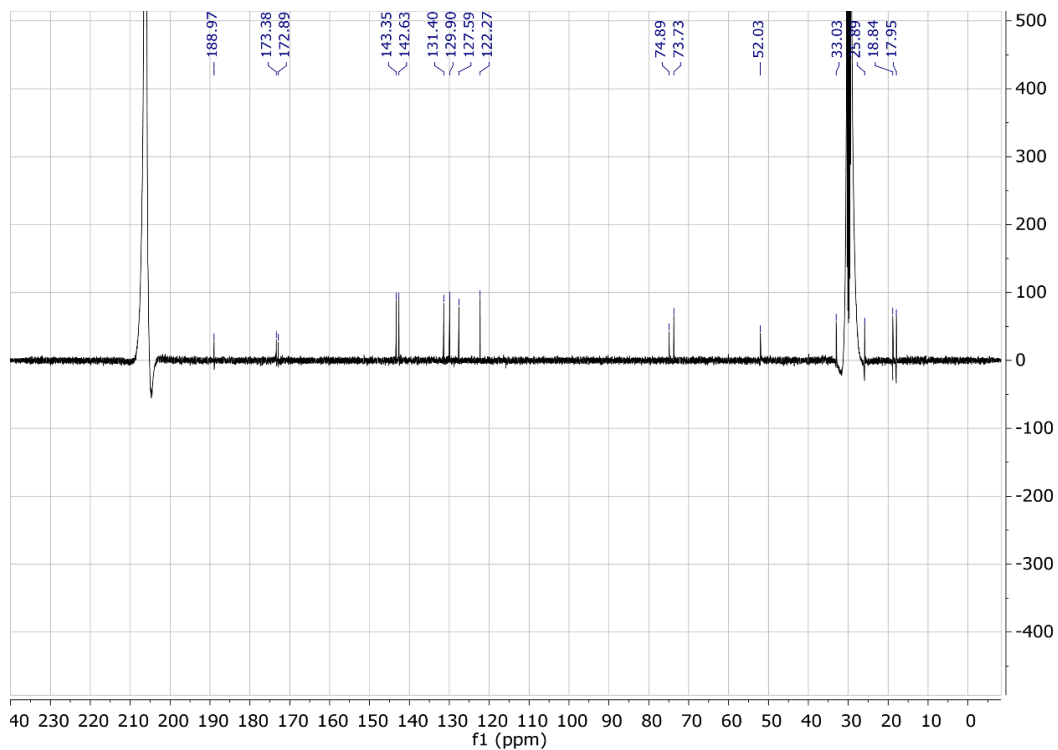


fig. S36.  $^{13}\text{C}$  NMR spectrum of compound 8 in acetone- $\text{d}_6$ .

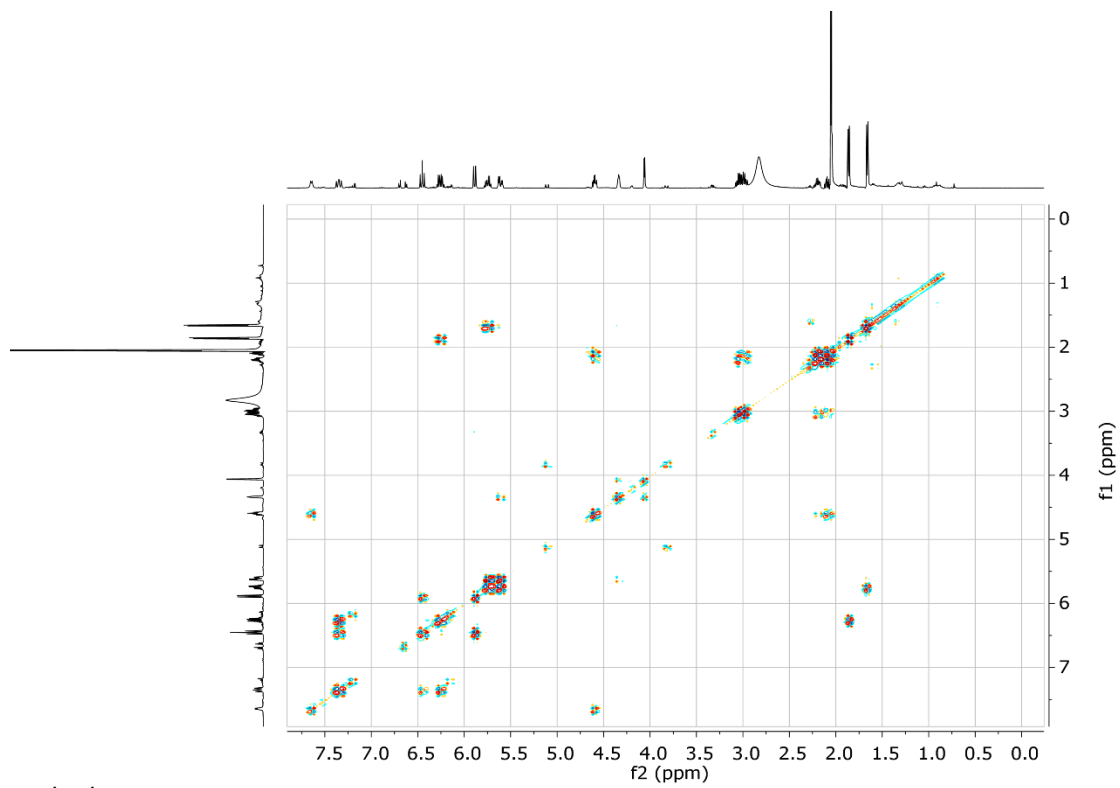


fig. S37.  $^1\text{H}$ - $^1\text{H}$  COSY spectrum of compound 8 in acetone- $\text{d}_6$ .

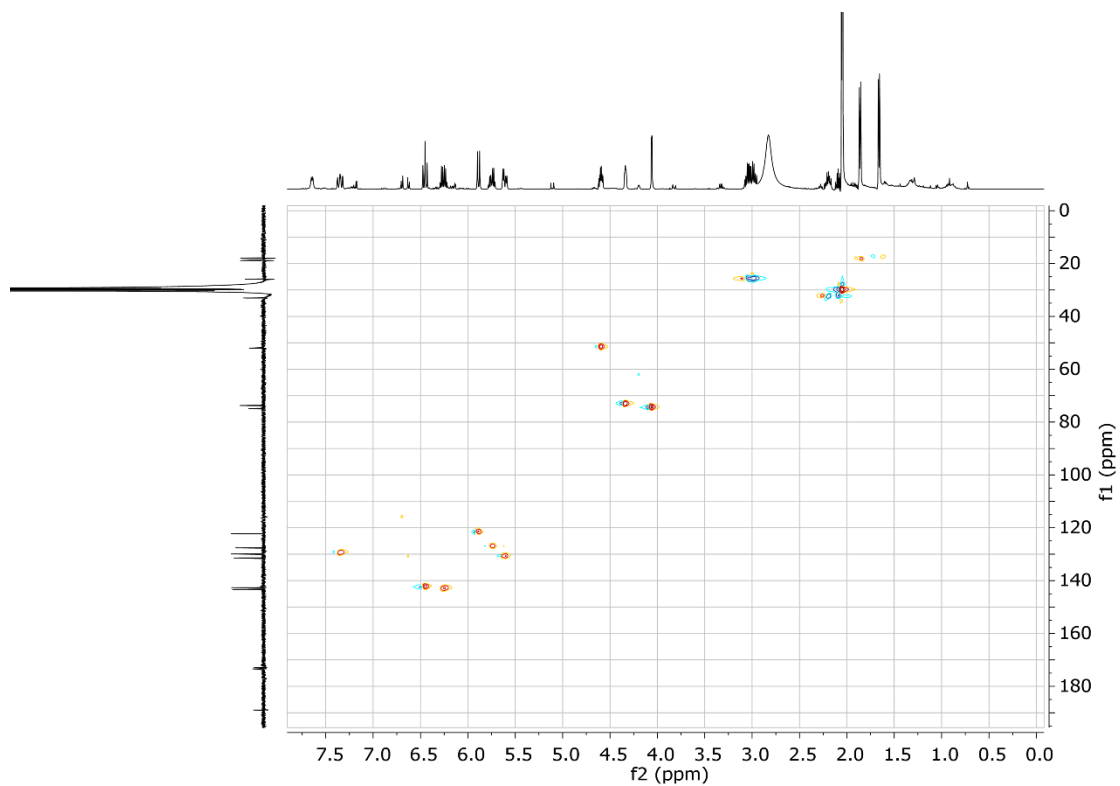


fig. S38. HSQC spectrum of compound 8 in acetone-d<sub>6</sub>.

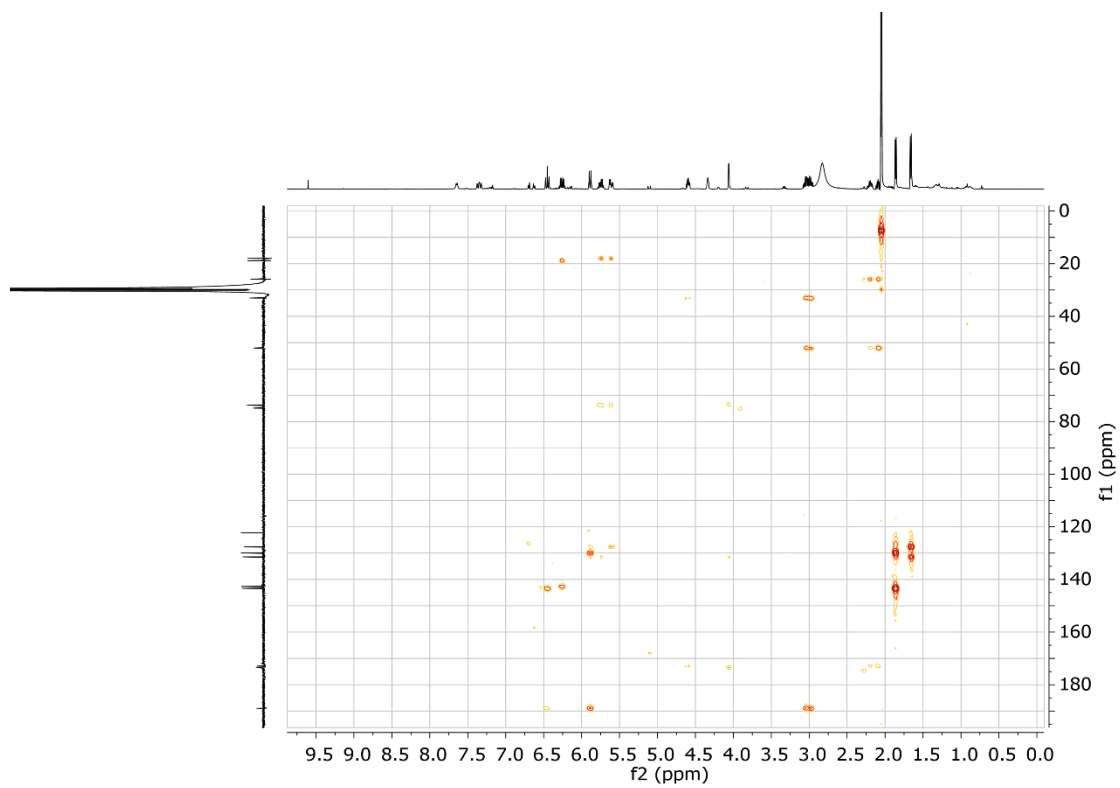


fig. S39. HMBC spectrum of compound 8 in acetone-d<sub>6</sub>.



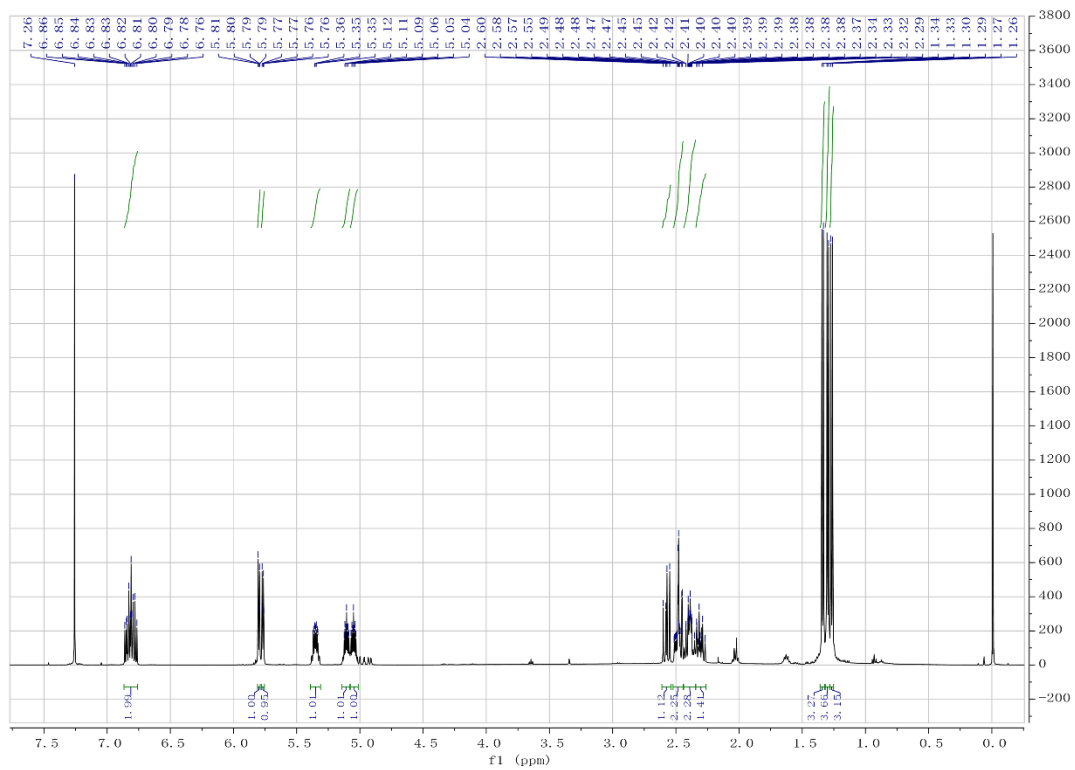


fig. S40.  $^1\text{H}$  NMR spectrum of compound 9 in  $\text{CDCl}_3$ .

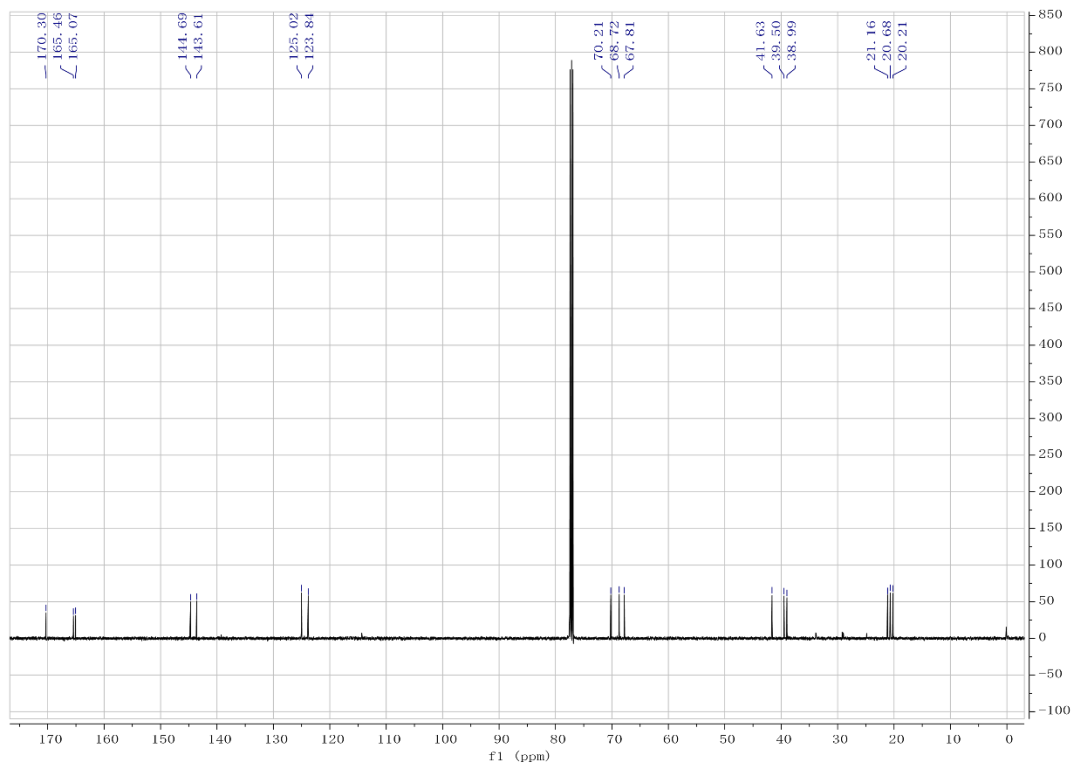


fig. S41.  $^{13}\text{C}$  NMR spectrum of compound 9 in  $\text{CDCl}_3$ .

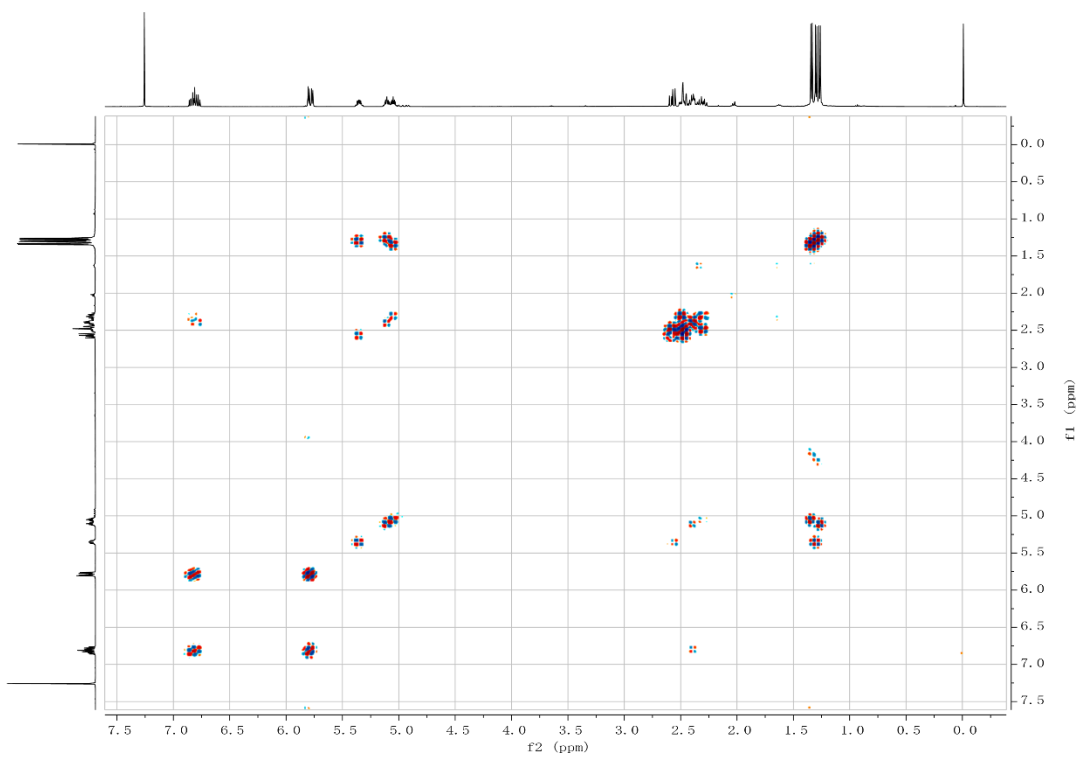


fig. S42.  $^1\text{H}$ - $^1\text{H}$  COSY spectrum of compound 9 in  $\text{CDCl}_3$ .

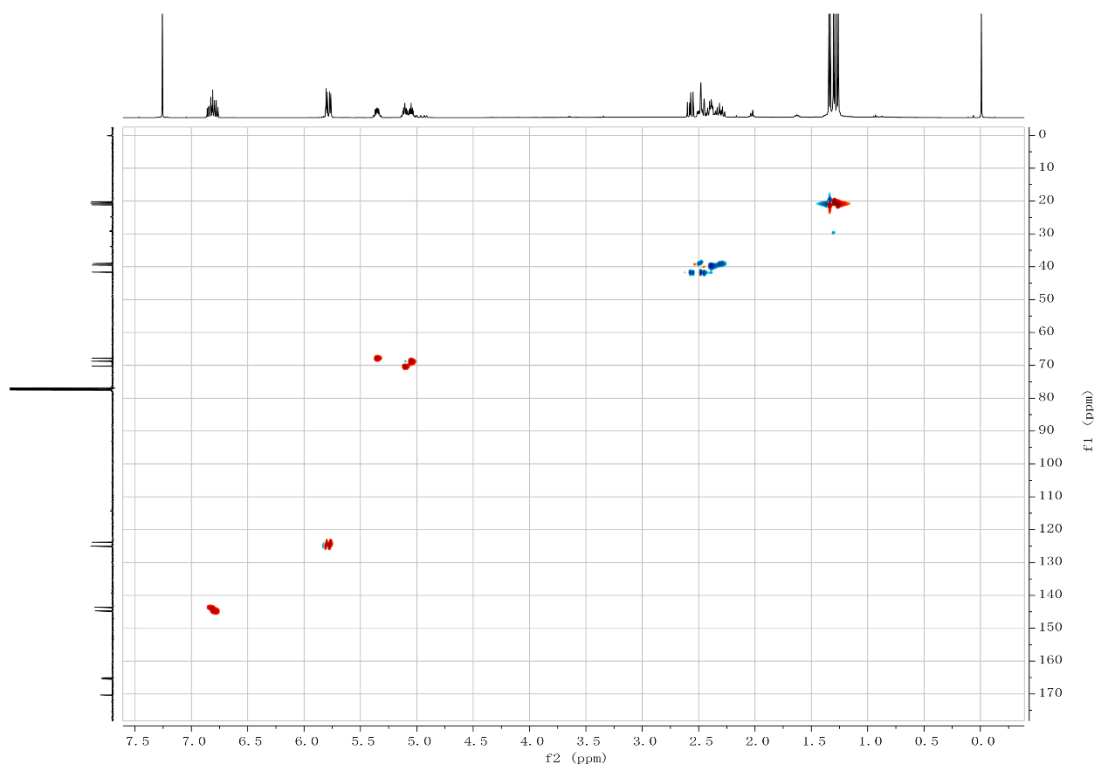


fig. S43. HSQC spectrum of compound 9 in  $\text{CDCl}_3$ .

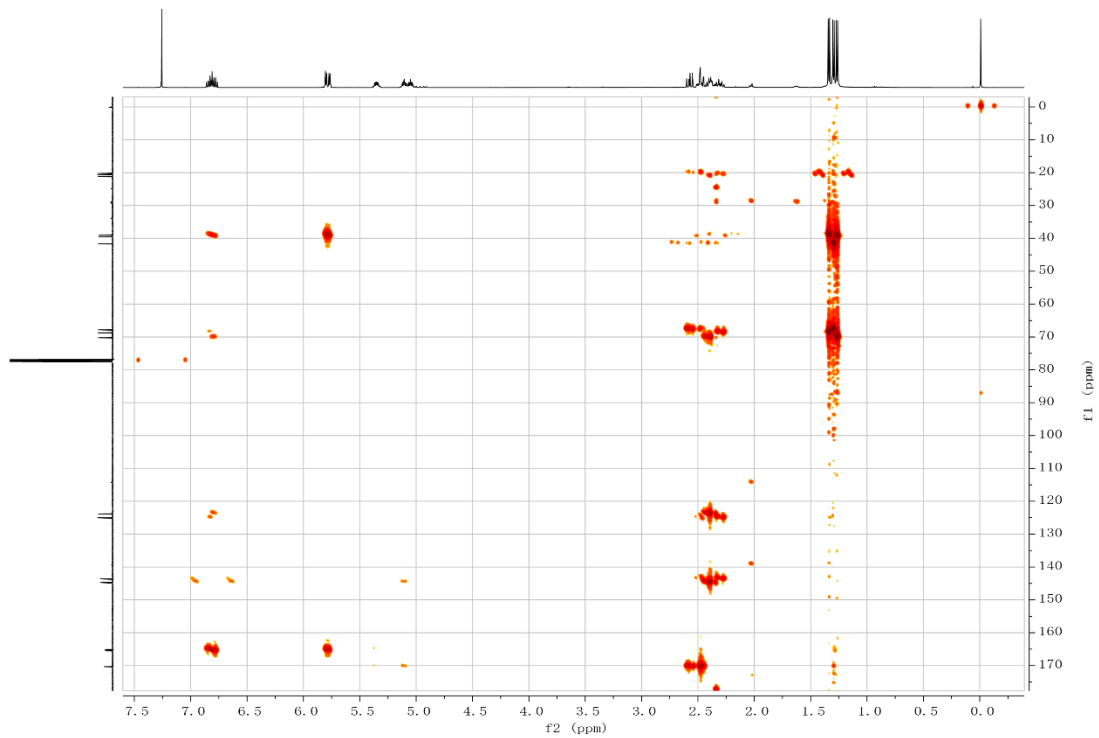


fig. S44. HMBC spectrum of compound 9 in CDCl<sub>3</sub>.

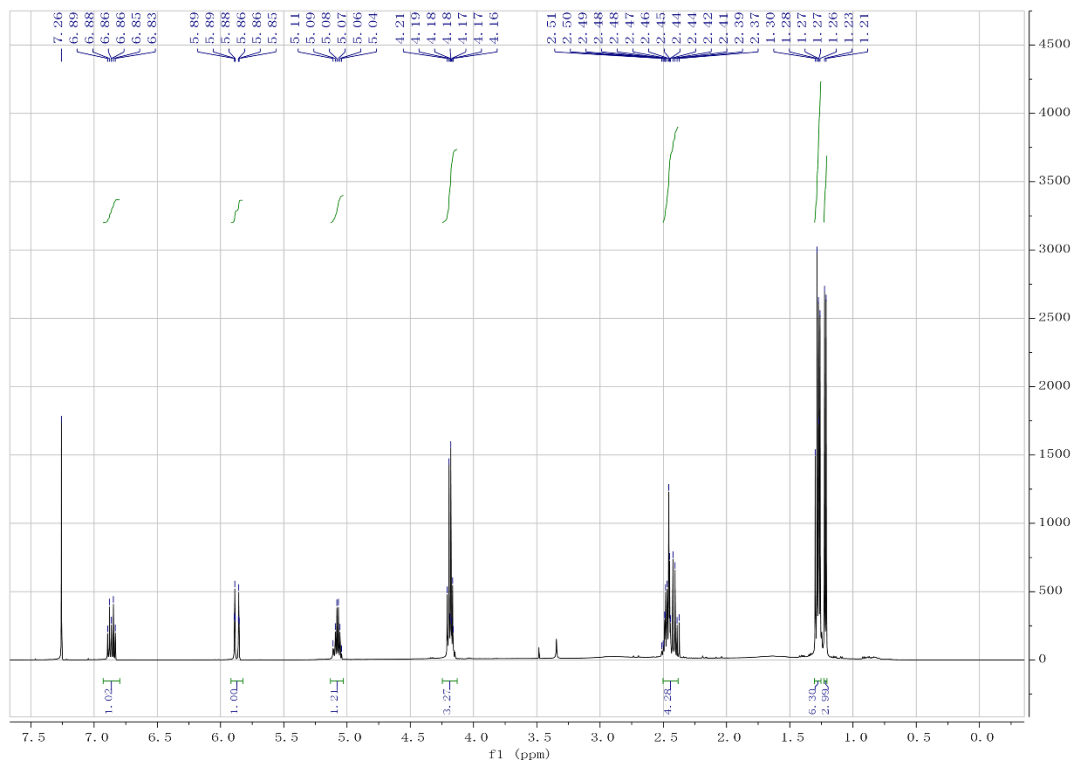


fig. S45. <sup>1</sup>H NMR spectrum of compound 10 in CDCl<sub>3</sub>.

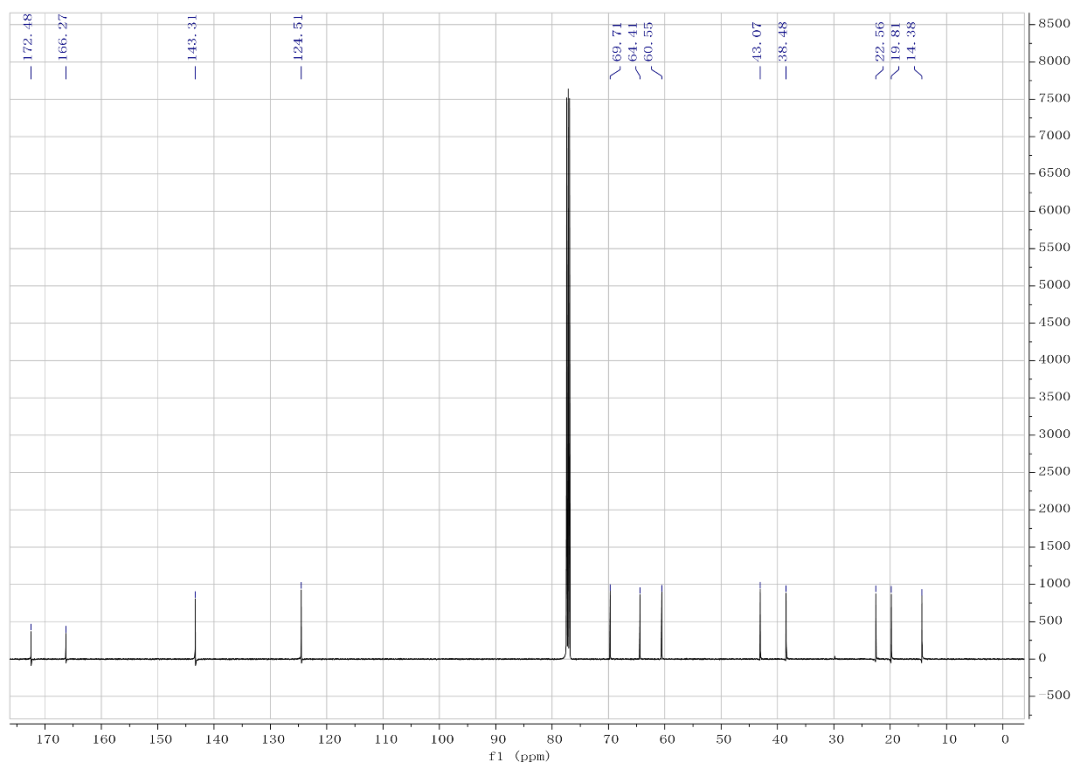


fig. S46.  $^{13}\text{C}$  NMR spectrum of compound 10 in  $\text{CDCl}_3$ .

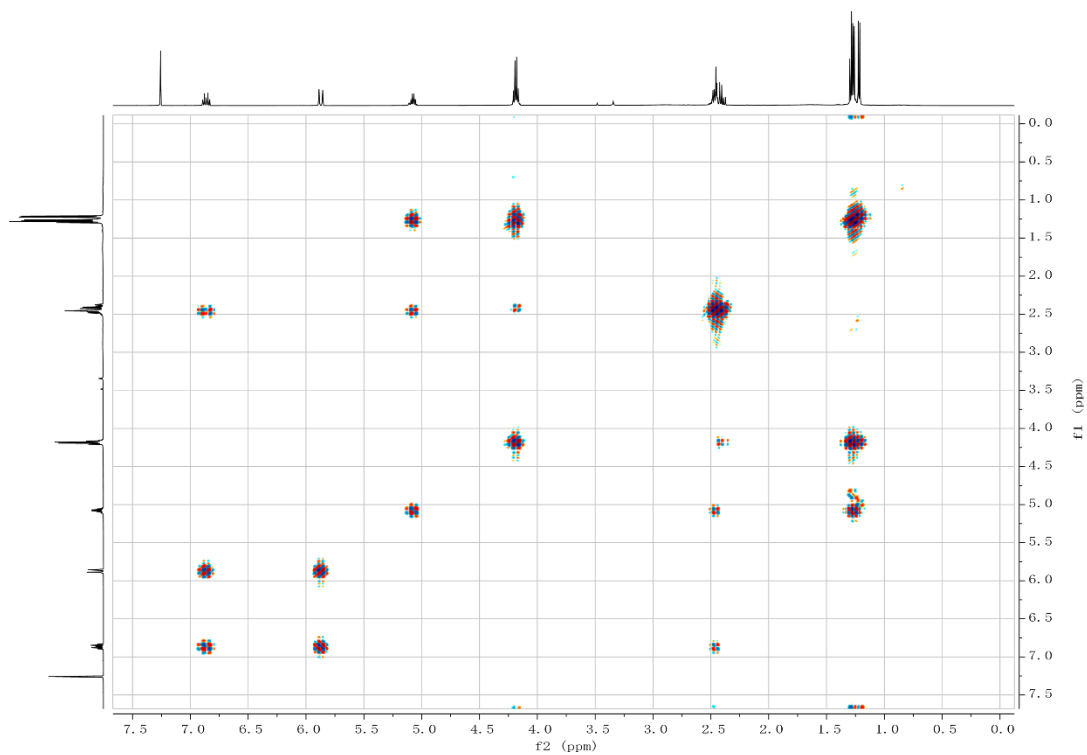


fig. S47.  $^1\text{H}$ - $^1\text{H}$  COSY spectrum of compound 10 in  $\text{CDCl}_3$ .

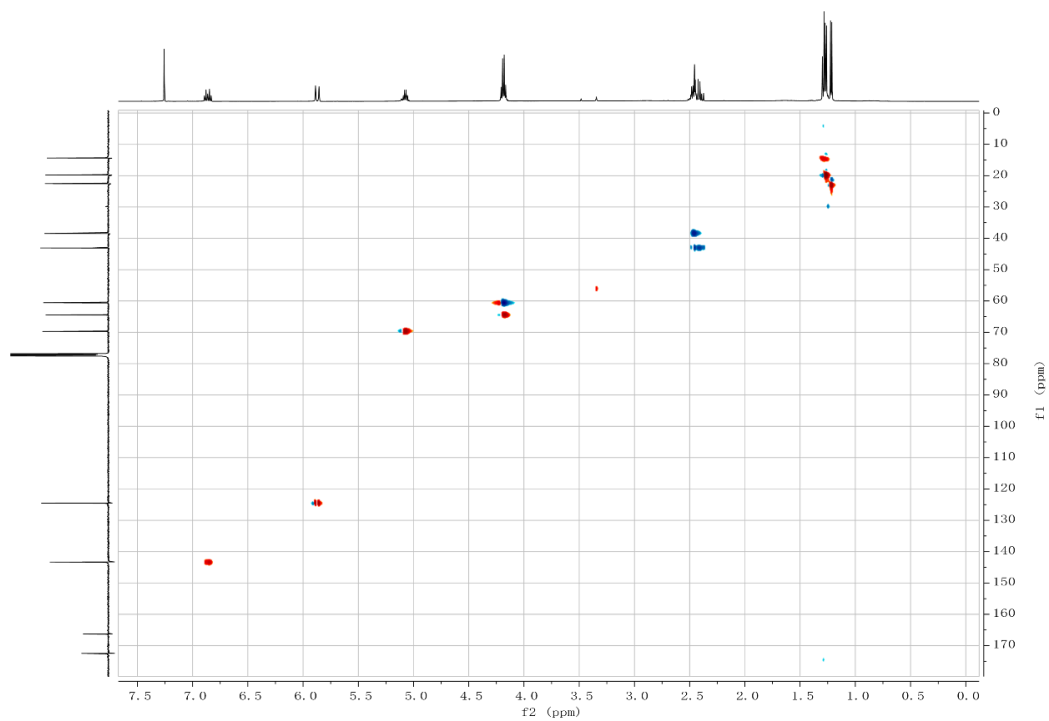


fig. S48. HSQC spectrum of compound 10 in  $\text{CDCl}_3$ .

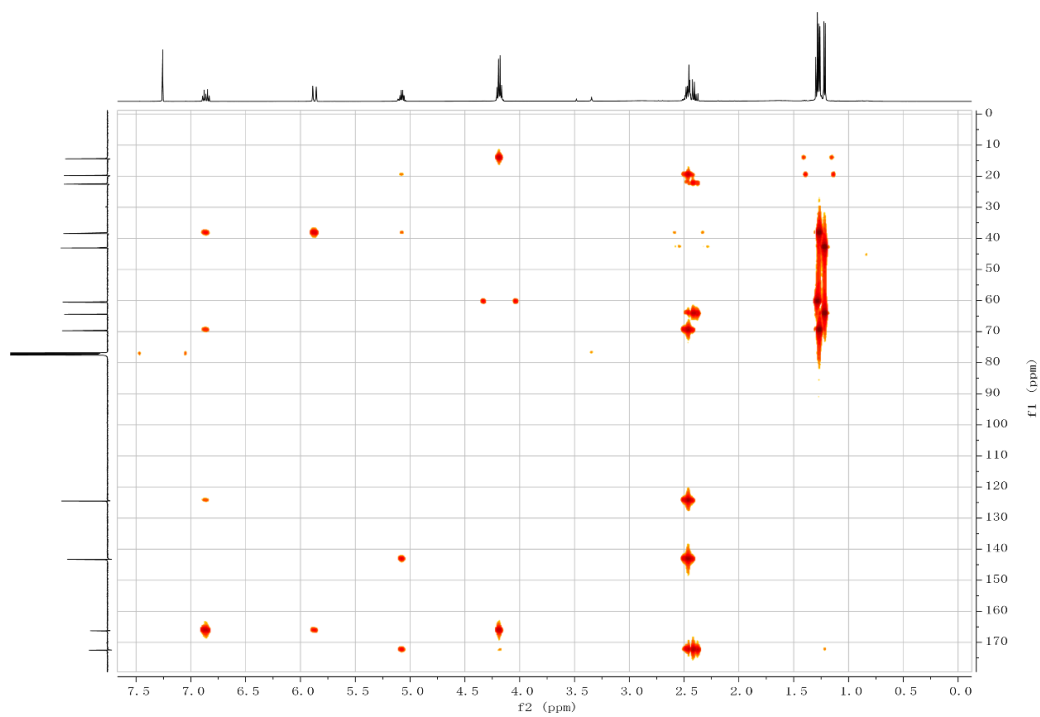


fig. S49. HMBC spectrum of compound 10 in  $\text{CDCl}_3$ .

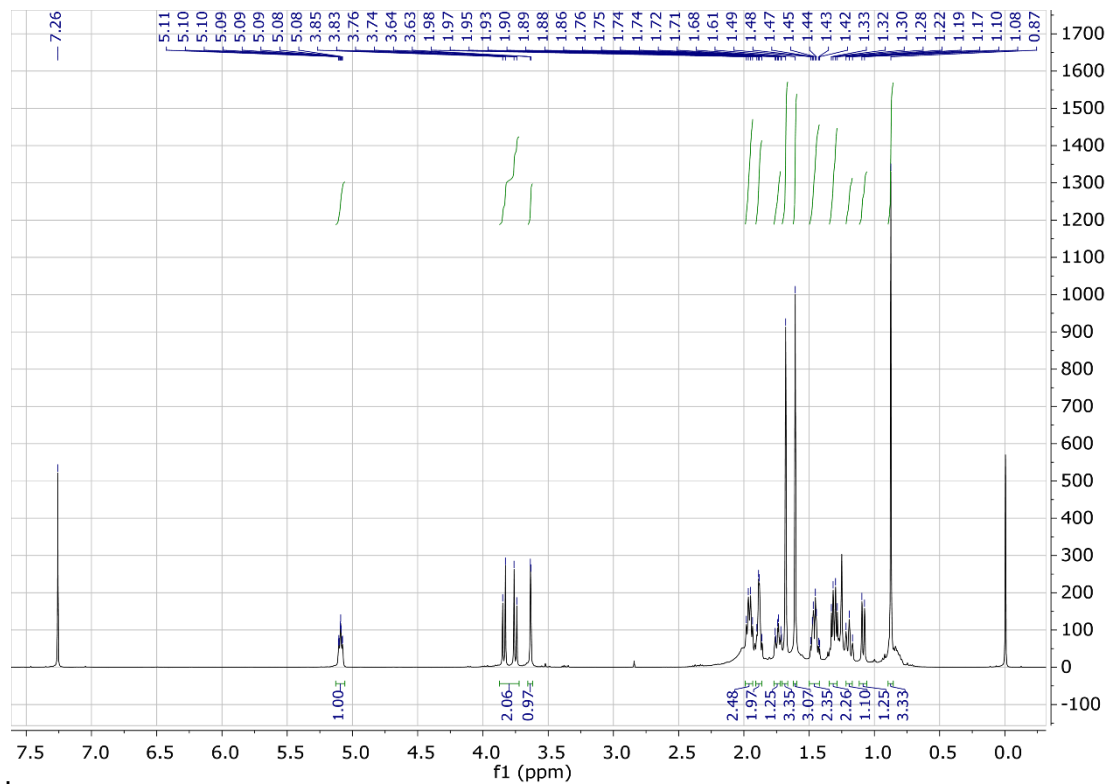


fig. S50.  $^1\text{H}$  NMR spectrum of compound 11 in  $\text{CDCl}_3$ .

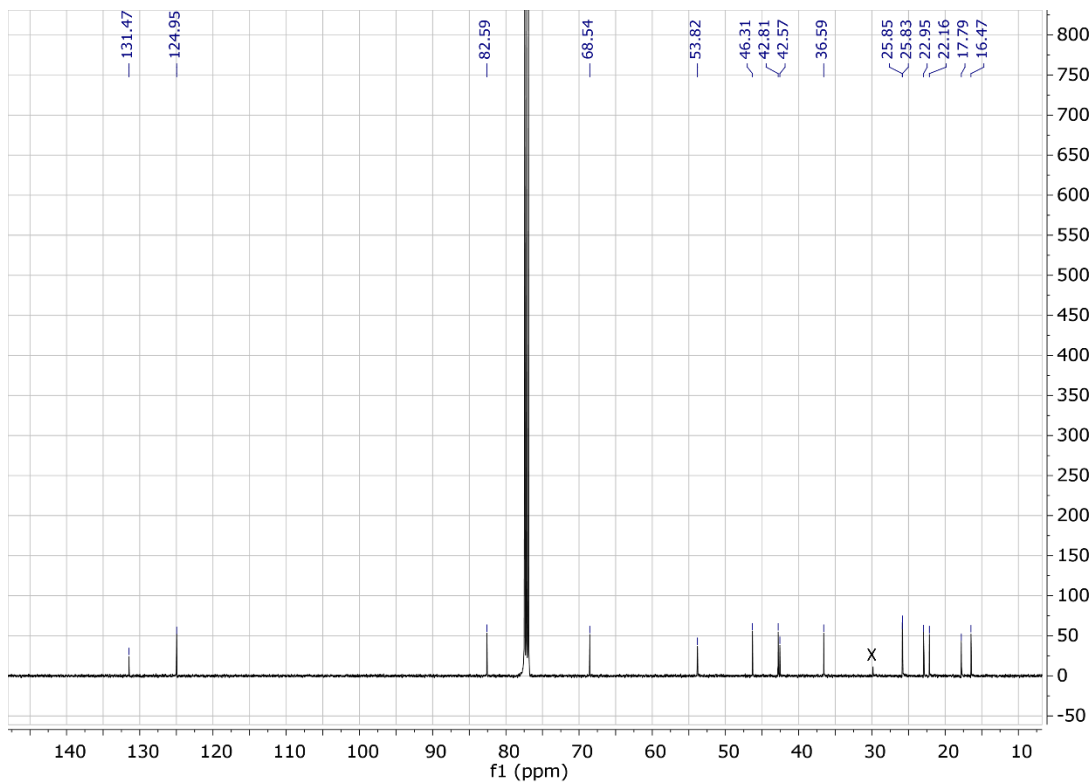


fig. S51.  $^{13}\text{C}$  NMR spectrum of compound 11 in  $\text{CDCl}_3$ .

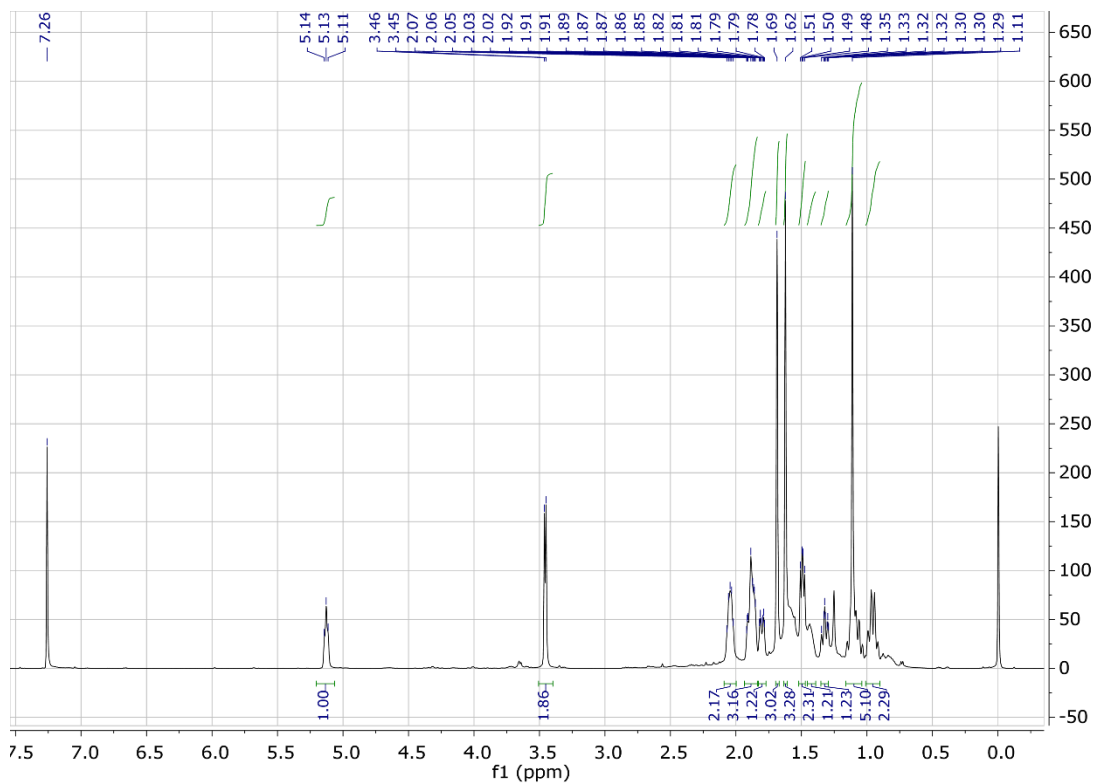


fig. S52.  $^1\text{H}$  NMR spectrum of compound 12 in  $\text{CDCl}_3$ .

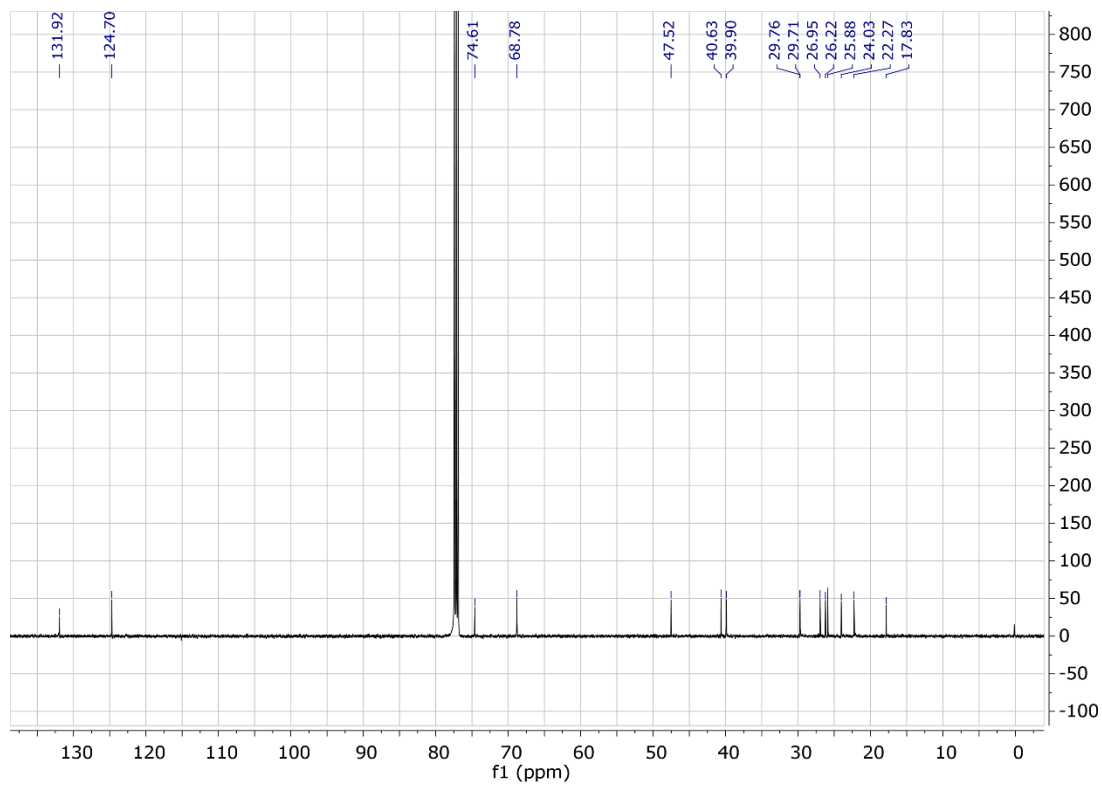


fig. S53.  $^{13}\text{C}$  NMR spectrum of compound 12 in  $\text{CDCl}_3$ .

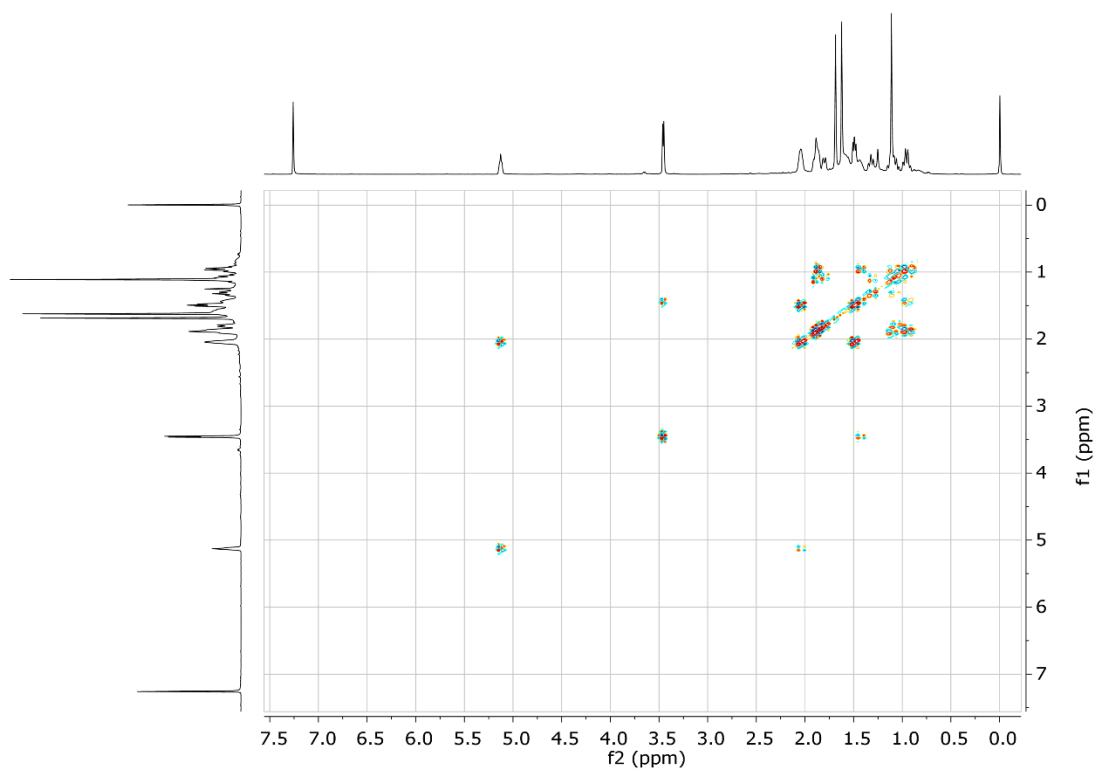


fig. S54.  $^1\text{H}$ - $^1\text{H}$  COSY spectrum of compound 12 in  $\text{CDCl}_3$ .

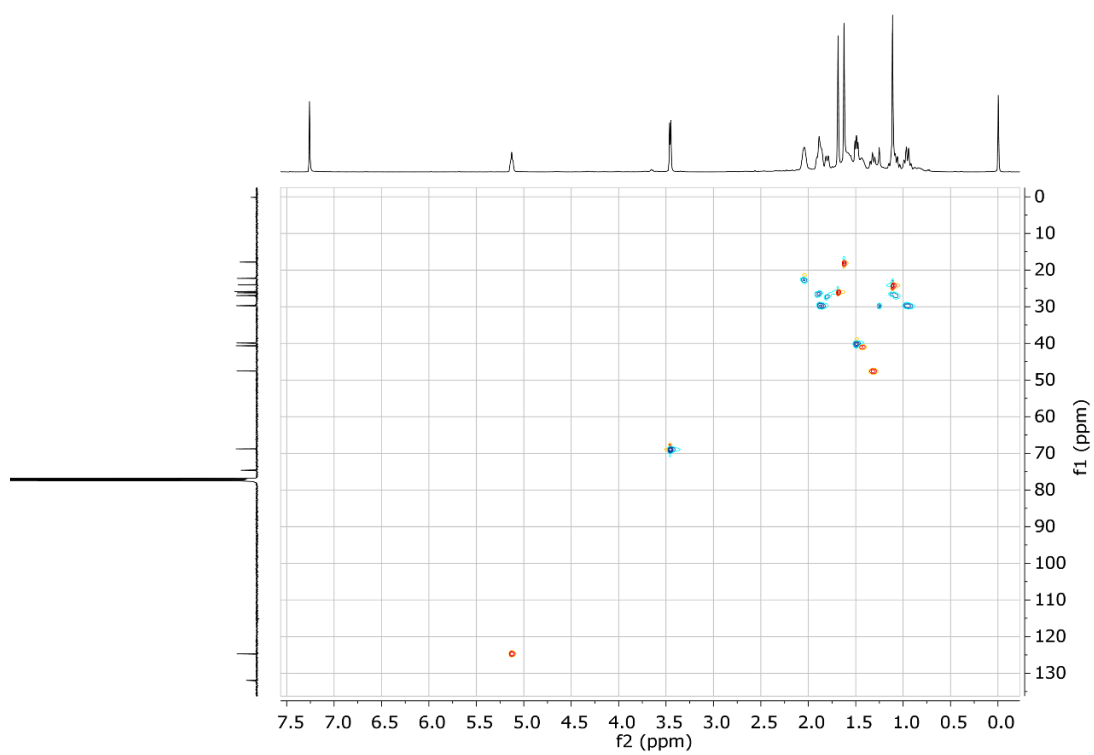


fig. S55. HSQC spectrum of compound 12 in  $\text{CDCl}_3$ .



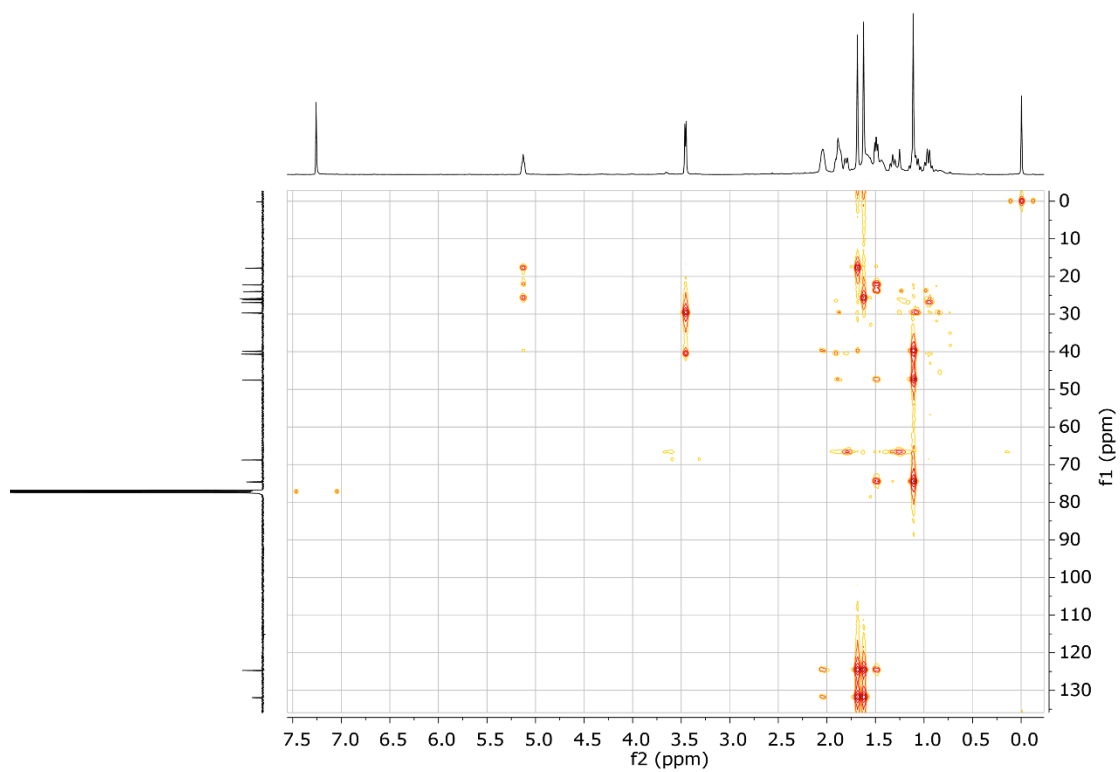


fig. S56. HMBC spectrum of compound 12 in  $\text{CDCl}_3$ .

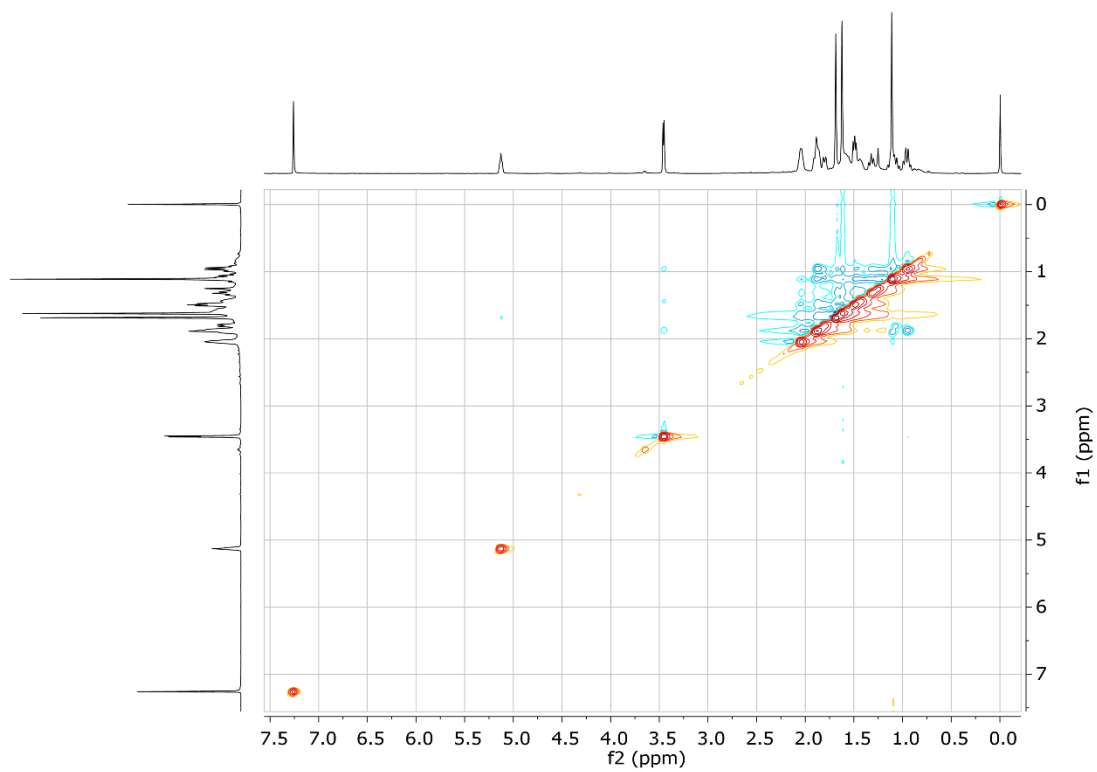


fig. S57. NOESY spectrum of compound 12 in  $\text{CDCl}_3$ .

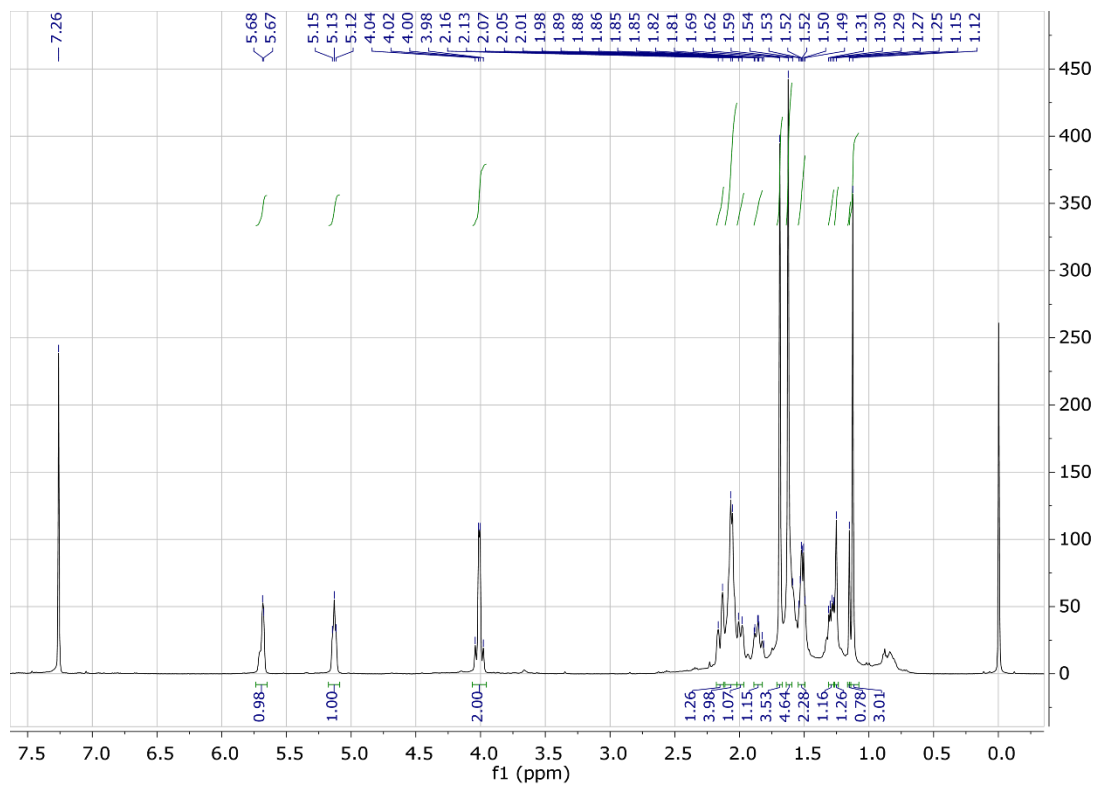


fig. S58.  $^1\text{H}$  NMR spectrum of compound 13 in  $\text{CDCl}_3$ .

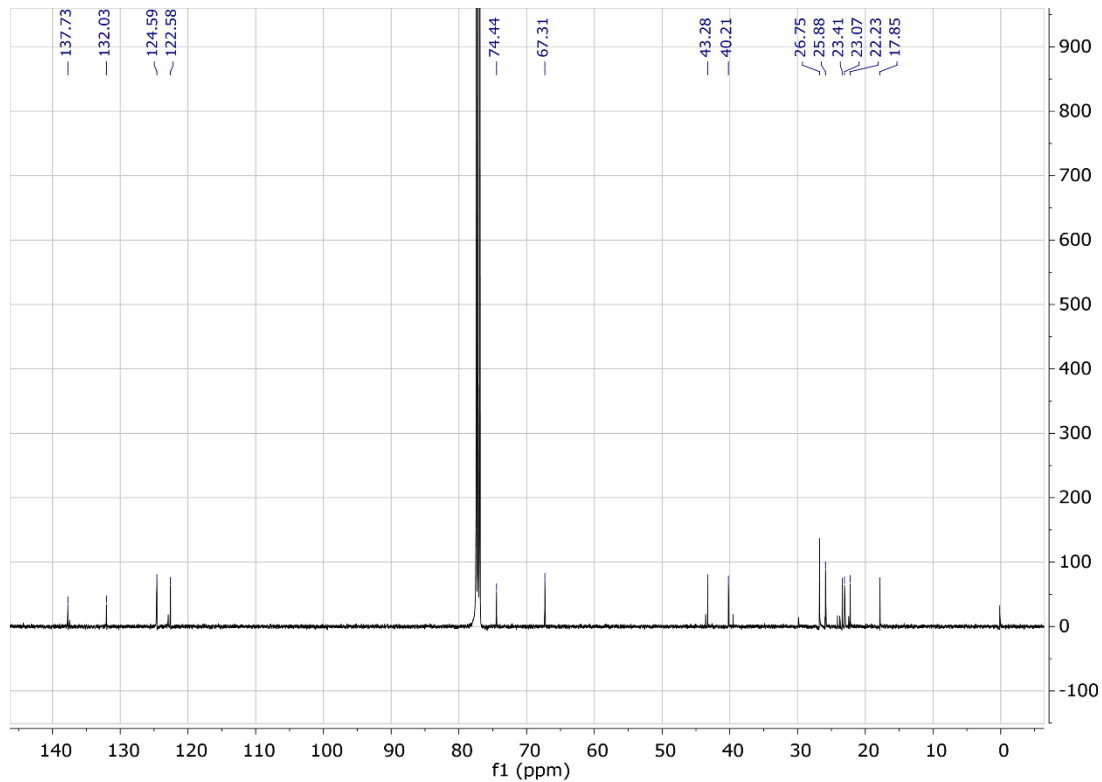


fig. S59.  $^{13}\text{C}$  NMR spectrum of compound 13 in  $\text{CDCl}_3$ .

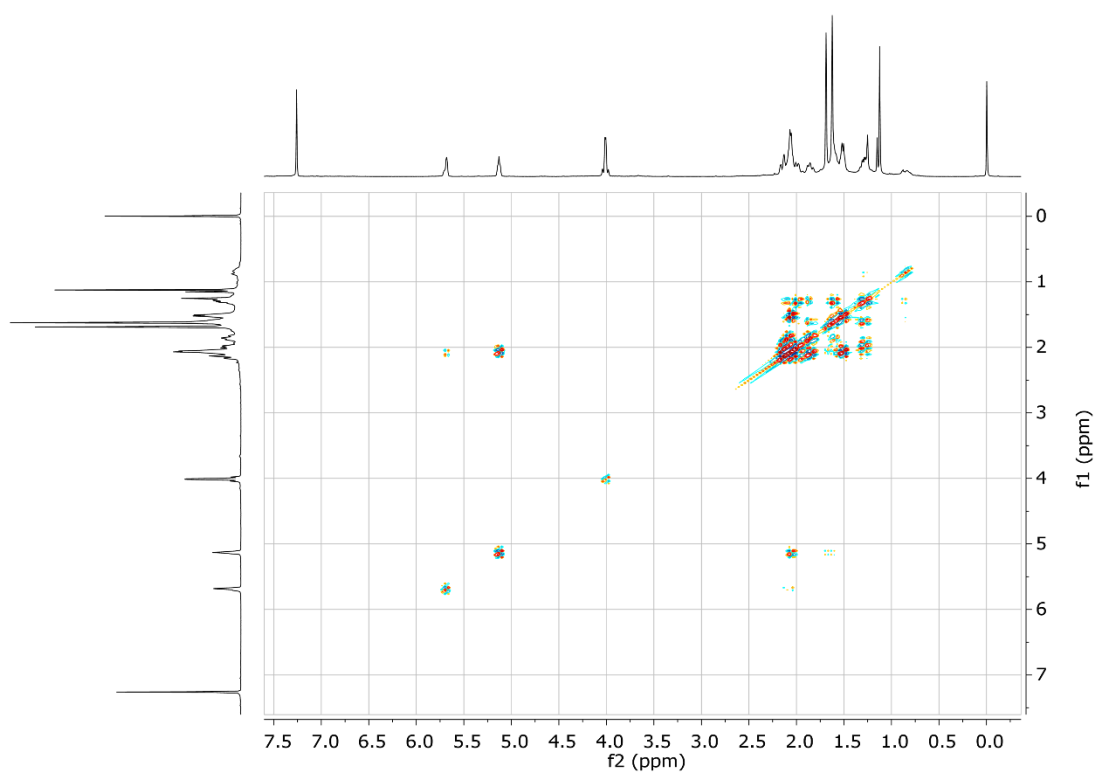


fig. S60.  $^1\text{H}$ - $^1\text{H}$  COSY spectrum of compound 13 in  $\text{CDCl}_3$ .

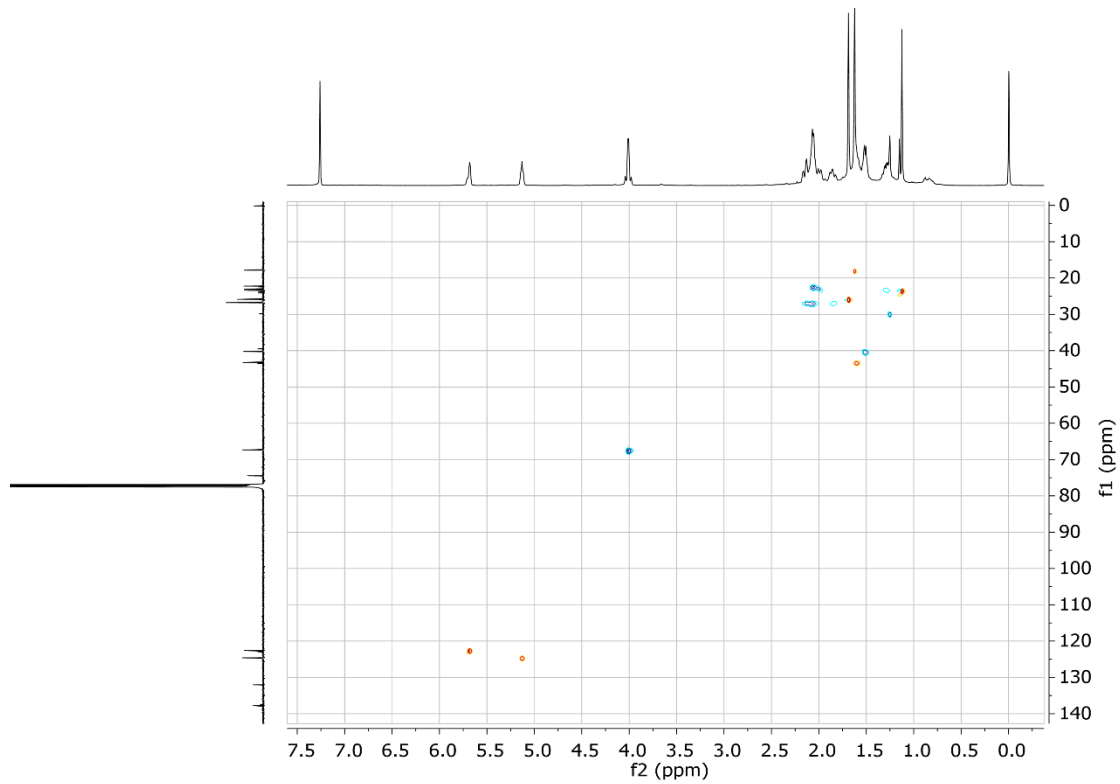


fig. S61. HSQC spectrum of compound 13 in  $\text{CDCl}_3$ .

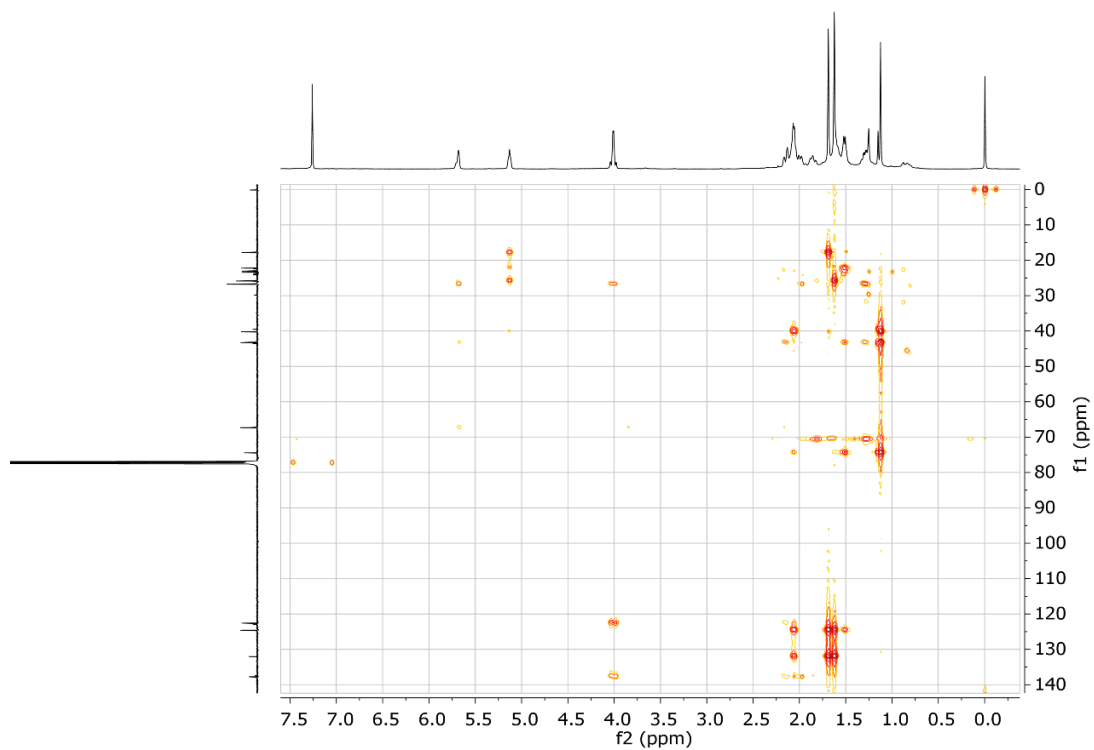


fig. S62. HMBC spectrum of compound 13 in  $\text{CDCl}_3$ .

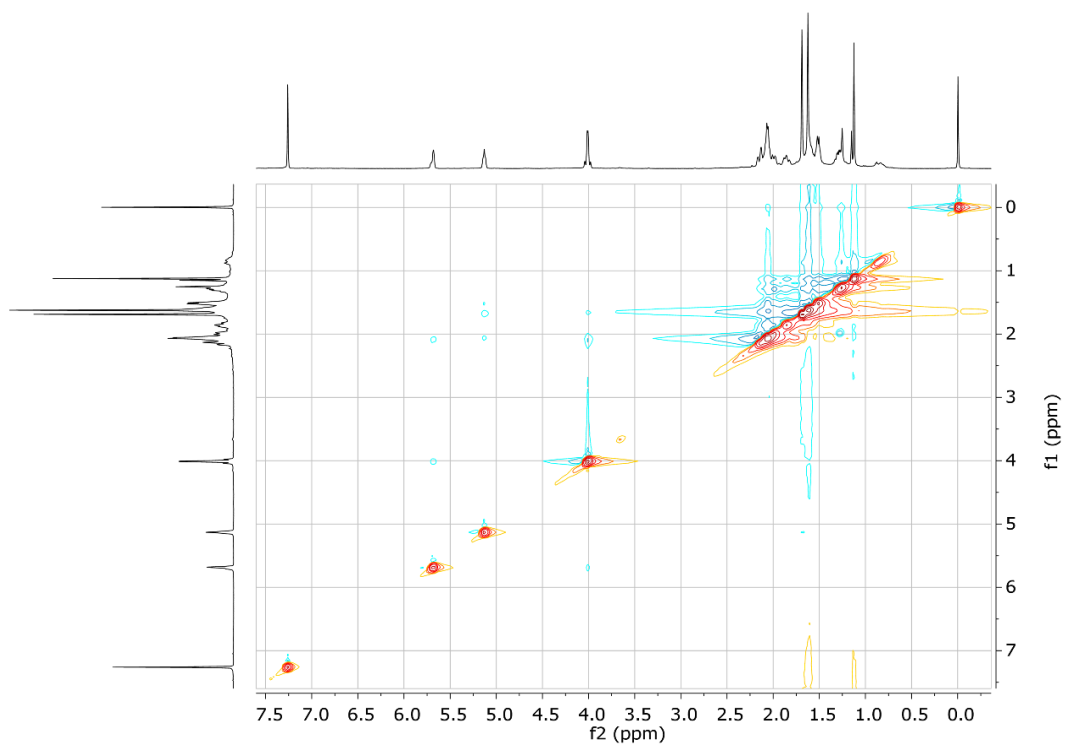


fig. S63. NOESY spectrum of compound 13 in  $\text{CDCl}_3$ .

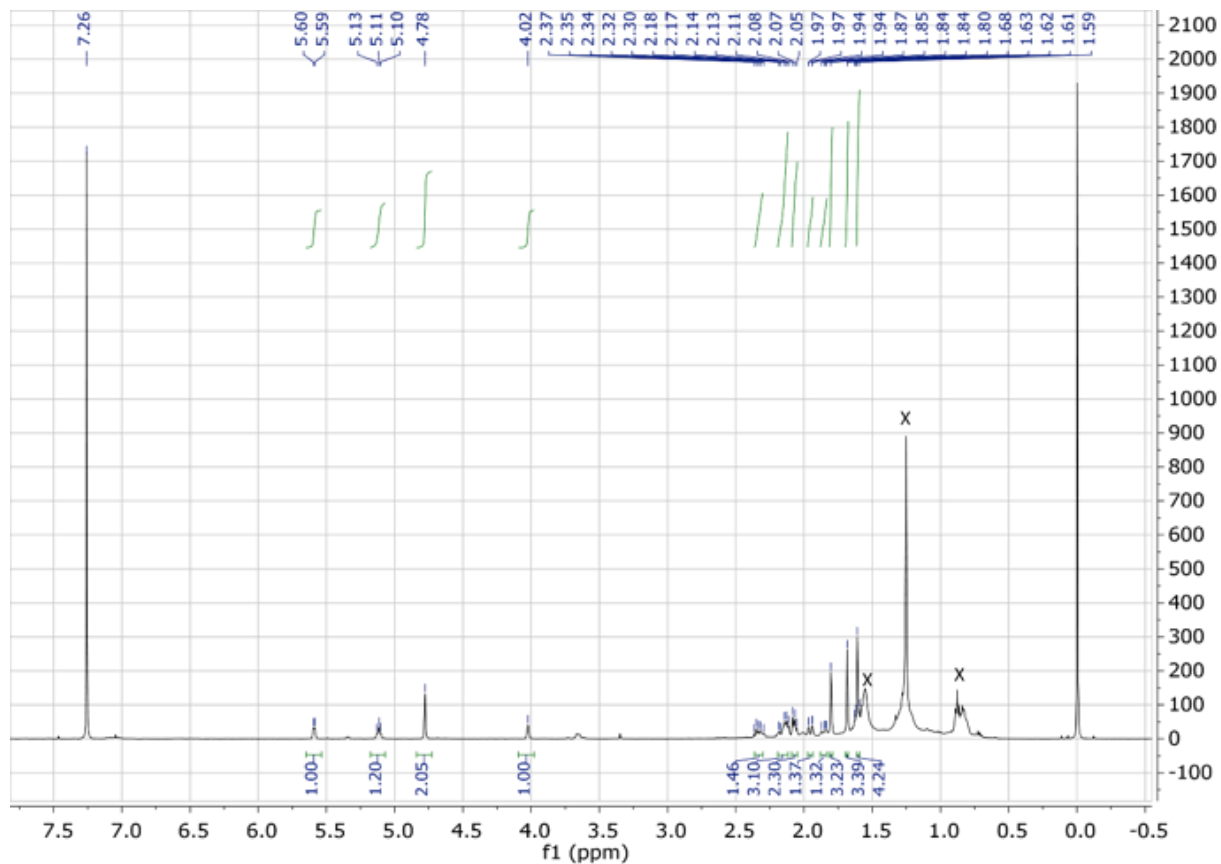


fig. S64.  $^1\text{H}$  NMR spectrum of compound 14 in  $\text{CDCl}_3$ .

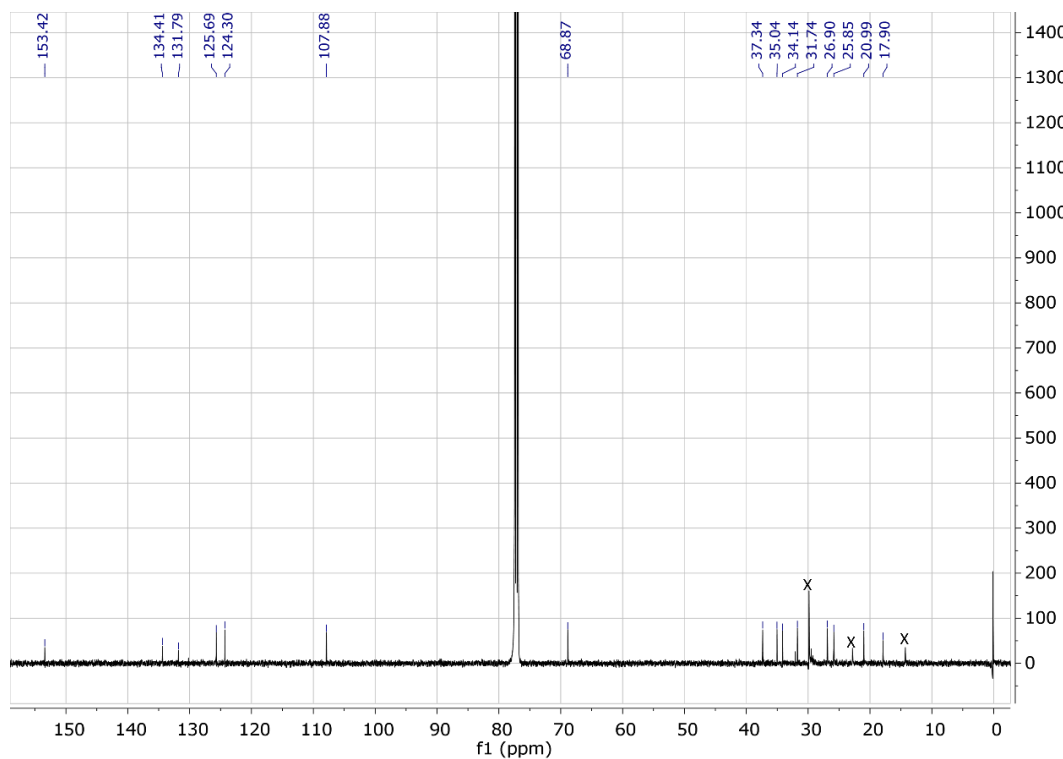


fig. S65.  $^{13}\text{C}$  NMR spectrum of compound 14 in  $\text{CDCl}_3$ .

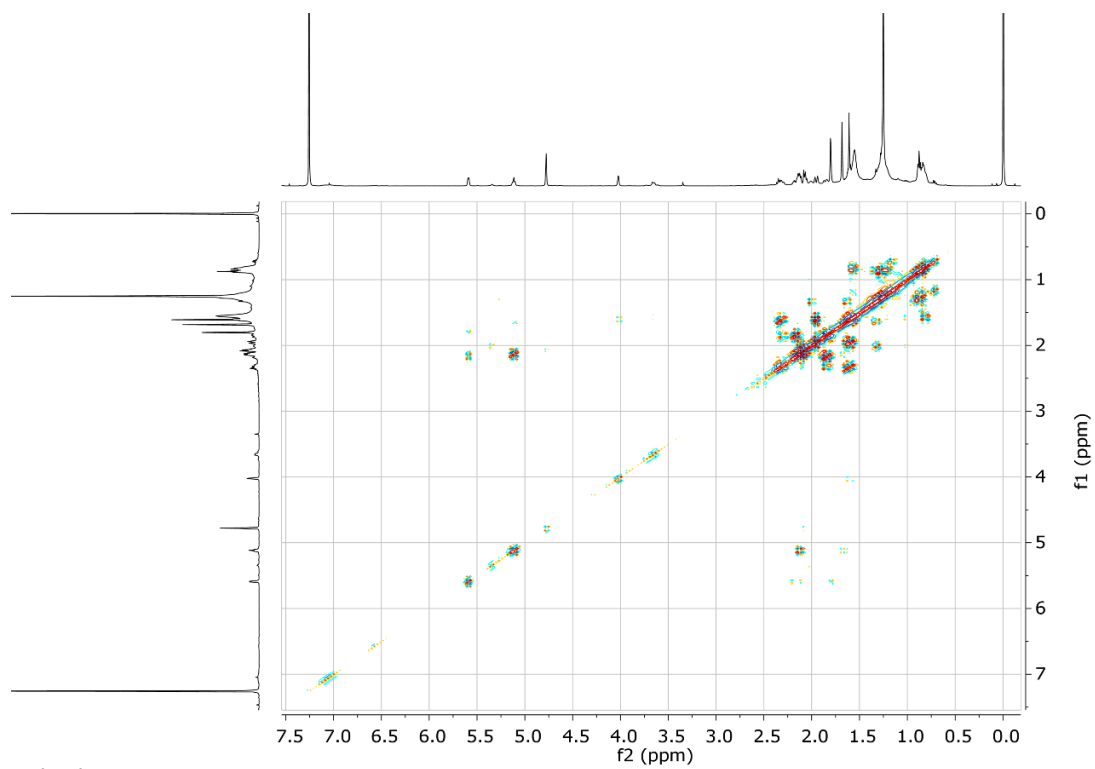


fig. S66.  $^1\text{H}$ - $^1\text{H}$  COSY spectrum of compound 14 in  $\text{CDCl}_3$ .

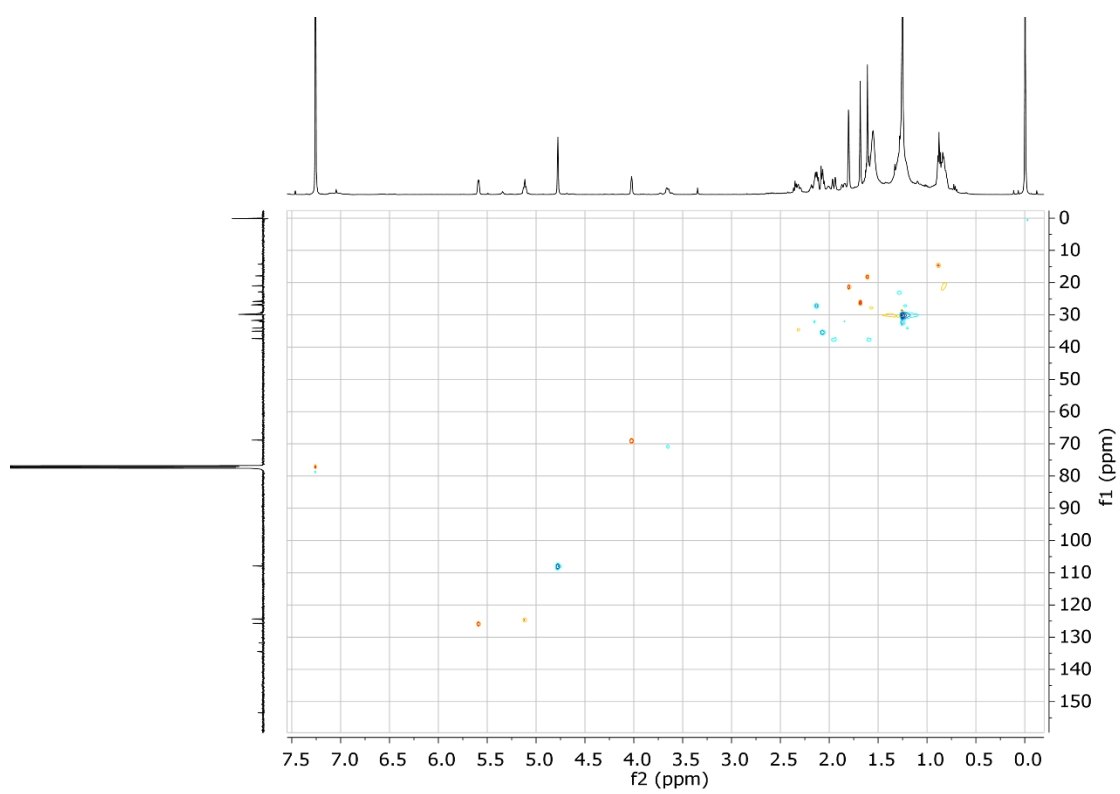


fig. S67. HSQC spectrum of compound 14 in  $\text{CDCl}_3$ .

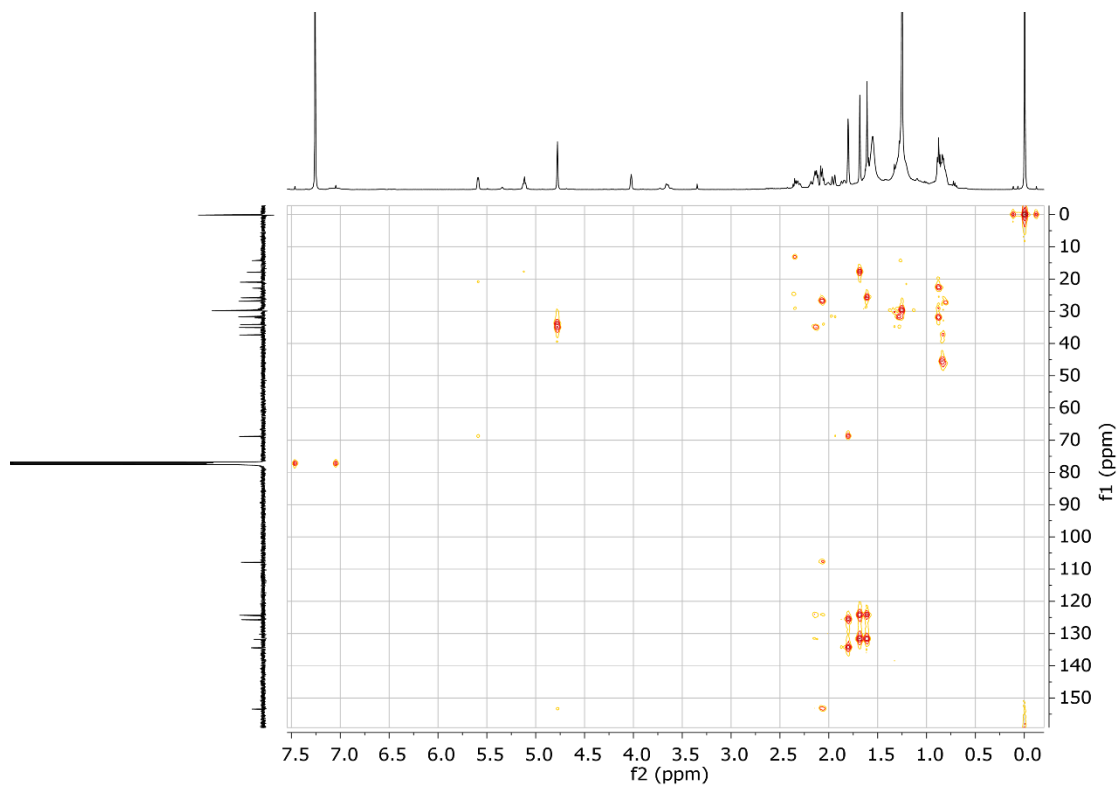


fig. S68. HMBC spectrum of compound 14 in  $\text{CDCl}_3$ .

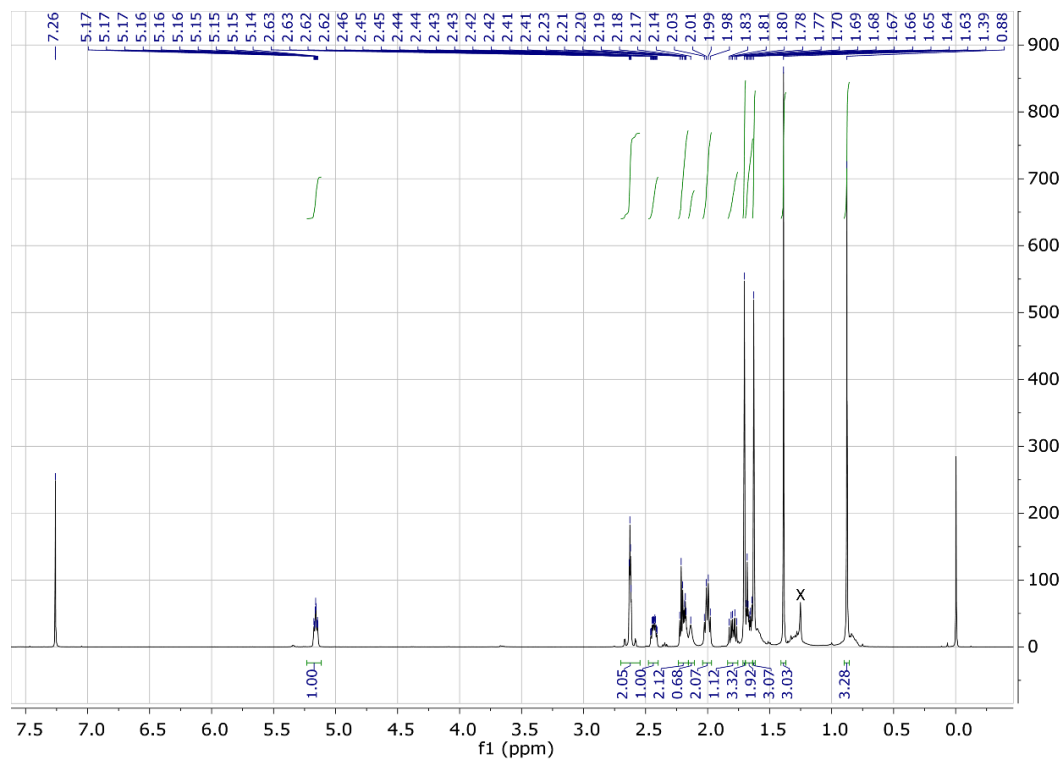


fig. S69.  $^1\text{H}$  NMR spectrum of compound 15 in  $\text{CDCl}_3$ .

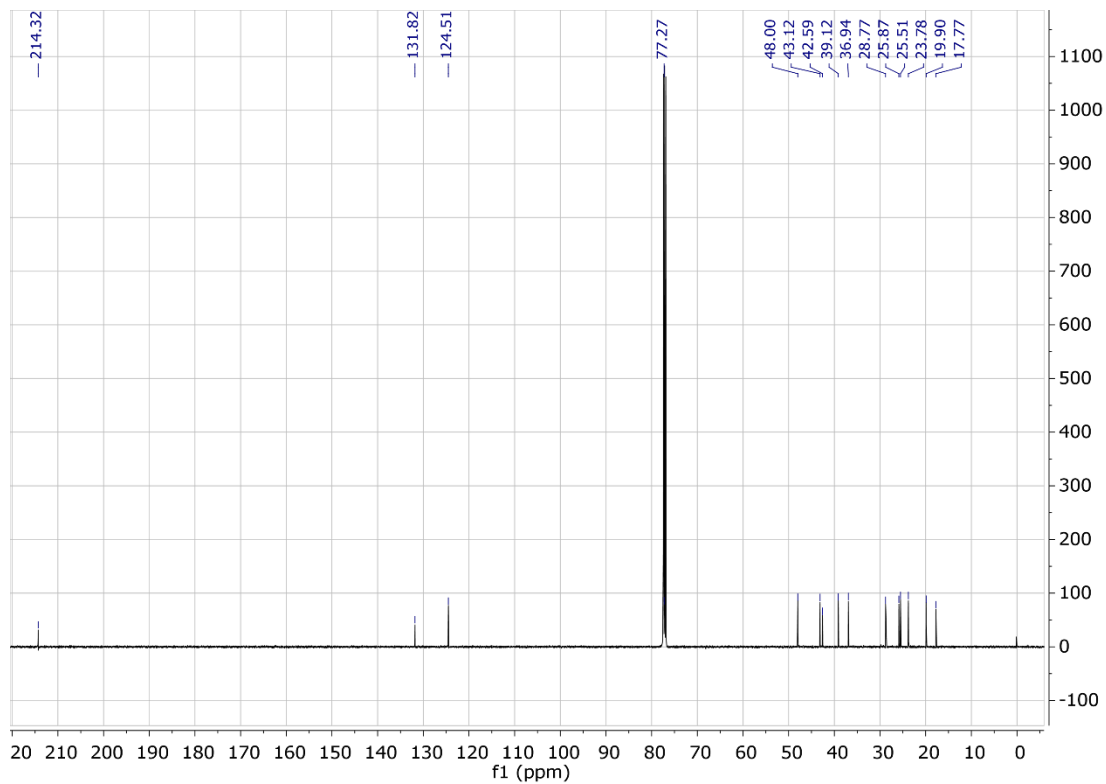


fig. S70. <sup>13</sup>C NMR spectrum of compound 15 in CDCl<sub>3</sub>.

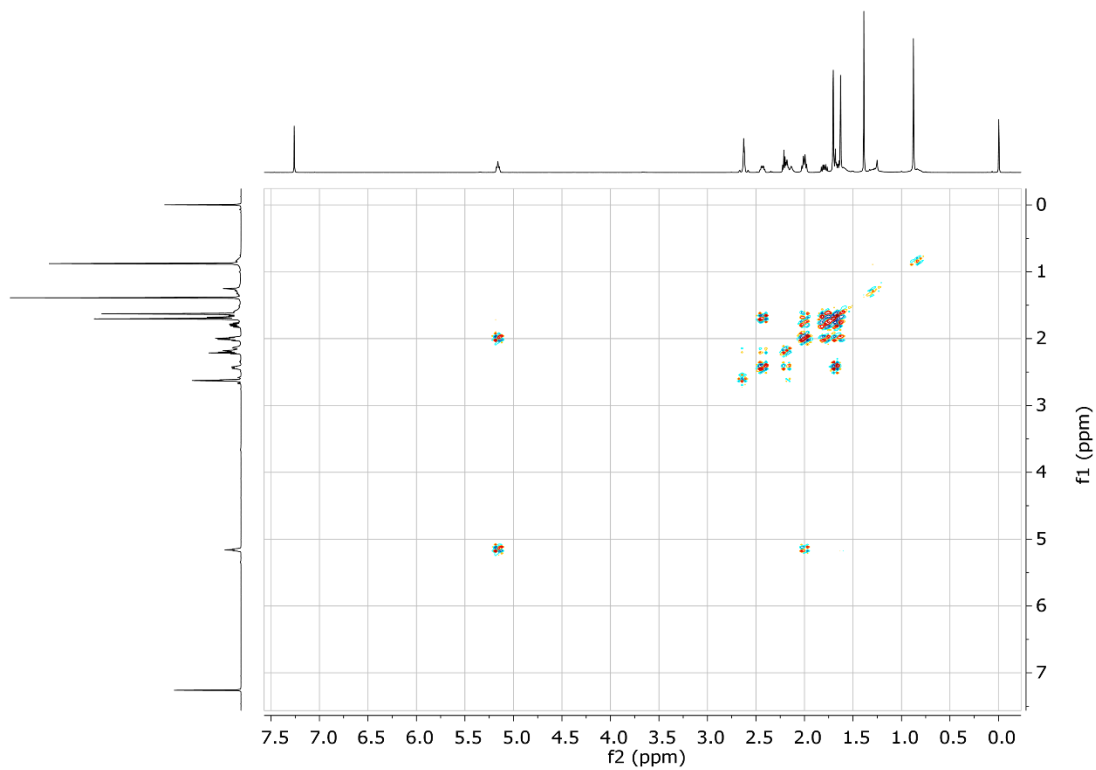


fig. S71. <sup>1</sup>H-<sup>1</sup>H COSY spectrum of compound 15 in CDCl<sub>3</sub>.



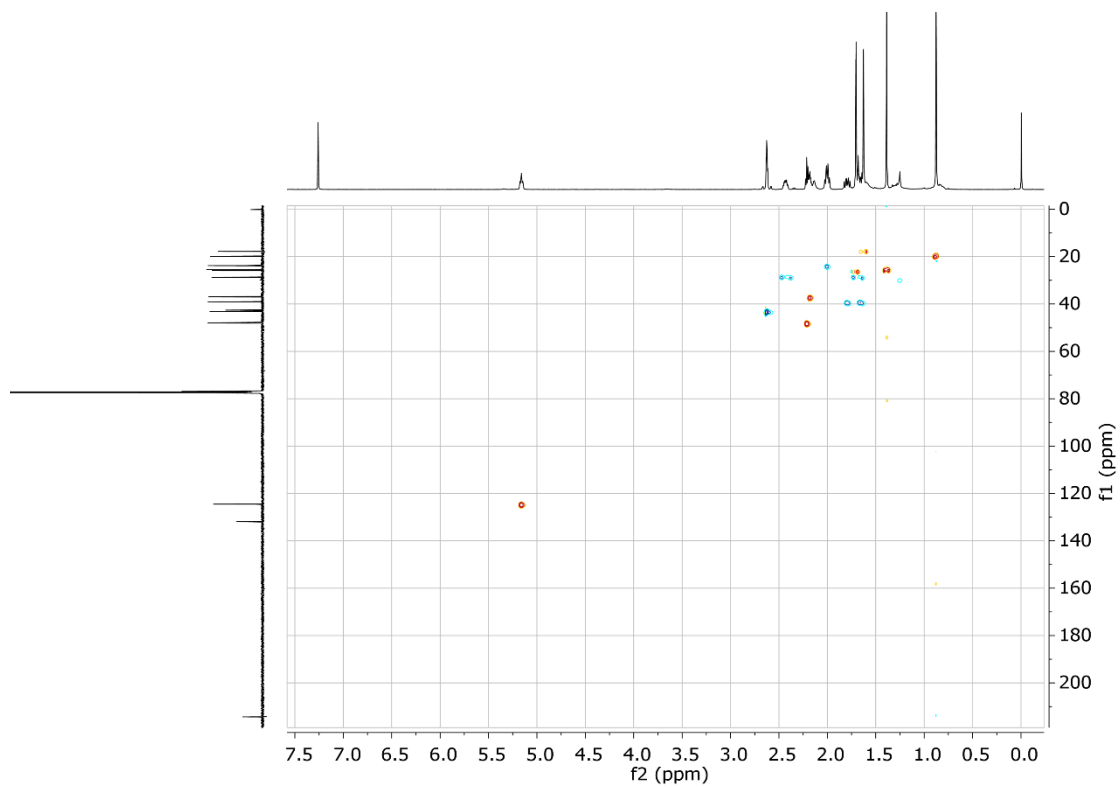


fig. S72. HSQC spectrum of compound 15 in CDCl<sub>3</sub>.

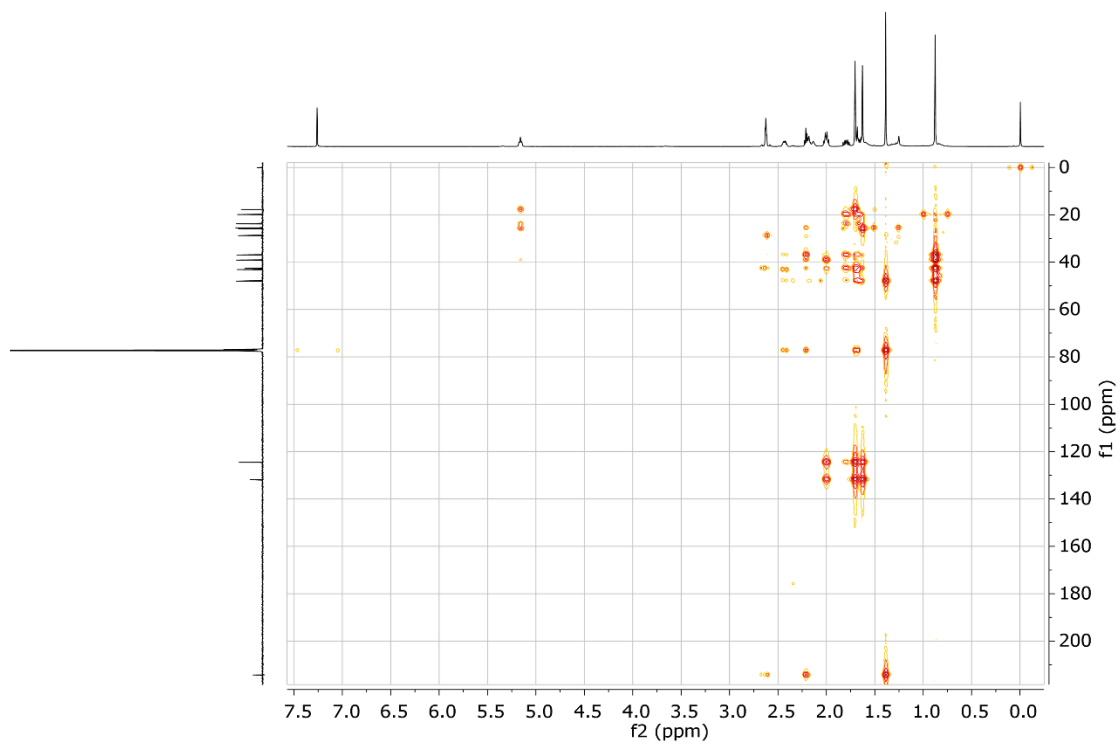


fig. S73. HMBC spectrum of compound 15 in CDCl<sub>3</sub>.

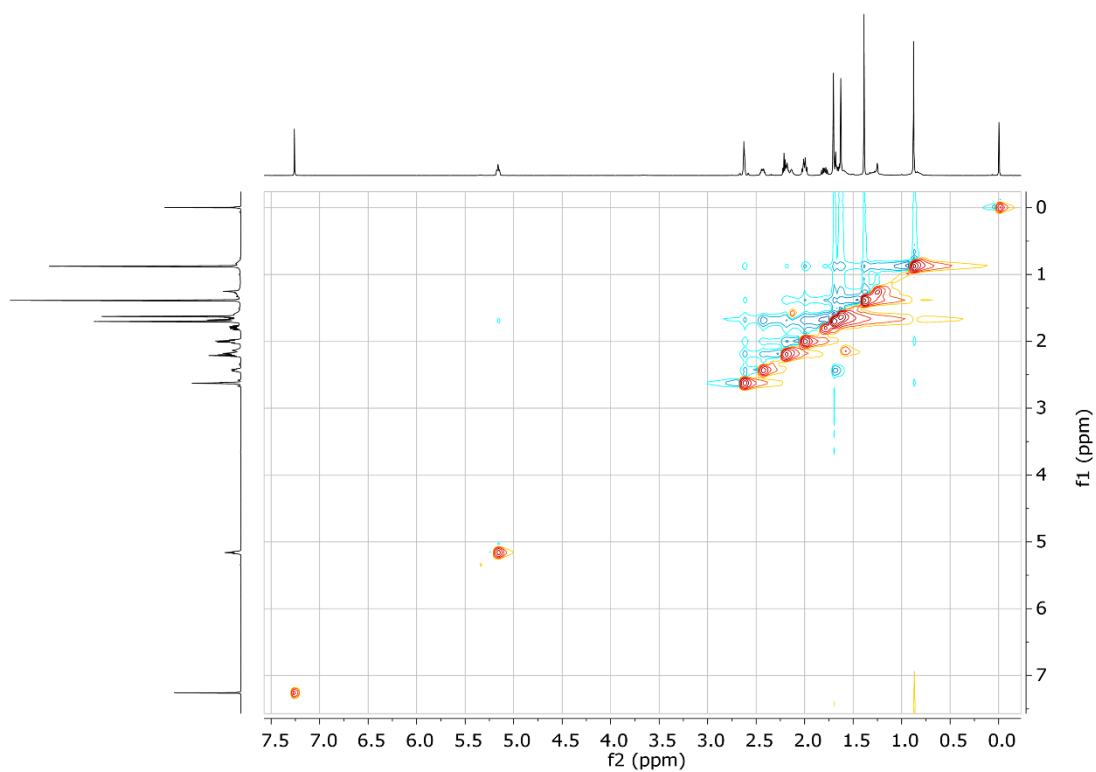


fig. S74. HMBC spectrum of compound 15 in  $\text{CDCl}_3$ .

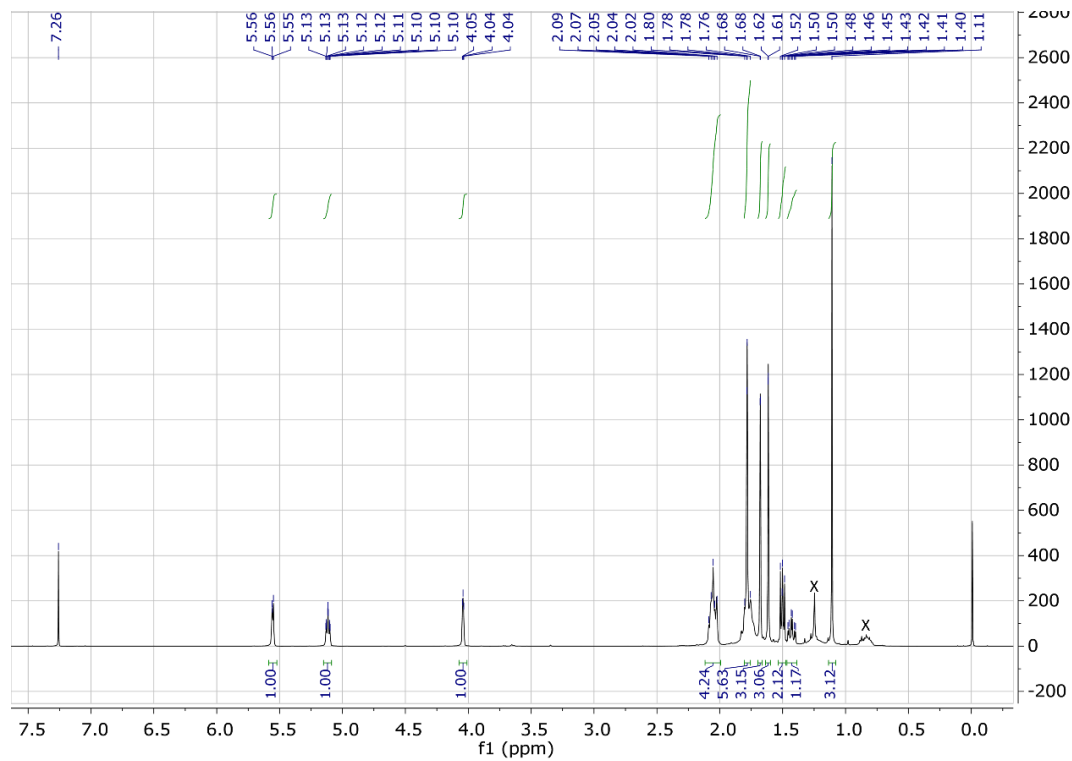


fig. S75.  $^1\text{H}$  NMR spectrum of compound 16 in  $\text{CDCl}_3$ .

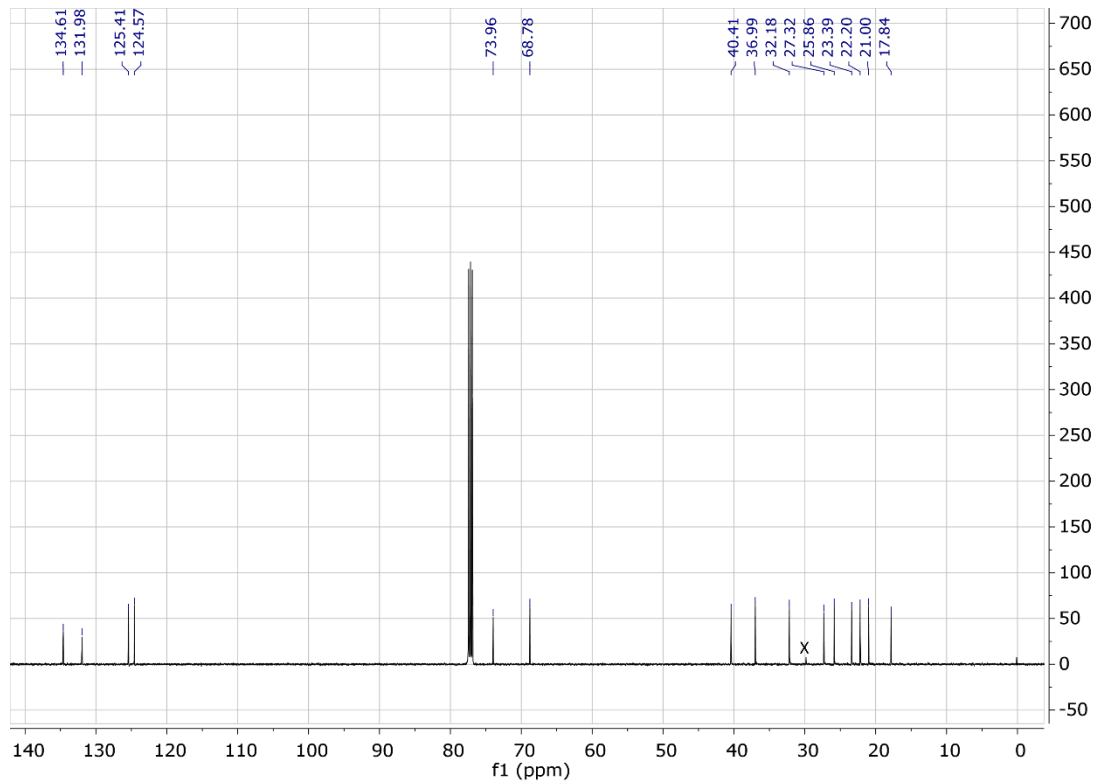


fig. S76.  $^{13}\text{C}$  NMR spectrum of compound 16 in  $\text{CDCl}_3$ .

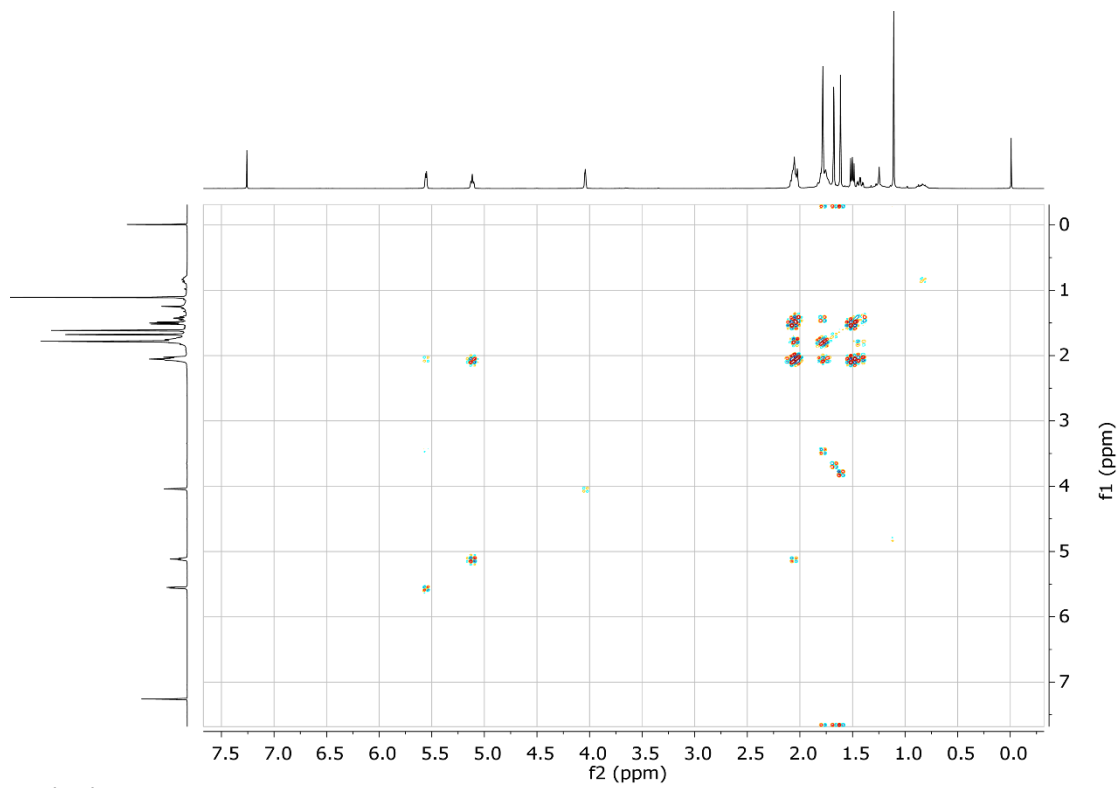


fig. S77.  $^1\text{H}$ - $^1\text{H}$  COSY spectrum of compound 16 in  $\text{CDCl}_3$ .

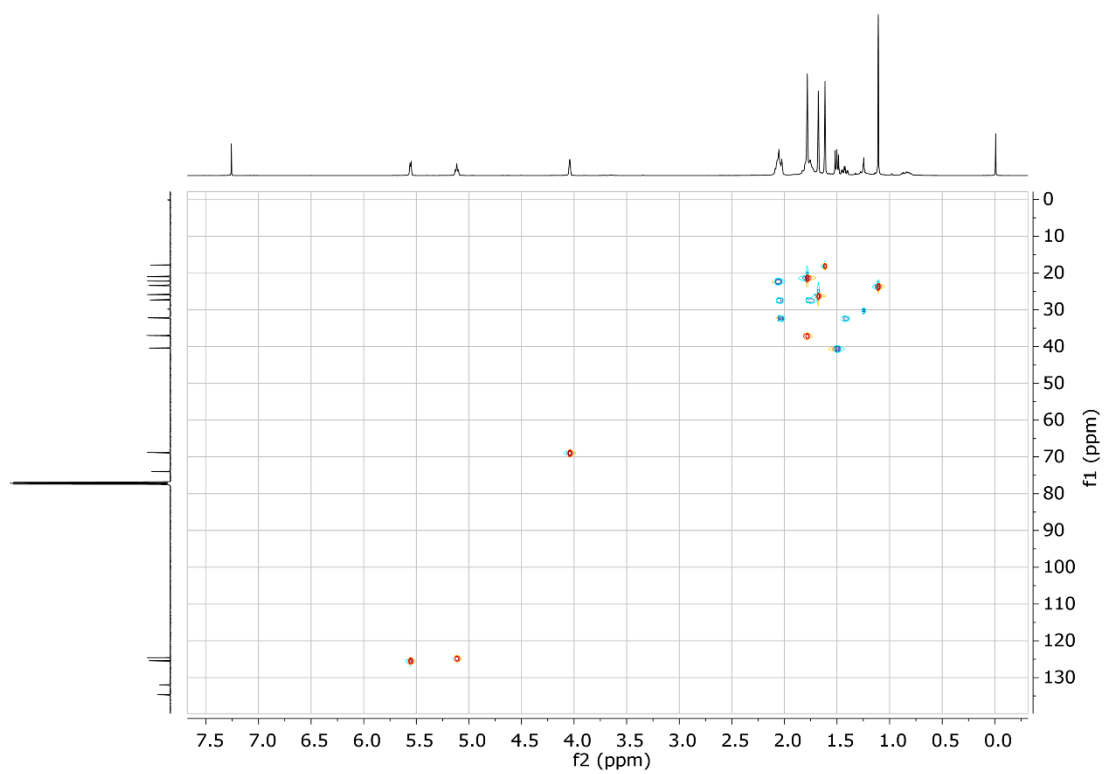


fig. S78. HSQC spectrum of compound 16 in CDCl<sub>3</sub>.

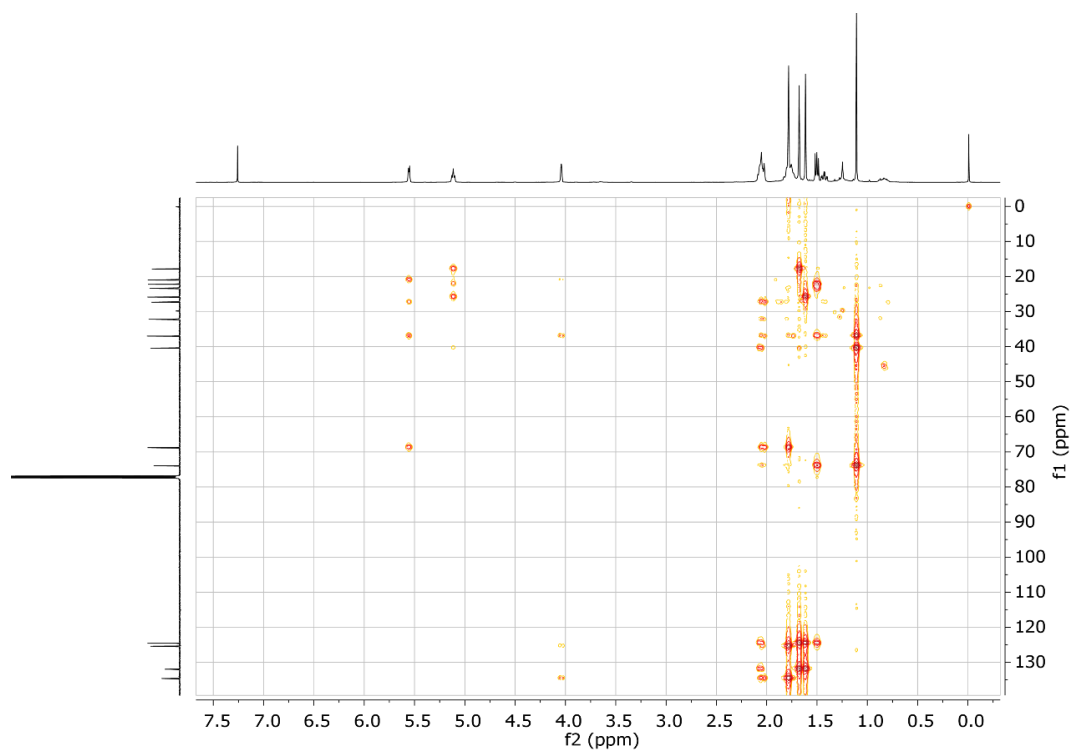


fig. S79. HMBC spectrum of compound 16 in CDCl<sub>3</sub>.